

Phonon spectra, quantum geometry, and the Goldstone theorem

Guglielmo Pellitteri,^{1,*} Zenan Dai,² Haoyu Hu,³ Yi Jiang,⁴ Guido Menichetti,^{5,6} Andrea Tomadin,⁵ B. Andrei Bernevig,^{3,4,7} and Marco Polini^{5,8}

¹*Scuola Normale Superiore, Piazza dei Cavalieri 7, I-56126 Pisa, Italy*

²*Zhiyuan College, Shanghai Jiao Tong University, Shanghai 200240, China*

³*Department of Physics, Princeton University, Princeton, New Jersey 08544, USA*

⁴*Donostia International Physics Center, P. Manuel de Lardizabal 4, 20018 Donostia-San Sebastian, Spain*

⁵*Dipartimento di Fisica dell'Università di Pisa, Largo Bruno Pontecorvo 3, I-56127 Pisa, Italy*

⁶*Istituto Italiano di Tecnologia, Graphene Labs, Via Morego 30, I-16163 Genova, Italy*

⁷*IKERBASQUE, Basque Foundation for Science, Maria Diaz de Haro 3, 48013 Bilbao, Spain*

⁸*ICFO-Institut de Ciències Fotòniques, The Barcelona Institute of Science and Technology, Av. Carl Friedrich Gauss 3, 08860 Castelldefels (Barcelona), Spain*

Phonons are essential quasi-particles of all crystals and play a key role in fundamental properties such as thermal transport and superconductivity. In particular, acoustic phonons can be interpreted as Goldstone modes that emerge due to the spontaneous breaking of translational symmetry. In this article, we investigate the quantum geometric contribution to the phonon spectrum in the absence of Holstein phonons. Using graphene as a case study, we decompose the dynamical matrix into distinct terms that exhibit different dependencies on the electron energy and wavefunction. We then examine the role of quantum geometry in shaping the material's phonon spectrum.

Introduction.—Every crystal supports elastic waves, which propagate as quanta of vibrational energy [1, 2] that Frenkel dubbed “*phonons*” in 1932. Phonons are quasi-particles that appear in a wide variety of condensed matter phenomena. Most notably, they serve as the bosonic glue that binds electrons into Cooper pairs in many conventional BCS superconductors [3]. They also play crucial roles in thermal and electrical transport, acting as an intrinsic and unavoidable source of scattering for electrons moving through a crystal. Additionally, phonons are important in atomically thin two-dimensional (2D) materials [4]: the authors of Ref. [5] demonstrated that graphene samples encapsulated in hexagonal Boron Nitride can display very large mobilities also at room temperature, which are solely limited by scattering of electrons against graphene’s acoustic phonons [6–10]. These are gapless modes near the center of the first Brillouin zone (FBZ)—see black lines labeled by “LA” and “TA” in Fig. 1—and play an important role in limiting plasmon lifetimes [11–14] in the same devices. From a theoretical point of view, acoustic phonons can be thought of as the Goldstones associated with the spontaneous breaking of continuous translation symmetry [15–18].

The physical properties listed above are critically dependent on the electron-phonon interaction (EPI) [19, 20]. The coexistence of electrons and phonons in a single host crystal has recently prompted various authors to search for topological contributions to phonons that originate microscopically from the EPI (see, for example, Refs. [21] and [22]). After two decades of intense research on the application of topology to properties of material science [23–26], a more general mathematical framework, now universally known as “quantum geometry”—is attracting significant attention in the community [27–29].

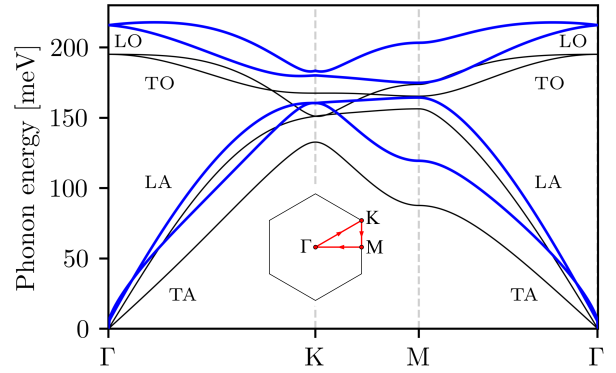


FIG. 1. (Color online) Dispersion of the four in-plane phonon branches (LA, TA, LO, and TO) in graphene. Results in this figure are plotted along the $\Gamma\text{K}\text{M}\Gamma$ high-symmetry path in the first Brillouin zone illustrated in the inset. Black lines: Phonon dispersion $\omega_\ell(\mathbf{q})$ calculated analytically within a next-nearest neighbor Born-von Karman framework [69]. The relevant parameters needed to produce these plots have been determined by fitting *ab initio* density functional theory results. Blue lines: Phonon dispersion $\tilde{\omega}_\ell(\mathbf{q})$ as calculated after removing from the full dynamical matrix $\mathcal{D}(\mathbf{q})$ the quantum geometric contribution $\mathcal{D}_g(\mathbf{q})$ —see Eq. (27). A finite mass $\Delta = 10$ meV (see App. VIII) of the Dirac node has been introduced to perform this calculation.

In 1980, Provost and Vallee [30] understood that the usual Hermitian product on the projective Hilbert space induces a meaningful metric tensor on any manifold of quantum states. This intuition led them to introduce the quantum geometric tensor (QGT):

$$\mathcal{Q}_{ij}(\mathbf{k}) = g_{ij}(\mathbf{k}) - \frac{i}{2} \mathcal{F}_{ij}(\mathbf{k}). \quad (1)$$

Here, $g_{ij}(\mathbf{k})$ is a real, symmetric, and gauge-invariant

tensor that is usually dubbed a quantum metric (or the Fubini-Study metric [31, 32]) and defined by

$$g_{ij}(\mathbf{k}) = \text{Re}[\langle \partial_{k_i} \psi_{\mathbf{k}} | \partial_{k_j} \psi_{\mathbf{k}} \rangle] - \langle \partial_{k_i} \psi_{\mathbf{k}} | \psi_{\mathbf{k}} \rangle \langle \psi_{\mathbf{k}} | \partial_{k_j} \psi_{\mathbf{k}} \rangle. \quad (2)$$

Here, $\{|\psi_{\mathbf{k}}\rangle\}$ is a family of normalized vectors of some Hilbert space which smoothly depend on an n -dimensional parameter $\mathbf{k} \in \mathbb{R}^n$ (this is usually the Bloch quasi-momentum in solid-state physics). The quantum metric tensor $g_{ij}(\mathbf{k})$ is a measure of the distance in amplitude between infinitely close wavefunctions in the \mathbf{k} space.

The second term in Eq. (1) is instead the more familiar Berry curvature [24, 26, 33]:

$$\mathcal{F}_{ij}(\mathbf{k}) = i \langle \partial_{k_i} \psi_{\mathbf{k}} | \partial_{k_j} \psi_{\mathbf{k}} \rangle - i \langle \partial_{k_j} \psi_{\mathbf{k}} | \partial_{k_i} \psi_{\mathbf{k}} \rangle \\ = -2 \text{Im} \langle \partial_{k_i} \psi_{\mathbf{k}} | \partial_{k_j} \psi_{\mathbf{k}} \rangle, \quad (3)$$

which, of course, is also gauge-invariant. A more modern and compact definition of the QGT is provided below in Eq. (21) and in App. I of the Supplemental Material [34].

The QGT plays a fundamental role in a vast number of physical phenomena. Its importance in the theory of the insulating state, for example, has been known for more than two decades [35–37], and has been recently revisited [38–43]. Interest in the QGT has been recently revitalized in the context of strongly correlated electron systems with flat bands, such as flat-band superconductors [44–50]. Quantum transport anomalies in systems with flat bands [51] as well as non-linear optical response functions [52] have also been linked to the quantum geometry of states. Direct measurements of QGT have been reported in optical lattices [53], qubits [54, 55], microcavities [56], and more recently in moiré materials [57]; however, more experimental replication is necessary.

A recent theoretical work [58] has incorporated the quantum geometry of electron bands into the theory of EPIs, demonstrating the crucial contributions of the Fubini-Study metric [31] or its orbital selective version [58] to the dimensionless electron-phonon coupling constant. Concrete estimates have been provided for two materials, i.e. graphene and MgB_2 , where the geometric contributions account for approximately 50% and 90% of the total electron-phonon coupling constant, respectively. In this work, we study the role of the QGT in the dispersion of phonons *directly*, using the same Gaussian approximation introduced in Ref. [58]. We do not consider Holstein-type EPI [59–61], for which the approximation used fails. The ions in the lattice experience both their mutual repulsion and the attractive force of the electron cloud. The latter is represented, within the Born-Oppenheimer approximation [1], by the variation of the electronic ground-state energy induced by the displacement of an ion from its equilibrium position. We show that this electronic term in the ionic equation of motion contains a contribution which is entirely due to the electronic QGT, thus affecting the phonon dispersion of the crystal. We then choose

graphene as a case study. The choice of this material is well motivated: it exhibits a non-zero QGT due to its two-site unit cell, the electron dispersion relation in graphene is very well-described by a simple tight-binding model, and the EPI has already been benchmarked in [58] to be well-described by the approximation used here.

Harmonic theory of phonons and Goldstone sum rules.—Consider a generic multipartite lattice in D dimensions, with N_{τ} atoms in the unit cell. In the following, we will denote with $\mathbf{R}_{p\nu} \equiv \mathbf{R}_p + \boldsymbol{\tau}_{\nu} + \mathbf{u}_{p\nu} \in \mathbb{R}^D$ The position of the ions in the lattice, where \mathbf{R}_p is a Bravais lattice vector labeled by an integer $p = 1, \dots, N$ in a finite N -unit-cell Born-von Karman (BvK) supercell [19], $\boldsymbol{\tau}_{\nu}$ is a basis vector in the $\mathbf{R}_p = \mathbf{0}$ unit cell labeled by a sublattice number $\nu = 1, \dots, N_{\tau}$, and $\mathbf{u}_{p\nu}$ is the displacement of an ion from its equilibrium position $\mathbf{R}_{p\nu}^0 \equiv \mathbf{R}_p + \boldsymbol{\tau}_{\nu}$.

Choosing a basis $\{\varphi_{\nu\alpha}(\mathbf{r})\}$ of sufficiently localized wavefunctions, the second-quantized one-electron Hamiltonian in the modified [58] tight-binding model can be expressed as

$$\hat{\mathcal{H}}_e(\{\mathbf{u}_{p\nu}\}) = \sum_{p\nu\alpha} \sum_{p'\nu'\alpha'} t_{\nu\nu'}^{\alpha\alpha'}(\mathbf{R}_{p\nu} - \mathbf{R}_{p'\nu'}) \hat{c}_{p\nu\alpha}^{\dagger} \hat{c}_{p'\nu'\alpha'}, \quad (4)$$

where $\hat{c}_{p\nu\alpha}^{\dagger}$ creates an electron in a generic orbital state identified by an additional set of quantum numbers α (including e.g. spin or internal atomic degrees of freedom) on the lattice site $\mathbf{R}_{p\nu}^0$, and $t_{\nu\nu'}^{\alpha\alpha'}(\mathbf{r}) = [t(\mathbf{r})]_{\nu\nu'}^{\alpha\alpha'}$ denotes the matrix elements of the hopping matrix $t(\mathbf{r})$, which carries both sublattice and orbital indices. Each matrix element is a smooth hopping function satisfying $[t(-\mathbf{r})]_{\nu\nu'}^{\alpha\alpha'} = [t^*(\mathbf{r})]_{\nu'\nu}^{\alpha'\alpha}$ in order to guarantee the Hermiticity of $\hat{\mathcal{H}}_e(\{\mathbf{u}_{p\nu}\})$.

The Hamiltonian (4), the many-electron ground state $|\phi_{\{\mathbf{u}_{p\nu}\}}^{(0)}\rangle$, and the electronic contribution $\mathcal{E}_0(\{\mathbf{u}_{p\nu}\})$ to the ground-state energy,

$$\mathcal{E}_0(\{\mathbf{u}_{p\nu}\}) \equiv \langle \phi_{\{\mathbf{u}_{p\nu}\}}^{(0)} | \hat{\mathcal{H}}_e(\{\mathbf{u}_{p\nu}\}) | \phi_{\{\mathbf{u}_{p\nu}\}}^{(0)} \rangle, \quad (5)$$

depend parametrically on the set of displacements $\{\mathbf{u}_{p\nu}\}$ of the ions from their equilibrium positions. Both the ground state and the ground-state energy, as well as the Hamiltonian's excited eigenstates introduced below, are evaluated within the one-electron approximation. Generalizations to include electron-electron interactions could be possible in the spirit of density functional perturbation theory [19] but are beyond the scope of the present work.

The standard tight-binding formalism is recovered by employing the Born-Oppenheimer approximation (BOA) [1], where the ions are assumed to be frozen in a fixed configuration while solving for the electronic degrees of freedom. In the BOA, the classical ionic Hamiltonian can be expanded up to second order in the ionic

displacements (harmonic approximation) as follows:

$$\hat{\mathcal{H}}_{\text{ion}} = \sum_{p\nu} \frac{P_{p\nu}^2}{2M_\nu} + \frac{1}{2} \sum_{pp'} \sum_{\nu\nu'} \sum_{ij} [\mathcal{C}]_{p\nu i}^{p'\nu'j} u_{p\nu i} u_{p'\nu'j}, \quad (6)$$

where i, j are Cartesian indices and we have defined the inter-atomic force constants as

$$\begin{aligned} [\mathcal{C}]_{p\nu i}^{p'\nu'j} &\equiv [\mathcal{C}^{(\text{ion})}]_{p\nu i}^{p'\nu'j} + [\mathcal{C}^{(\text{el})}]_{p\nu i}^{p'\nu'j} \\ &= \left. \frac{\partial^2 \mathcal{V}}{\partial u_{p\nu i} \partial u_{p'\nu'j}} \right|_0 + \left. \frac{\partial^2 \mathcal{E}_0}{\partial u_{p\nu i} \partial u_{p'\nu'j}} \right|_0. \end{aligned} \quad (7)$$

This expression of the inter-atomic force constants highlights the natural separation into a term due to the ion-ion repulsive interactions, i.e. the first term in Eq. (7), and one which depends on the electronic degrees of freedom only, i.e. the second term in Eq. (7). Here and in what follows, the symbol $|_0$ denotes that the quantity A is evaluated in the mechanical equilibrium configuration, i.e. for $\{\mathbf{u}_{p\nu} = \mathbf{0}\}$. Consistently with the above mentioned one-electron approximation, the equilibrium-configuration ground state $|\phi_{\{\mathbf{0}\}}^{(0)}\rangle \equiv |\phi_{\{\mathbf{u}_{p\nu}=\mathbf{0}\}}^{(0)}\rangle$ is taken to be the non-interacting Fermi sea [62].

We are now ready to introduce the dynamical matrix, whose diagonalization results in the phonon dispersion. Indeed, the dispersion $\omega_\ell(\mathbf{q})$ of the ℓ -th phononic branch, where $\ell = 1, \dots, D \times N_\tau$ and \mathbf{q} is the phonon wave vector, is determined by the eigenvalue equation.

$$\sum_{\nu'j} [\mathcal{D}(\mathbf{q})]_{\nu i}^{\nu'j} w_{\nu'j}^{(\ell)}(\mathbf{q}) = \omega_\ell^2(\mathbf{q}) w_{\nu i}^{(\ell)}(\mathbf{q}). \quad (8)$$

Here, $w_{\nu}^{(\ell)}(\mathbf{q})$ is the ℓ -th normal mode of vibration and $[\mathcal{D}(\mathbf{q})]_{\nu i}^{\nu'j}$ is the *dynamical matrix* (DM):

$$[\mathcal{D}(\mathbf{q})]_{\nu i}^{\nu'j} \equiv \frac{1}{\sqrt{M_\nu M_{\nu'}}} \sum_p e^{-i\mathbf{q} \cdot (\mathbf{R}_p + \boldsymbol{\tau}_\nu - \boldsymbol{\tau}_{\nu'})} [\mathcal{C}]_{p\nu i}^{p'\nu'j}. \quad (9)$$

This is the key quantity of this work. It can be decomposed in the same fashion as in Eq. (7), i.e. $\mathcal{D}(\mathbf{q}) = \mathcal{D}^{(\text{ion})}(\mathbf{q}) + \mathcal{D}^{(\text{el})}(\mathbf{q})$, with the latter term depending exclusively on electronic degrees of freedom. As shown in App. II, due to the invariance under global translations of the entire crystal, both the complete DM and, separately, its ionic and electronic parts, obey the so-called acoustic sum rules [63]:

$$\sum_{\nu'} \sqrt{M_{\nu'}} [\mathcal{D}(\mathbf{0})]_{\nu i}^{\nu'j} = 0 \quad \forall \nu, i, j, \quad (10)$$

$$\sum_{\nu'} \sqrt{M_{\nu'}} [\mathcal{D}^{(\text{ion})}(\mathbf{0})]_{\nu i}^{\nu'j} = 0 \quad \forall \nu, i, j, \quad (11)$$

and

$$\sum_{\nu'} \sqrt{M_{\nu'}} [\mathcal{D}^{(\text{el})}(\mathbf{0})]_{\nu i}^{\nu'j} = 0 \quad \forall \nu, i, j. \quad (12)$$

These sum rules imply that the acoustic phonon modes, i.e. those eigenmodes $\mathbf{w}_\nu^{(\ell)}(\mathbf{q})$ in which atoms in the unit cell vibrate in phase with each other, have to be *Goldstones*, i.e. their frequency must go to zero in the long-wavelength limit $\mathbf{q} \rightarrow \mathbf{0}$. Indeed, when $\mathbf{q} = \mathbf{0}$, acoustic modes correspond to global translations of the lattice, which are part of the symmetry group of the crystal.

The purely electronic contribution to the force-constant matrix (7) can be calculated directly from Eq. (5)—see App. III—by exploiting the Hellmann-Feynman theorem [62] and its Epstein generalization [1]. The result is

$$[\mathcal{C}^{(\text{el})}]_{p\nu i}^{p'\nu'j} = [\mathcal{C}^{(\text{el},1)}]_{p\nu i}^{p'\nu'j} + [\mathcal{C}^{(\text{el},2)}]_{p\nu i}^{p'\nu'j}, \quad (13)$$

with

$$\begin{aligned} [\mathcal{C}^{(\text{el},1)}]_{p\nu i}^{p'\nu'j} &\equiv \sum_{m \neq 0} \frac{1}{\mathcal{E}_0 - \mathcal{E}_m} \left\langle \phi_{\{\mathbf{0}\}}^{(m)} \left| \partial_{p\nu i} \hat{\mathcal{H}}_e \right| \phi_{\{\mathbf{0}\}}^{(0)} \right\rangle \\ &\quad \times \left\langle \phi_{\{\mathbf{0}\}}^{(0)} \left| \partial_{p'\nu'j} \hat{\mathcal{H}}_e \right| \phi_{\{\mathbf{0}\}}^{(m)} \right\rangle + \text{H.c.}, \end{aligned} \quad (14)$$

$$[\mathcal{C}^{(\text{el},2)}]_{p\nu i}^{p'\nu'j} \equiv \left\langle \phi_{\{\mathbf{0}\}}^{(0)} \left| \partial_{p\nu i} \partial_{p'\nu'j} \hat{\mathcal{H}}_e \right| \phi_{\{\mathbf{0}\}}^{(0)} \right\rangle, \quad (15)$$

where $\partial_{p\nu i} \equiv \partial/\partial u_{p\nu i}$, $|\phi_{\{\mathbf{0}\}}^{(m)}\rangle$ with $m \neq 0$ is an excited state of $\hat{\mathcal{H}}_e(\{\mathbf{u}_{p\nu} = \mathbf{0}\})$ and \mathcal{E}_m is the associated eigenenergy.

Eqs. (14)-(15) have a very appealing physical interpretation. In calculating the electronic contribution to the force constants, one studies the response of the electronic Hamiltonian $\hat{\mathcal{H}}_e(\{\mathbf{u}_{p\nu}\})$ to a static displacement field $\mathbf{u}_{p\nu}$, for small displacements. The latter quantity plays the role of a time-independent vector potential $\mathbf{A}(\mathbf{r})$ [64] in the usual linear response theory for electronic systems coupled to the electromagnetic field [62]. In such an analogy, it is easy to recognize that two key operators entering Eqs. (14)-(15) are: i) the “paramagnetic” current operator

$$\hat{j}_{p\nu i} \equiv \left. \frac{\partial \hat{\mathcal{H}}_e}{\partial u_{p\nu i}} \right|_0, \quad (16)$$

which controls the first-order (i.e. linear) coupling between the electronic degrees of freedom and $\mathbf{u}_{p\nu}$, and ii) the “diamagnetic” tensor

$$\hat{\mathcal{T}}_{p\nu i}^{p'\nu'j} \equiv \left. \frac{\partial^2 \hat{\mathcal{H}}_e}{\partial u_{p\nu i} \partial u_{p'\nu'j}} \right|_0, \quad (17)$$

which controls the second-order coupling between the electronic degrees of freedom and $\mathbf{u}_{p\nu}$. Recognizing these operators in Eqs. (14)-(15) leads to the following identities:

$$[\mathcal{C}^{(\text{el},1)}]_{p\nu i}^{p'\nu'j} \equiv \chi_{j_{p\nu i} j_{p'\nu'j}}, \quad (18)$$

$$[\mathcal{C}^{(\text{el},2)}]_{p\nu i}^{p'\nu'j} \equiv \left\langle \phi_{\{\mathbf{0}\}}^{(0)} \left| \hat{\mathcal{T}}_{p\nu i}^{p'\nu'j} \right| \phi_{\{\mathbf{0}\}}^{(0)} \right\rangle, \quad (19)$$

where $\chi_{j_{p\nu i} j_{p'\nu' j}}$ is the “paramagnetic” contribution to the $T = 0$ current-current response function [62], in the static (i.e. $\omega = 0$) limit. We therefore conclude that Eq. (14) is simply $\chi_{j_{p\nu i} j_{p'\nu' j}}$ in the Lehmann representation [62], while Eq. (15) is the “diamagnetic” contribution. The sum of these two contributions appearing in Eq. (13), which is the force constant matrix, actually coincides with the *physical* current-current response function of the electronic system.

In light of this formal analogy, we can rederive the acoustic sum rule (12) in a manner that emphasizes the Goldstone nature of the acoustic branches. Indeed, it is clear that a finite physical electronic current cannot flow in response to a static and *uniform* displacement $\mathbf{u}_{p\nu} \equiv \mathbf{u} \ (\forall p, \nu)$ of all the atoms, which is simply a global translation of the lattice. Mathematically, this statement is translated into the so-called TRK sum rule [65]:

$$\sum_{p'\nu'} \left[\chi_{j_{p\nu i} j_{p'\nu' j}} + \left\langle \phi_{\{0\}}^{(0)} \left| \hat{T}_{p\nu i}^{p'\nu' j} \right| \phi_{\{0\}}^{(0)} \right\rangle \right] = 0, \quad (20)$$

which must hold $\forall p, \nu, i, j$. Eq. (20) is just the real-space version of the acoustic sum rule (12) for the electronic contribution to the force constants. In linear response theory to a static gauge field $\mathbf{A}(\mathbf{r})$ the TRK sum rule expresses the fact that a finite physical current cannot flow in response to a static and spatially-uniform vector potential $\mathbf{A}(\mathbf{r}) = \mathbf{A}$ since this constant field can be gauged away [66]. We refer the reader to Apps. III and IV for all the necessary technical details on the calculation of the electronic contribution to the DM, App. V for the construction of the formal analogy with linear response theory, and App. VI for the explicit proof of the TRK sum rule in a simple 1D toy model. Furthermore, in App. X we calculate the geometric group velocity renormalization for the acoustic mode in the case of the EFK model.

Quantum geometric terms in the dynamical matrix.—

We now proceed to single out the quantum geometric contribution to $\mathcal{D}^{(\text{el})}(\mathbf{q})$. As mentioned above, $\hbar\mathbf{k}$ has a sharp physical meaning in a crystal: it is the quasi-momentum of a Bloch electron and spans the FBZ. Each band, labeled by a discrete index n , can be interpreted as a separate manifold of states and is thus characterized by its own QGT, i.e. $\mathcal{Q}_{ij}^{(n)}(\mathbf{k})$. As shown in App. I, the QGT defined in Eq. (1) can be calculated from the following equivalent expression:

$$\mathcal{Q}_{ij}^{(n)}(\mathbf{k}) = \text{Tr} \left\{ \partial_{k_i} P_n(\mathbf{k}) [1 - P_n(\mathbf{k})] \partial_{k_j} P_n(\mathbf{k}) \right\}, \quad (21)$$

where $P_n(\mathbf{k})$ is the projection matrix onto a Bloch eigenvector [58, 67]. As the group velocity $\partial_{k_i} E_n(\mathbf{k})$ characterizes the dispersion properties of a band [1], the derivatives $\partial_{k_i} P_n(\mathbf{k})$ of the projector fully characterize the quantum geometric properties. For single-band systems, $P(\mathbf{k}) = 1$ is the only non-zero projector, leading to a trivial quantum geometry.

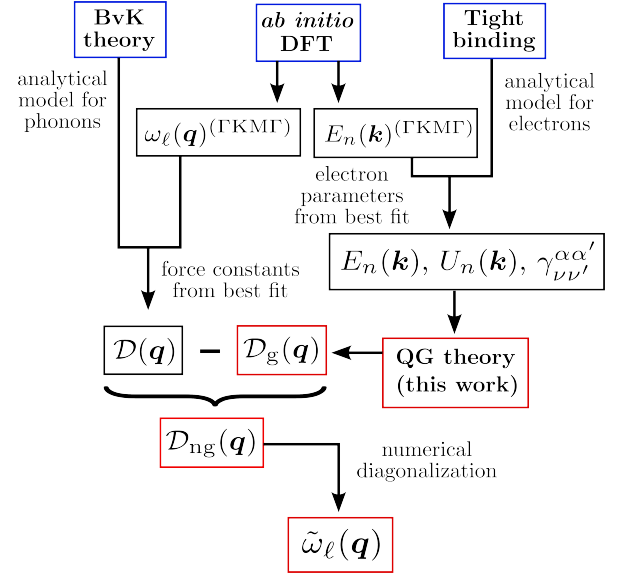


FIG. 2. (Color online) Workflow followed for the case of graphene. The same method can be applied to any material for which the relevant hopping integrals are well-described by the GA. Fitting the BvK model to *ab initio* data on the high-symmetry line ΓKMF allows us to extract the force constants and thus calculate the DM on the entire FBZ. The same fitting procedure is followed in order to obtain all the relevant information on electrons, thus allowing us to calculate the geometric contribution to the DM $\mathcal{D}_g(\mathbf{q})$, from which we obtained the phonon dispersion lines $\tilde{\omega}_\ell(\mathbf{q})$ illustrated in Figs. 1 and 4.

We now isolate the non-trivial geometric terms in the DM, i.e., the terms of the DM that would be zero in the case of bands with trivial quantum geometry. To this end, we exploit the same Gaussian approximation (GA) for the hopping amplitude $t_{\nu\nu'}^{\alpha\alpha'}(\mathbf{r})$ that was proposed and extensively discussed in Ref. [58], i.e. we take

$$t_{\nu\nu'}^{\alpha\alpha'}(\mathbf{r}) = t_{\nu\nu'}^{\alpha\alpha'}(\mathbf{0}) \exp\left(\gamma_{\nu\nu'}^{\alpha\alpha'} r^2/2\right), \quad (22)$$

with $\gamma_{\nu\nu'}^{\alpha\alpha'} \equiv [\gamma]_{\nu\nu'}^{\alpha\alpha'} < 0$. The theory described in this work relies on the GA for the hopping matrix elements and is, therefore, appropriate for materials whose hopping functions are well described by a spatial profile with a Gaussian shape. Within the GA, we are able to neatly separate the geometric contribution to the electronic force constants (13). We start from the Fourier transforms of the hopping matrix and of its derivatives, i.e. $h(\mathbf{k}) = \sum_p e^{-i\mathbf{k}\cdot(\mathbf{R}_p + \boldsymbol{\tau}_\nu - \boldsymbol{\tau}_{\nu'})} t(\mathbf{r})|_{\mathbf{R}_p + \boldsymbol{\tau}_\nu - \boldsymbol{\tau}_{\nu'}}$, $f_i(\mathbf{k}) = \sum_p e^{-i\mathbf{k}\cdot(\mathbf{R}_p + \boldsymbol{\tau}_\nu - \boldsymbol{\tau}_{\nu'})} \partial_{r_i} t(\mathbf{r})|_{\mathbf{R}_p + \boldsymbol{\tau}_\nu - \boldsymbol{\tau}_{\nu'}}$ and $M_{ij}(\mathbf{k}) = \sum_p e^{-i\mathbf{k}\cdot(\mathbf{R}_p + \boldsymbol{\tau}_\nu - \boldsymbol{\tau}_{\nu'})} \partial_{r_i r_j}^2 t(\mathbf{r})|_{\mathbf{R}_p + \boldsymbol{\tau}_\nu - \boldsymbol{\tau}_{\nu'}}$. The key property of the GA is that the following identities hold true [67]: $\partial_{r_i} t(\mathbf{r}) = \gamma r_i t(\mathbf{r})$ and $\partial_{r_i r_j}^2 t(\mathbf{r}) = (\gamma \delta_{ij} + \gamma^2 r_i r_j) t(\mathbf{r})$. We thus obtain the following results, which

hold within the framework of the GA:

$$f_i(\mathbf{k}) = i\gamma\partial_{k_i}h(\mathbf{k}) , \quad (23)$$

$$M_{ij}(\mathbf{k}) = (\gamma\delta_{ij} - \gamma^2\partial_{k_i}\partial_{k_j})h(\mathbf{k}) . \quad (24)$$

The Bloch Hamiltonian $h(\mathbf{k})$ defines both the energy bands $E_n(\mathbf{k})$ and the Bloch eigenvectors $U_n(\mathbf{k})$ via the eigenvalue equation $h(\mathbf{k})U_n(\mathbf{k}) = E_n(\mathbf{k})U_n(\mathbf{k})$, thus providing the following explicit form $P_n(\mathbf{k}) = U_n(\mathbf{k})U_n^\dagger(\mathbf{k})$ for the projection matrices. Identities (23) and (24), together with the spectral decomposition $h(\mathbf{k}) = \sum_n E_n(\mathbf{k})P_n(\mathbf{k})$, allow us to decompose $f_i(\mathbf{k})$ and $M_{ij}(\mathbf{k})$ into dispersive (or energetic) and geometric parts. For $f_i(\mathbf{k})$, we have $f_i(\mathbf{k}) = f_i^E(\mathbf{k}) + f_i^G(\mathbf{k})$, with

$$f_i^E(\mathbf{k}) = i\gamma\sum_n \partial_{k_i}E_n(\mathbf{k})P_n(\mathbf{k}) , \quad (25)$$

$$f_i^G(\mathbf{k}) = i\gamma\sum_n E_n(\mathbf{k})\partial_{k_i}P_n(\mathbf{k}) . \quad (26)$$

The quantity $f_i^G(\mathbf{k})$ is the geometric contribution to $f_i(\mathbf{k})$ [58], since it arises due to the momentum dependence of $P_n(\mathbf{k})$ and is zero in the case of trivial geometry. The term $f_i^E(\mathbf{k})$, on the other hand, is a *dispersive* term, as it scales with the group velocity and is zero in the case of a perfectly flat band. The Fourier transform $M_{ij}(\mathbf{k})$ of the Hessian tensor is decomposed in the same fashion, as shown in detail in App. VII. While the geometric nature of the gradient $f_i(\mathbf{k})$ of the Bloch Hamiltonian has been discussed at length in Ref. [58]—where it was shown that $f_i(\mathbf{k})$ controls the strength of the EPI—in this work we deal with higher-order contributions contained in the Hessian tensor $M_{ij}(\mathbf{k})$, which scale as the second-order derivatives $\partial_{k_i}\partial_{k_j}P_n(\mathbf{k})$ of the projection matrix. While these are obviously recognizable as non-trivial geometric terms, they do not enter the QGT. This suggests the intriguing possibility that higher-order geometric structures have a role in defining the properties of crystals [68].

The purely electronic contribution to the force-constant matrix in Eq. (13) is a function of Hamiltonian derivatives only. Inserting the different contributions (25)-(26) to $f_i(\mathbf{k})$ into Eqs. (14)-(15) and doing the same for $M_{ij}(\mathbf{k})$, we can decompose the purely electronic part of the DM, $\mathcal{D}^{(\text{el})}(\mathbf{q})$, which has been introduced immediately after Eq. (9) into the sum of non-geometric and geometric contributions: $\mathcal{D}^{(\text{el})}(\mathbf{q}) = \mathcal{D}_{\text{ng}}^{(\text{el})}(\mathbf{q}) + \mathcal{D}_{\text{g}}(\mathbf{q})$. Here, $\mathcal{D}_{\text{g}}(\mathbf{q})$ is the non-trivial geometric contribution to the DM, which is solely of electronic nature and therefore has no ionic contribution, while $\mathcal{D}_{\text{ng}}^{(\text{el})}(\mathbf{q})$ is that part of the electronic term in the DM which would be non-zero also in the case of a trivial quantum geometry. The entire DM can thus be decomposed as

$$\mathcal{D}(\mathbf{q}) = \mathcal{D}_{\text{ng}}(\mathbf{q}) + \mathcal{D}_{\text{g}}(\mathbf{q}) , \quad (27)$$

where $\mathcal{D}_{\text{ng}}(\mathbf{q}) \equiv \mathcal{D}^{(\text{ion})}(\mathbf{q}) + \mathcal{D}_{\text{ng}}^{(\text{el})}(\mathbf{q})$. Explicit expressions for the geometric contribution $\mathcal{D}_{\text{g}}(\mathbf{q})$ to the DM

are provided in App. VII. Additionally, we demonstrate in Appendix VII that $\mathcal{D}_{\text{g}}(\mathbf{q})$ and $\mathcal{D}_{\text{ng}}^{(\text{el})}(\mathbf{q})$ each satisfy the sum rule.

Graphene as a case study.—The calculation of the geometric contribution to the phonons in graphene proceeds as schematized in Fig. 2. The DM is calculated analytically within a next-nearest-neighbor (NNN) BvK model [69], leaving the force constants as free parameters. The force constants are then determined by fitting the analytical results to *ab initio* density functional perturbation theory (DFPT) [70] calculations along the high-symmetry $\Gamma\text{K}\Gamma$ path. Details on the *ab initio* calculations can be found in App. VIII and Refs. [71–79].

The electronic Hamiltonian is calculated analytically by using a linear combination of atomic orbitals (LCAO) within the next-next-nearest-neighbor (NNNN) tight-binding approximation, leaving hopping and overlap integrals as free parameters [80]. These are in turn determined by fitting the analytical model to *ab initio* density functional theory (DFT) data on the $\Gamma\text{K}\Gamma$ high-symmetry path. This allows us to reconstruct the Hamiltonian on the full FBZ, thus obtaining, by means of numerical diagonalization, all the information on the π bands and their geometric structure, i.e., the energy bands $E_{\pm}(\mathbf{k})$ and the Bloch eigenvectors $U_{\pm}(\mathbf{k})$, where the subscript $+$ ($-$) denotes the conduction (valence) band. Only these two bands are considered in this calculation, as the hopping integrals that generate them are very well-described by the GA, as shown in App. VIII. We therefore fix $\alpha = \alpha' = p_z$ and omit orbital labels from here on. The spatial dependence of $t_{AA}(\mathbf{r})$ and $t_{AB}(\mathbf{r})$, where A and B are sublattice labels, is obtained by repeating the best-fit procedure to determine the hopping integrals on a strained lattice, i.e. a graphene lattice on which a lattice constant different from that of the relaxed structure has been imposed.

Before presenting our primary numerical results, it is essential to examine the peculiarities of quantum geometry in graphene. The relevant quantum number in this material is the sublattice label, commonly referred to as the *pseudospin* [81]. Bloch states corresponding to the π bands at a fixed wave vector \mathbf{k} are obtained by producing a linear combination of states localized on the A and B sublattices. Due to this superposition, the quantum geometry of graphene exhibits nontrivial characteristics [27]. However, the singularity in the energy gradient at the Dirac points—i.e. at the \mathbf{K} and \mathbf{K}' points in the FBZ—gives rise to an infrared singularity in the \mathbf{k} -derivatives of the projection matrices, specifically $\nabla_{\mathbf{k}}P_n(\mathbf{k}) \sim 1/k$, rendering the QGT (21) ill-defined. To address this issue, we propose a natural regularization by introducing a small energy shift Δ for the p_z orbitals localized on A -type sublattice sites with respect to that of the B -type sublattice sites. This staggered potential breaks inversion symmetry (as in the case of graphene aligned to hBN [82]) and opens a gap Δ be-

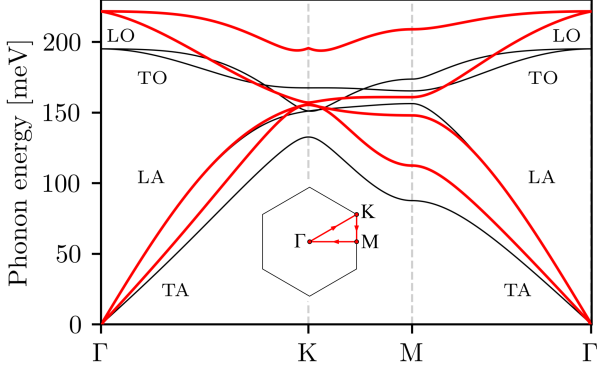


FIG. 3. (Color online) Black lines: Phonon dispersions in graphene along ΓKMF , calculated as in Fig. 1. Red lines: eigenvalues of $\mathcal{D}(\mathbf{q}) - \mathcal{D}^{(\text{el})}(\mathbf{q})$. The acoustic modes still behave linearly in $|\mathbf{q}|$ for $\mathbf{q} \rightarrow \Gamma$ after the removal of the electronic contribution to the dynamical matrix.

tween the two π bands, thereby generating a finite Semenoff mass [81]. The trace of the Fubini-Study metric and the Berry curvature for Semenoff-gapped graphene are shown in App. VIII. We now examine the electronic contribution to the dynamical matrix of graphene. Our analysis begins with the contribution from a single gapless Dirac cone, where analytical results can be explicitly derived. To this end, we consider the following effective Hamiltonian, which describes the behavior of the gapless Dirac node:

$$h(\mathbf{k}) = \hbar v_F \begin{pmatrix} 0 & k_x - ik_y \\ k_x + ik_y & 0 \end{pmatrix}, \quad (28)$$

We consider the total electronic contribution to the acoustic modes from the gapless Dirac cone. Specifically, we denote the geometric contribution as $[\mathcal{D}_g^{\text{ac}}(\mathbf{q})]$ and the total electronic contribution as $[\mathcal{D}_{\text{el}}^{\text{ac}}(\mathbf{q})]$:

$$\begin{aligned} [\mathcal{D}_g^{\text{ac}}(\mathbf{q})]_i^j &\equiv \sum_{\nu\nu'} [v^{\text{ac}}]_{\nu}^* [\mathcal{D}_g(\mathbf{q})]_{\nu i}^{\nu' j} [v^{\text{ac}}]_{\nu'}^{\nu}, \\ [\mathcal{D}_{\text{el}}^{\text{ac}}(\mathbf{q})]_i^j &\equiv \sum_{\nu\nu'} [v^{\text{ac}}]_{\nu}^* [\mathcal{D}^{(\text{el})}(\mathbf{q})]_{\nu i}^{\nu' j} [v^{\text{ac}}]_{\nu'}^{\nu}. \end{aligned} \quad (29)$$

where the superscript “ac” denotes the dynamical matrix projected onto the acoustic branches (see App. IX), and $i, j \in \{x, y\}$. The vector $[v^{\text{ac}}]_{\nu} = \frac{1}{\sqrt{2}}$ characterizes the wavefunction of the acoustic mode. Given that the unit cell of graphene contains only two atoms of equal mass, the vector v^{ac} assumes the same value for all its components.

Analytically, we find $[\mathcal{D}_{\text{el}}^{\text{ac}}(\mathbf{q})]_i^j = 0$ as we have proved in App. IX. Therefore, the total electronic contributions to the dynamical matrix of acoustic mode vanishes. We now turn to the geometric contribution $[\mathcal{D}_g^{\text{ac}}(\mathbf{q})]$. Unlike the total contributions, the geometric contribution $[\mathcal{D}_g^{\text{ac}}(\mathbf{q})]$ is non-zero. However, since the total contribu-

tion vanishes, this indicates that the geometric and non-geometric contributions cancel each other. Analytically, we observe that the geometric contribution exhibits non-analytical behavior. To illustrate such a non-analyticity, we consider the case of $\mathbf{q} = (q_x, 0)$, and as we proved in App. IX, we find $[\mathcal{D}_{\text{el}}^{\text{ac}}((q_x, 0))]_i^j \propto |q_x|$. Thus, the dispersion of the acoustic mode behaves like $\sqrt{|q_x|}$.

The non-analyticity arises from the singular behaviors induced by the gapless Dirac node and can be regularized by introducing a finite fermion mass. We, therefore, also provide the result for the gapped Dirac node

$$h^{(\Delta)}(\mathbf{k}) = \begin{pmatrix} \Delta/2 & \hbar v_F(k_x - ik_y) \\ \hbar v_F(k_x + ik_y) & -\Delta/2 \end{pmatrix}, \quad (30)$$

where $\Delta/2$ is the Semenoff mass. Similar to the case of gapless Dirac node, the total contribution $[\mathcal{D}_{\text{el}}^{\text{ac}}(\mathbf{q})]_i^j = 0$ vanishes. For the electronic contribution, we have

$$[\mathcal{D}_g^{\text{ac}}(\mathbf{q})]_i^j \approx \frac{-8\gamma^2\pi\hbar^2v_F^2}{15\Delta M_C\Omega} \begin{pmatrix} 3q_x^2 + q_y^2 & 2q_xq_y \\ 2q_xq_y & 3q_y^2 + q_x^2 \end{pmatrix}, \quad (31)$$

where M_C is the mass of carbon atom, and Ω is the area of the Brillouin zone. We observe that the leading-order contribution is of order \mathbf{q}^2 , as in the complete dynamical matrix. The coefficient of the leading-order contribution is proportional to $1/\Delta$, reflecting the non-analytic behavior of the geometric contribution in the case of the gapless Dirac node ($\Delta \rightarrow 0$).

We have, at this point, an analytic understanding of the quantum geometric contribution for the cases of gapless and gapped Dirac nodes. We now turn to the discussion of the full phonon spectrum of graphene, considering a realistic tight-binding model rather than the simplified Dirac Hamiltonian.

The tight-binding model is constructed by fitting GA parameters from *ab initio* data. Subsequently, we numerically evaluate both the geometric and total electronic contributions to the dynamical matrix. To capture the singular behavior at the Dirac node, we introduce a finite value for Δ , which characterizes the sublattice energy difference and introduces a finite gap at the Dirac point K.

We first explore the total electronic contributions. As shown numerically in Fig. 3, we find that these contributions result in only a small renormalization of the acoustic mode's dispersion. Since the Dirac node does not alter the behaviors of the acoustic modes, the contribution due to high-energy spectrum of graphene, which cannot be described by a simple Dirac node Hamiltonian, leads to a weak renormalization of the acoustic mode (within 20% change in velocity).

In Fig. 1, we show the phonon spectrum with the geometric contribution removed. A zoom-in plot for the acoustic modes, along the ΓK contour line for different values of Δ , is shown in Fig. 4. Similar behaviors in the acoustic modes have also been found along ΓM

line, as discussed in App. VIII. For a relatively large Δ ($= 0.5$ eV), we observe the conventional linear-in- q long-wavelength behavior of the acoustic mode dispersion, as shown in Fig. 4 (a). For a small value of Δ ($= 0.01$ eV), the acoustic mode follows a $\sqrt{|q|}$ -like dispersion, starting from a very small value of $|q| \sim 10^{-2} [\text{\AA}]^{-1}$ (which is the smallest non-zero momentum we picked in our numerical calculations), as demonstrated in Fig. 4(b). The threshold wavevector for which we can distinguish the two regimes can be inferred to be of the order of $q_{\text{thr}} = \Delta/\hbar v_F$, as shown in Fig. 4(a)-(b). We note that the symmetry of the phonon spectrum [83] is preserved when either the electronic or geometric contribution is removed, as evidenced by the retention of the twofold degenerate bands at Γ and K (see Figs. 1 and 3). Although a nonzero Δ breaks inversion symmetry and, in principle, gaps the twofold degeneracy at K, this effect is negligible for small Δ . We conclude that our numerical and analytical results are consistent with each other.

Summary. In this article, we explored the electronic contribution to the dynamical matrix within the framework of the Gaussian approximation. We demonstrated that this contribution can be divided into geometric and non-geometric components, that we found to individually satisfy acoustic sum rules. Using graphene as a case study, we examined the behavior of these contributions to the acoustic mode through both analytical and numerical methods. We found that the geometric contribution behaves in a highly non-analytical fashion in the long-wavelength limit $q \rightarrow 0$, while the total electronic contributions remains regular at every q . This indicates a cancellation between the non-analytical terms of the geometric and non-geometric contributions. Additionally, we found that the total electronic contribution to the acoustic mode from a gapless Dirac node with linear dispersion vanishes. However, in a realistic tight-binding model, high-energy electrons, which are not captured by the simple gapless Dirac Hamiltonian, can still contribute nonzero terms, leading to a weak renormalization of the velocity of the acoustic mode.

Acknowledgments.—G. P. and M. P. wish to thank Angelo Esposito for useful and inspiring discussions. This work was supported by the MUR - Italian Ministry of University and Research under the “Research projects of relevant national interest - PRIN 2020” - Project No. 2020JLZ52N (“Light-matter interactions and the collective behavior of quantum 2D materials, q-LIMA”) and by the European Union under grant agreements No. 101131579 - Exqiral and No. 873028 - Hydrotronics. Views and opinions expressed are however those of the author(s) only and do not necessarily reflect those of the European Union or the European Commission. Neither the European Union nor the granting authority can be held responsible for them. B.A.B. and H.H. were supported by the Gordon and Betty Moore Foundation through Grant No. GBMF8685 towards the Princeton

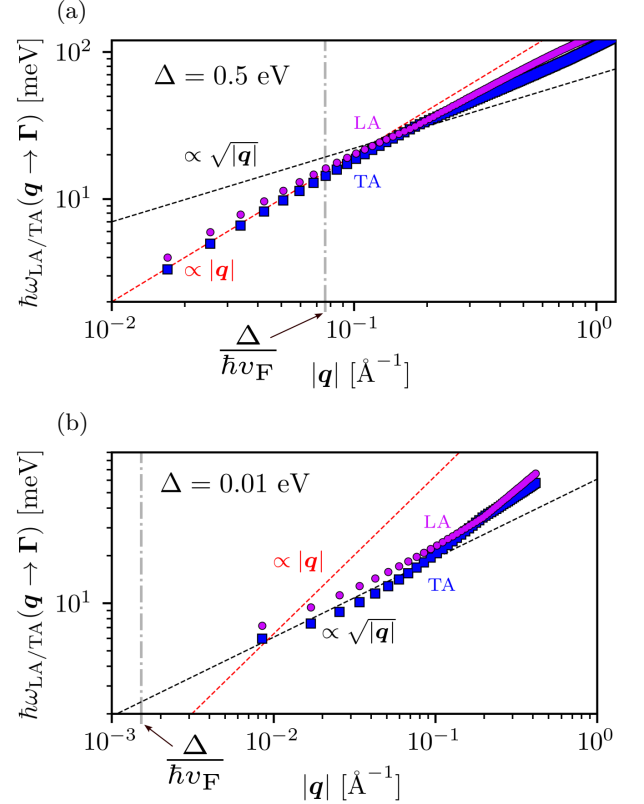


FIG. 4. (Color online) (a) The TA (blue squares) and LA (purple dots) modes, calculated for NNNN graphene, are shown to behave linearly for $q \rightarrow \Gamma$, as described by the analytics for the case of a gapped Dirac node. The dashed lines are guides-to-the-eye that illustrate linear and $\propto \sqrt{|q|}$ trends. The electronic gap $\Delta = 0.5$ eV is exaggerated for illustrative purposes. (b) Same plot for an electronic gap $\Delta = 10$ meV, showing the behavior of TA and LA modes: the dispersion of the TA/LA modes follows a $\propto \sqrt{|q|}$ trend, as described by the massless fermion theory. We note that the considered wavevectors belong to the $K \rightarrow \Gamma$ fraction of the high-symmetry contour, but that the similar behavior has been found along $M \rightarrow \Gamma$ line, as shown in App. IX. The dashed-dotted grey line indicates the threshold value $|q| = q_{\text{thr}} = \Delta/\hbar v_F$.

theory program, the Gordon and Betty Moore Foundation’s EPIQS Initiative (Grant No. GBMF11070), the Office of Naval Research (ONR Grant No. N00014-20-1-2303), the Global Collaborative Network Grant at Princeton University, the Simons Investigator Grant No. 404513, the BSF Israel US foundation No. 2018226, the NSF-MERSEC (Grant No. MERSEC DMR 2011750), the Simons Collaboration on New Frontiers in Superconductivity (Grant No. SFI-MPS-NFS-00006741-01), and the Schmidt Foundation at the Princeton University. Y.J. was supported by the European Research Council (ERC) under the European Union’s Horizon 2020 research and innovation program (Grant Agreement No. 101020833), as well as by the IKUR Strategy under the

collaboration agreement between Ikerbasque Foundation and DIPIC on behalf of the Department of Education of the Basque Government.

* guglielmo.pellitteri@sns.it

- [1] G. Grosso and G. Pastori Parravicini, *Solid State Physics*, 2nd edition (Academic Press, Oxford, 2014).
- [2] M. P. Marder, *Condensed Matter Physics*, 2nd edition (John Wiley & Sons, Inc., New Jersey, 2010).
- [3] M. Tinkham, *Introduction to Superconductivity*, 2nd edition (Dover Publications, New York, 2004).
- [4] A. K. Geim and I. V. Grigorieva, Van der Waals heterostructures *Nature* **499**, 419 (2013).
- [5] L. Wang, I. Meric, P. Y. Huang, Q. Gao, Y. Gao, H. Tran, T. Taniguchi, K. Watanabe, L. M. Campos, D. A. Muller, J. Guo, P. Kim, J. Hone, K.L. Shepard, and C. R. Dean, One-dimensional electrical contact to a two-dimensional material, *Science* **342**, 614 (2013).
- [6] N. Mounet and N. Marzari, First-principles determination of the structural, vibrational and thermodynamic properties of diamond, graphite, and derivatives, *Phys. Rev. B* **71**, 205214 (2005).
- [7] A. C. Ferrari, J. C. Meyer, V. Scardaci, C. Casiraghi, M. Lazzeri, F. Mauri, S. Piscanec, D. Jiang, K. S. Novoselov, S. Roth, and A. K. Geim, Raman spectrum of graphene and graphene layers, *Phys. Rev. Lett.* **97**, 187401 (2006).
- [8] A. C. Ferrari, Raman spectroscopy of graphene and graphite: Disorder, electron-phonon coupling, doping and nonadiabatic effects, *Solid State Commun.* **143**, 47 (2007).
- [9] D. L. Nika and A. A. Balandin, Two-dimensional phonon transport in graphene, *J. Phys. Condens. Matter* **24**, 233203 (2012).
- [10] A. C. Ferrari and D. Basko, Raman spectroscopy as a versatile tool for studying the properties of graphene, *Nat. Nanotech.* **8**, 235 (2013).
- [11] A. Principi, M. Carrega, M. B. Lundeberg, A. Woessner, F. H. L. Koppens, G. Vignale, and M. Polini, Plasmon losses due to electron-phonon scattering: The case of graphene encapsulated in hexagonal boron nitride. *Phys. Rev. B* **90**, 165408 (2014).
- [12] A. Woessner, M. B. Lundeberg, Y. Gao, A. Principi, P. Alonso-González, M. Carrega, K. Watanabe, T. Taniguchi, G. Vignale, M. Polini, J. Hone, R. Hillenbrand, and F. H. L. Koppens, Highly confined low-loss plasmons in graphene-boron nitride heterostructures, *Nat. Mater.* **14**, 421 (2015).
- [13] M. B. Lundeberg, Y. Gao, R. Asgari, C. Tan, B. Van Duppen, M. Autore, P. Alonso-González, A. Woessner, K. Watanabe, T. Taniguchi, R. Hillenbrand, J. Hone, M. Polini, and F. H. L. Koppens, Tuning quantum nonlocal effects in graphene plasmonics, *Science* **357**, 187 (2017).
- [14] G. X. Ni, A. S. McLeod, Z. Sun, L. Wang, L. Xiong, K. W. Post, S. S. Sunku, B.-Y. Jiang, J. Hone, C. R. Dean, M. M. Fogler, and D. N. Basov, Fundamental limits to graphene plasmonics, *Nature* **557**, 530 (2018).
- [15] H. Leutwyler, Phonons as Goldstone bosons, *Helv. Phys. Acta* **70**, 275 (1997).
- [16] S. Endlich, A. Nicolis, and J. Wang, Solid inflation, *J. Cosmol. Astropart. Phys.* **10**, 011 (2013).
- [17] A. Nicolis, R. Penco, F. Piazza, and R. Rattazzi, Zoology of condensed matter: framids, ordinary stuff, extraordinary stuff, *J. High Energ. Phys.* **2015**, 155 (2015).
- [18] A. Esposito, E. Geoffray, and T. Melia, Effective field theory for acoustic and pseudoacoustic phonons in solids, *Phys. Rev. D* **102**, 105009 (2020).
- [19] F. Giustino, Electron-phonon interactions from first principles, *Rev. Mod. Phys.* **89**, 015003 (2017).
- [20] M. Engel, M. Marsman, C. Franchini, and G. Kresse, Electron-phonon interactions using the projector augmented-wave method and Wannier functions, *Phys. Rev. B* **101**, 184302 (2020).
- [21] J. Li, J. Li, J. Tang, Z. Tao, S. Xue, J. Liu, H. Peng, X.-Q. Chen, J. Guo, and X. Zhu, Direct observation of topological phonons in graphene, *Phys. Rev. Lett.* **131**, 116602 (2023).
- [22] Y. Xu, M. G. Vergniory, D.-S. Ma, J. L. Mañes, Z.-D. Song, B. A. Bernevig, N. Regnault, and L. Elcoro, Catalog of topological phonon materials, *Science* **384**, 638 (2024).
- [23] R. Resta, Manifestations of Berry's phase in molecules and condensed matter, *J. Phys. Condens. Matter* **12**, R107 (2000).
- [24] D. Vanderbilt, *Berry Phases in Electronic Structure Theory* (Cambridge University Press, Cambridge, 2018).
- [25] D. Xiao, M.-C. Chang, and Q. Niu, Berry phase effects on electronic properties, *Rev. Mod. Phys.* **82**, 1959 (2010).
- [26] B. A. Bernevig and T. L. Hughes, *Topological Insulators and Topological Superconductors* (Princeton University Press, Princeton and Oxford, 2013).
- [27] P. Törmä, Essay: where can quantum geometry lead us?, *Phys. Rev. Lett.* **131**, 240001 (2023).
- [28] J. Yu, B. A. Bernevig, R. Queiroz, E. Rossi, P. Törmä, and B.-J. Yang, Quantum geometry in quantum materials, [arXiv:2501.00098](https://arxiv.org/abs/2501.00098).
- [29] A. Bouhon, A. Timmel, and R.-J. Slager, Quantum geometry beyond projective single bands, [arXiv:2303.02180](https://arxiv.org/abs/2303.02180).
- [30] J. P. Provost and G. Vallee, Riemannian structure on manifolds of quantum states, *Comm. Math. Phys.* **76**, 289 (1980).
- [31] D. N. Page, Geometrical description of Berry's phase, *Phys. Rev. A* **36**, 3479 (1987).
- [32] J. Anandan and Y. Aharonov, Geometry of quantum evolution, *Phys. Rev. Lett.* **65**, 1697 (1990).
- [33] M. V. Berry, Quantal phase factors accompanying adiabatic changes, *Proc. R. Soc. London, Ser. A* **392**, 45 (1984).
- [34] See Supplemental Material for additional information on the QGT in crystals, proof of the acoustic sum rules, calculation of electronic force constants within the BOA, explicit formulas for the dynamical matrix, discussion of the analogy between phonon theory and linear response theory, proof of the TRK sum rule for a 1D toy model, isolation of non-trivial geometric terms via the Gaussian approximation, details on the application of the theory to graphene, and explicit analytical calculation of some terms in $\mathcal{D}_g(\mathbf{q})$ for massless Dirac fermions.
- [35] R. Resta and S. Sorella, Electron localization in the insulating state, *Phys. Rev. Lett.* **82**, 370 (1999).
- [36] I. Souza, T. Wilkens, and R. M. Martin, Polarization and localization in insulators: Generating function approach, *Phys. Rev. B* **62**, 1666 (2000).
- [37] R. Resta, The insulating state of matter: A geometrical

- theory, *Eur. Phys. J. B* **79**, 121 (2011).
- [38] M. F. Lapa and T. L. Hughes, Semiclassical wave packet dynamics in nonuniform electric fields, *Phys. Rev. B* **99**, 121111 (2019).
- [39] S. Kwon and B.-J. Yang, Quantum geometric bound and ideal condition for Euler band topology, *Phys. Rev. B* **109**, L161111 (2024).
- [40] W. J. Jankowski, A. S. Morris, A. Bouhon, F. N. Ünal, and R.-J. Slager, Optical manifestations and bounds of topological Euler class, *Phys. Rev. B* **111**, L081103 (2025).
- [41] Y. Onishi and L. Fu, Fundamental bound on topological gap, *Phys. Rev. X* **14**, 011052 (2024).
- [42] I. Komissarov, T. Holder, and R. Queiroz, The quantum geometric origin of capacitance in insulators, *Nat. Comm.* **15**, 4621 (2024).
- [43] N. Verma and R. Queiroz, Instantaneous response and quantum geometry of insulators, *arXiv:2403.07052*.
- [44] S. Peotta and P. Törmä, Superfluidity in topologically nontrivial flat bands, *Nat. Comm.* **6**, 8944 (2015).
- [45] J. S. Hofmann, E. Berg, and D. Chowdhury, Superconductivity, pseudogap, and phase separation in topological flat bands, *Phys. Rev. B* **102**, 201112 (2020).
- [46] J. Herzog-Arbeitman, A. Chew, K.-E. Huhtinen, P. Törmä, and B. A. Bernevig, Many-Body superconductivity in topological flat bands, *arXiv:2209.00007*.
- [47] E. Rossi, Quantum metric and correlated states in two-dimensional systems, *Curr. Opin. Solid State Mater. Sci.* **25**, 100952 (2021).
- [48] P. Törmä, S. Peotta, and B. A. Bernevig, Superconductivity, superfluidity and quantum geometry in twisted multilayer systems, *Nat. Rev. Phys.* **4**, 528 (2022).
- [49] S. Peotta, K.-E. Huhtinen, and P. Törmä, Quantum geometry in superfluidity and superconductivity, *arXiv:2308.08248*.
- [50] J. S. Hofmann, E. Berg, and D. Chowdhury, Superconductivity, charge density wave, and supersolidity in flat bands with a tunable quantum metric, *Phys. Rev. Lett.* **130**, 226001 (2023).
- [51] A. Kruchkov, Quantum transport anomalies in dispersionless quantum states, *Phys. Rev. B* **107**, L241102 (2023).
- [52] J. Ahn, G.-Y. Guo, N. Nagaosa, and A. Vishwanath, Riemannian geometry of resonant optical responses, *Nat. Phys.* **18**, 290 (2021).
- [53] C.-R. Yi, J. Yu, H. Yuan, R.-H. Jiao, Y.-M. Yang, X. Jiang, J.-Y. Zhang, S. Chen, and J.-W. Pan, Extracting the quantum geometric tensor of an optical Raman lattice by Bloch-state tomography, *Phys. Rev. Res.* **5**, L032016 (2023).
- [54] M. Yu, P. Yang, M. Gong, Q. Cao, Q. Lu, H. Liu, S. Zhang, M. B. Plenio, F. Jelezko, T. Ozawa, N. Goldman, and J. Cai, Experimental measurement of the quantum geometric tensor using coupled qubits in diamond, *Nat. Sci. Rev.* **7**, 254 (2019).
- [55] W. Zheng, J. Xu, Z. Ma, Y. Li, Y. Dong, Y. Zhang, X. Wang, G. Sun, P. Wu, J. Zhao, S. Li, D. Lan, X. Tan, and Y. Yu, Measuring quantum geometric tensor of non-Abelian system in superconducting circuits, *Chin. Phys. Lett.* **39**, 100202 (2022).
- [56] A. Gianfrate, O. Bleu, L. Dominici, V. Ardizzone, M. De Giorgi, D. Ballarini, G. Lerario, K. W. West, L. N. Pfeiffer, D. D. Solnyshkov, D. Sanvitto, and G. Malpuech, Measurement of the quantum geometric tensor and of the anomalous Hall drift, *Nature* **578**, 381 (2020).
- [57] R. K. Kumar, G. Li, R. Bertini, S. Chaudhary, K. Nowakowski, J. M. Park, S. Castilla, Z. Zhan, P. A. Pantaleón, H. Agarwal, S. Battle-Porro, E. Icking, M. Ceccanti, A. Reserbat-Plantey, G. Piccinini, J. Barrier, E. Khestanova, T. Taniguchi, K. Watanabe, C. Stampfer, G. Refael, F. Guinea, P. Jarillo-Herrero, J. C. W. Song, P. Stepanov, C. Lewandowski, and F. H. L. Koppens, Terahertz photocurrent probe of quantum geometry and interactions in magic-angle twisted bilayer graphene, *arXiv:2406.16532*.
- [58] J. Yu, C. J. Ciccarino, R. Bianco, I. Errea, P. Narang, and B. A. Bernevig, Non-trivial quantum geometry and the strength of electron-phonon coupling, *Nat. Phys.* **20**, 1262 (2024).
- [59] T. Holstein, Studies of polaron motion: Part I. The molecular-crystal model, *Ann. Phys.* **8**, 325 (1959).
- [60] T. Holstein, Studies of polaron motion: Part II. The “small” polaron, *Ann. Phys.* **8**, 343 (1959).
- [61] J. Sous, B. Kloss, D. M. Kennes, D. R. Reichman, and A. J. Millis, Phonon-induced disorder in dynamics of optically pumped metals from nonlinear electron-phonon coupling, *Nat. Comm.* **12**, 5803 (2021).
- [62] G. F. Giuliani and G. Vignale, *Quantum Theory of the Electron Liquid* (Cambridge University Press, Cambridge, 2005).
- [63] X. Gonze and C. Lee, Dynamical matrices, Born effective charges, dielectric permittivity tensors, and interatomic force constants from density-functional perturbation theory, *Phys. Rev. B* **55**, 10355 (1997).
- [64] M. A. H. Vozmediano, M. I. Katsnelson, and F. Guinea, Gauge fields in graphene, *Phys. Rep.* **496**, 109 (2010).
- [65] J. J. Sakurai and J. Napolitano, *Modern Quantum Mechanics, 2nd edition* (Cambridge University Press, Cambridge, 2017).
- [66] G. M. Andolina, F. M. D. Pellegrino, V. Giovannetti, A. H. MacDonald, and M. Polini, Cavity quantum electrodynamics of strongly correlated electron systems: A no-go theorem for photon condensation, *Phys. Rev. B* **100**, 121109 (2019).
- [67] Throughout this work we have taken the liberty to omit orbital and sublattice indices when referring to the projection matrix $[P_n(\mathbf{k})]_{\nu\alpha}^{\nu'\alpha'}$ and the Bloch eigenvectors $[U_n(\mathbf{k})]_{\nu\alpha}$. These indices have instead been written down explicitly for the hopping matrix $[t(\mathbf{r})]_{\nu\alpha}^{\nu'\alpha'}$, the force-constant matrix $[C]_{p\nu i}^{p'\nu'j}$, and the DM $[D]_{\nu i}^{\nu'j}$. Other quantities defined in the following, such as the Bloch Hamiltonian $h(\mathbf{k})$ and its derivatives $f_i(\mathbf{k})$ and $M_{ij}(\mathbf{k})$, trivially inherit their matrix structure from the hopping matrix $t(\mathbf{r})$. Wherever the γ symbol appears in front of a matrix, e.g. $\gamma t(\mathbf{r})$, the product is intended to be element-wise, i.e. $[\gamma t(\mathbf{r})]_{\nu\alpha}^{\nu'\alpha'} = [\gamma]_{\nu\alpha}^{\nu'\alpha'} [t(\mathbf{r})]_{\nu\alpha}^{\nu'\alpha'}$ and $[\gamma^2 t(\mathbf{r})]_{\nu\alpha}^{\nu'\alpha'} = ([\gamma]_{\nu\alpha}^{\nu'\alpha'})^2 [t(\mathbf{r})]_{\nu\alpha}^{\nu'\alpha'}$. The same applies when $t(\mathbf{r}) \leftrightarrow h(\mathbf{k})$.
- [68] B. Hetényi and P. Lévy, Fluctuations, uncertainty relations, and the geometry of quantum state manifolds, *Phys. Rev. A* **108**, 032218 (2023).
- [69] L. Falkovsky, Phonon dispersion in graphene, *J. Exp. Theor. Phys.* **105**, 397 (2007).
- [70] S. Baroni, S. de Gironcoli, A. Dal Corso, and P. Giannozzi, Phonons and related crystal properties from density-functional perturbation theory, *Rev. Mod. Phys.* **73**, 515 (2001).

- [71] P. Giannozzi, S. Baroni, N. Bonini, M. Calandra, R. Car, C. Cavazzoni, D. Ceresoli, G. L. Chiarotti, M. Cococcioni, I. Dabo, A. Dal Corso, S. de Gironcoli, S. Fabris, G. Fratesi, R. Gebauer, U. Gerstmann, C. Gougousis, A. Kokalj, M. Lazzeri, L. Martin-Samos, N. Marzari, F. Mauri, R. Mazzarello, S. Paolini, A. Pasquarello, L. Paulatto, C. Sbraccia, S. Scandolo, G. Sclauzero, A. P. Seitsonen, A. Smogunov, P. Umari, and R. M. Wentzcovitch, QUANTUM ESPRESSO: a modular and open-source software project for quantum simulations of materials, *J. Phys. Condens. Matter* **21**, 395502 (2009).
- [72] P. Giannozzi, O. Andreussi, T. Brumme, O. Bunau, M. Buongiorno Nardelli, M. Calandra, R. Car, C. Cavazzoni, D. Ceresoli, M. Cococcioni, N. Colonna, I. Carnimeo, A. Dal Corso, S. de Gironcoli, P. Delugas, R. A. DiStasio, A. Ferretti, A. Floris, G. Fratesi, G. Fugallo, R. Gebauer, U. Gerstmann, F. Giustino, T. Gorni, J. Jia, M. Kawamura, H.-Y. Ko, A. Kokalj, E. Küçükbenli, M. Lazzeri, M. Marsili, N. Marzari, F. Mauri, N. L. Nguyen, H.-V. Nguyen, A. Otero-de-la-Roza, L. Paulatto, S. Poncé, D. Rocca, R. Sabatini, B. Santra, M. Schlipf, A. P. Seitsonen, A. Smogunov, I. Timrov, T. Thonhauser, P. Umari, N. Vast, X. Wu, and S. Baroni, Advanced capabilities for materials modelling with Quantum ESPRESSO, *J. Phys. Condens. Matter* **29**, 465901 (2017).
- [73] G. Prandini, A. Marrazzo, I. E. Castelli, N. Mounet, and N. Marzari, Precision and efficiency in solid-state pseudopotential calculations, *npj Comput. Mater.* **4**, 72 (2018).
- [74] A. Dal Corso, Pseudopotentials periodic table: From H to Pu, *Comput. Mater. Sci.* **95**, 337 (2014).
- [75] J. P. Perdew, K. Burke, and M. Ernzerhof, Generalized gradient approximation made simple, *Phys. Rev. Lett.* **77**, 3865 (1996).
- [76] S. Grimme, Semiempirical GGA-type density functional constructed with a long-range dispersion correction, *J. Comput. Chem.* **27**, 1787 (2006).
- [77] M. Methfessel and A. T. Paxton, High-precision sampling for Brillouin-zone integration in metals, *Phys. Rev. B* **40**, 3616 (1989).
- [78] H. J. Monkhorst and J. D. Pack, Special points for Brillouin-zone integrations, *Phys. Rev. B* **13**, 5188 (1976).
- [79] T. Sohler, M. Calandra, and F. Mauri, Density functional perturbation theory for gated two-dimensional heterostructures: Theoretical developments and application to flexural phonons in graphene, *Phys. Rev. B* **96**, 075448 (2017).
- [80] S. Reich, J. Maultzsch, C. Thomsen, and P. Ordejón, Tight-binding description of graphene, *Phys. Rev. B* **66**, 035412 (2002).
- [81] M. I. Katsnelson, *The Physics of Graphene*, 2nd edition (Cambridge University Press, Cambridge, 2020).
- [82] G. Giovannetti, P. A. Khomyakov, G. Brocks, V. M. Karpan, J. van den Brink, and P. J. Kelly, Substrate-induced band gap in graphene on hexagonal boron nitride: Ab initio density functional calculations, *Phys. Rev. B* **76**, 073103 (2007).
- [83] J. L. Mañes, Symmetry-based approach to electron-phonon interactions in graphene, *Phys. Rev. B* **76**, 045430 (2007).

Supplemental Material for: “Phonon spectra, quantum geometry, and the Goldstone theorem”

Guglielmo Pellitteri,^{1,*} Zenan Dai,² Haoyu Hu,³ Yi Jiang,⁴ Guido Menichetti,^{5,6} Andrea Tomadin,⁵ B. Andrei Bernevig^{3,4,7} and Marco Polini^{5,8}

¹*Scuola Normale Superiore, Piazza dei Cavalieri 7, I-56126 Pisa, Italy*

²*Zhiyuan College, Shanghai Jiao Tong University, Shanghai 200240, China*

³*Department of Physics, Princeton University, Princeton, New Jersey 08544, USA*

⁴*Donostia International Physics Center, P. Manuel de Lardizabal 4, 20018 Donostia-San Sebastian, Spain*

⁵*Dipartimento di Fisica dell'Università di Pisa, Largo Bruno Pontecorvo 3, I-56127 Pisa, Italy*

⁶*Istituto Italiano di Tecnologia, Graphene Labs, Via Morego 30, I-16163 Genova, Italy*

⁷*IKERBASQUE, Basque Foundation for Science, Maria Diaz de Haro 3, 48013 Bilbao, Spain*

⁸*ICFO-Institut de Ciències Fotòniques, The Barcelona Institute of Science and Technology, Av. Carl Friedrich Gauss 3, 08860 Castelldefels (Barcelona), Spain*

This Supplemental Material is organized into nine Appendices. In App. I, we briefly present some fundamental identities regarding the QGT in a crystal. In App. II, we give a proof of the acoustic sum rules for the interatomic force constants. In App. III, we show how to write the electronic part of the force-constant matrix in terms of derivatives of the electronic Hamiltonian only. In App. IV we derive explicit, general analytical formulas for the electronic part of the dynamical matrix of a crystal. App. V contains details on the construction of the formal analogy between phonon theory and linear response theory. In App. VI, we verify the TRK sum rule for a simple 1D toy model. App. VII is devoted to the isolation of nontrivial geometric terms in the dynamical matrix. In App. VIII, we further discuss the application of the theory to graphene. In App. IX, we calculate $\mathcal{D}_g(\mathbf{q})$ in the long-wavelength limit for the case of massive and massless Dirac fermions. In App. X, we derive the geometric dynamical matrix and the group velocity renormalization analytically for the EFK Hamiltonian.

Appendix I: The Quantum Geometric Tensor in solid-state systems

The problem of electrons in a periodic potential is described by the Hamiltonian

$$\hat{\mathcal{H}}_e = \frac{\hat{\mathbf{p}}^2}{2m_e} + \hat{V}(\mathbf{r}) \quad \text{with} \quad \hat{V}(\mathbf{r} + \mathbf{R}_{p\nu}^0) = \hat{V}(\mathbf{r}) , \quad (\text{I1})$$

where we have used the same notation for the lattice structure as in the main text. The eigenstates $\psi_{n\mathbf{k}}(\mathbf{r})$ of the Hamiltonian (I1) are of the Bloch type [S1], i.e. $\psi_{n\mathbf{k}}(\mathbf{r}) = e^{i\mathbf{k}\cdot\hat{\mathbf{r}}} u_{n\mathbf{k}}(\mathbf{r})$, with $u_{n\mathbf{k}}(\mathbf{r}) = u_{n\mathbf{k}}(\mathbf{r} + \mathbf{R}_{p\nu}^0)$. They are labeled by a discrete band number n and depend parametrically on the Bloch quasi-momentum $\mathbf{k} \in \text{FBZ}$. The crystal is therefore described by the Hamiltonian $\hat{\mathcal{H}}_e$ which does not explicitly depend on the Bloch quasi-momentum, with boundary conditions that do depend on it. To transition to a formulation where the boundary conditions remain \mathbf{k} -independent while the Hamiltonian retains its \mathbf{k} -dependence, it is useful to apply a momentum shift [S2]:

$$\hat{\mathcal{H}}_e \rightarrow \hat{\mathcal{H}}_e(\mathbf{k}) \equiv e^{-i\mathbf{k}\cdot\hat{\mathbf{r}}} \hat{\mathcal{H}}_e e^{i\mathbf{k}\cdot\hat{\mathbf{r}}} = \frac{(\hat{\mathbf{p}} + \hbar\mathbf{k})^2}{2m_e} + \hat{V}(\mathbf{r}) . \quad (\text{I2})$$

The eigenstates of the Hamiltonian (I2) reduce from being of the Bloch type to being only the periodic part of the Bloch wavefunction, i.e. they coincide with the quantity $u_{n\mathbf{k}}(\mathbf{r})$. This representation is well-suited to discuss topology and, more in general, quantum geometry.

As stated in the main text, in the case in which bands do *not* touch, the analysis of the geometry of wavefunctions requires the definition of a different QGT for each band [S3]:

$$\mathcal{Q}_{ij}^{(n)}(\mathbf{k}) = \text{Tr} \left\{ \partial_{k_i} \hat{P}_n(\mathbf{k}) \left[1 - \hat{P}_n(\mathbf{k}) \right] \partial_{k_j} \hat{P}_n(\mathbf{k}) \right\} , \quad (\text{I3})$$

where $\hat{P}_n(\mathbf{k}) \equiv |u_{n\mathbf{k}}\rangle\langle u_{n\mathbf{k}}|$ is the projection operator on the state $|u_{n\mathbf{k}}\rangle$. The expression (I3) of the QGT is appropriate for numerical calculations, as it does not require any type of gauge smoothing. Indeed, the projectors $\hat{P}_n(\mathbf{k})$ are

manifestly gauge-invariant. We note that, due to the presence of a Semenoff mass Δ acting as a regularizer in our description of the quantum geometry of graphene, we do not need to deal with band crossings.

We now show that the definition (I3) is equivalent to the original definition provided by Provost and Vallee [S4] and given in Eqs. (1)-(3) of the main text. We begin by transforming the projector-based expression (I3) into a formulation that explicitly incorporates an exact eigenstate representation:

$$\begin{aligned}
\mathcal{Q}_{ij}^{(n)}(\mathbf{k}) &= \text{Tr}\{\partial_{k_i} \left[|u_{n\mathbf{k}}\rangle\langle u_{n\mathbf{k}}| \right] \left[1 - |u_{n\mathbf{k}}\rangle\langle u_{n\mathbf{k}}| \right] \partial_{k_j} \left[|u_{n\mathbf{k}}\rangle\langle u_{n\mathbf{k}}| \right] \} \\
&= \sum_m \langle u_{m\mathbf{k}} | \left[|\partial_{k_i} u_{n\mathbf{k}}\rangle\langle u_{n\mathbf{k}}| + |u_{n\mathbf{k}}\rangle\langle \partial_{k_i} u_{n\mathbf{k}}| \right] \left[\sum_{l \neq n} |u_{l\mathbf{k}}\rangle\langle u_{l\mathbf{k}}| \right] \left[|\partial_{k_j} u_{n\mathbf{k}}\rangle\langle u_{n\mathbf{k}}| + |u_{n\mathbf{k}}\rangle\langle \partial_{k_j} u_{n\mathbf{k}}| \right] |u_{m\mathbf{k}}\rangle \\
&= \sum_m \langle u_{m\mathbf{k}} | u_{n\mathbf{k}}\rangle\langle \partial_{k_i} u_{n\mathbf{k}} | \left[\sum_{l \neq n} |u_{l\mathbf{k}}\rangle\langle u_{l\mathbf{k}}| \right] | \partial_{k_j} u_{n\mathbf{k}}\rangle\langle u_{n\mathbf{k}} | u_{m\mathbf{k}}\rangle \\
&= \sum_m \delta_{mn} \langle \partial_{k_i} u_{n\mathbf{k}} | \left[\sum_{l \neq n} |u_{l\mathbf{k}}\rangle\langle u_{l\mathbf{k}}| \right] | \partial_{k_j} u_{n\mathbf{k}}\rangle \delta_{nm} \\
&= \langle \partial_{k_i} u_{n\mathbf{k}} | \partial_{k_j} u_{n\mathbf{k}}\rangle - \langle \partial_{k_i} u_{n\mathbf{k}} | u_{n\mathbf{k}}\rangle\langle u_{n\mathbf{k}} | \partial_{k_j} u_{n\mathbf{k}}\rangle .
\end{aligned} \tag{I4}$$

Here, we used the completeness relation $\sum_n |u_{n\mathbf{k}}\rangle\langle u_{n\mathbf{k}}| = \mathbf{1}$ and orthogonality of the eigenstates, i.e. $\langle u_{n\mathbf{k}} | u_{m\mathbf{k}}\rangle = \delta_{nm}$, which are both valid at each fixed value of \mathbf{k} , as well as the definition of the trace on the parametric Hilbert space, $\text{Tr}[\dots] = \sum_m \langle u_{m\mathbf{k}} | \dots | u_{m\mathbf{k}}\rangle$, again valid at each fixed value of \mathbf{k} .

We now note that the second term in the last line of Eq. (I4) is real. We therefore have:

$$\text{Re } \mathcal{Q}_{ij}^{(n)}(\mathbf{k}) = \text{Re} \left[\langle \partial_{k_i} u_{n\mathbf{k}} | \partial_{k_j} u_{n\mathbf{k}}\rangle \right] - \langle \partial_{k_i} u_{n\mathbf{k}} | u_{n\mathbf{k}}\rangle\langle u_{n\mathbf{k}} | \partial_{k_j} u_{n\mathbf{k}}\rangle , \tag{I5a}$$

$$2i \text{Im } \mathcal{Q}_{ij}^{(n)}(\mathbf{k}) = \mathcal{Q}_{ij}^{(n)}(\mathbf{k}) - [\mathcal{Q}_{ij}^{(n)}(\mathbf{k})]^* = \langle \partial_{k_i} u_{n\mathbf{k}} | \partial_{k_j} u_{n\mathbf{k}}\rangle - \langle \partial_{k_j} u_{n\mathbf{k}} | \partial_{k_i} u_{n\mathbf{k}}\rangle . \tag{I5b}$$

By substituting $|u_{n\mathbf{k}}\rangle \leftrightarrow |\psi_{\mathbf{k}}\rangle$, we see that Eqs. (I5a) and (I5b) coincide with the definitions of $g_{ij}(\mathbf{k})$ and $\mathcal{F}_{ij}(\mathbf{k})$ given in Eqs. (2) and (3) of the main text, respectively.

The form given in Eq. (I3), however, is not quite equivalent to that provided in Eq. (21) of the main text: the formal correspondence $\hat{P}_n(\mathbf{k}) \rightarrow P_n(\mathbf{k}) \equiv U_n(\mathbf{k})U_n^\dagger(\mathbf{k})$ between the projection operator and the projection matrix is only valid under the tight-binding approximation, within which all the information on the \mathbf{k} -dependence of the Bloch eigenstates $|u_{n\mathbf{k}}\rangle$ is contained in the Bloch eigenvector $U_n(\mathbf{k})$. A proof of this statement can be found in the Supplementary information of Ref. [S5].

Appendix II: Proof of the acoustic sum rules

We start by proving the acoustic sum rule for the complete dynamical matrix and for the ionic and electronic contributions to it. It is sufficient to impose invariance of the interatomic potential energy $V(\{\mathbf{u}_{p\nu}\})$ felt by each atom under a global translation of the entire crystal by a constant vector \mathbf{b} . Let us calculate the potential energy felt by an atom in the $p = 0$ unit cell, with basis vector $\boldsymbol{\tau}_\nu$:

$$V(\mathbf{u}_{0\nu}) = \sum_{p'} \sum_{\nu'} u_{0\nu i} [\mathcal{C}]_{0\nu i}^{p'\nu'j} u_{p'\nu'j} = \sum_{p'} \sum_{\nu'} (u_{0\nu i} + b_i) [\mathcal{C}]_{0\nu i}^{p'\nu'j} (u_{p'\nu'j} + b_j) , \tag{II1}$$

implying

$$\sum_{p'} \sum_{\nu'} b_i [\mathcal{C}]_{0\nu i}^{p'\nu'j} b_j = 0 \quad \forall \mathbf{b} \in \mathbb{R}^D , \tag{II2}$$

and therefore

$$\sum_{\nu'} \sqrt{M_{\nu'}} [\mathcal{D}(\mathbf{q} = \mathbf{0})]_{\nu i}^{\nu'j} = \frac{1}{\sqrt{M_\nu}} \sum_{p', \nu'} [\mathcal{C}]_{0\nu i}^{p'\nu'j} = 0 \quad \forall \nu, i, j . \tag{II3}$$

The same line of reasoning can be applied to $\mathcal{D}^{(\text{ion})}(\mathbf{q} = \mathbf{0})$, substituting the interatomic potential with the bare Coulomb repulsive potential, and thus to the electronic contribution $\mathcal{D}^{(\text{el})}(\mathbf{q} = \mathbf{0})$.

With the two-center approximation of the tight-binding model, we can also derive the sum rule for the electronic contribution. To demonstrate this, we examine the sum of the derivatives of the Hamiltonian.

$$\begin{aligned}
\sum_{p\nu} \partial_{p\nu i} \hat{\mathcal{H}}_e &= \sum_{p\nu} \sum_{p'\nu'\alpha'} \sum_{p''\nu''\alpha''} \partial_{p\nu i} t_{\nu'\nu''}^{\alpha'\alpha''} (\mathbf{R}_{p'\nu'} - \mathbf{R}_{p''\nu''}) \hat{c}_{p'\nu'\alpha'}^\dagger \hat{c}_{p''\nu''\alpha''} \\
&= \sum_{p\nu} \sum_{p'\nu'\alpha'} \sum_{p''\nu''\alpha''} \delta_{p,p'} \delta_{\nu,\nu'} \partial_{p'\nu' i} t_{\nu'\nu''}^{\alpha'\alpha''} (\mathbf{R}_{p'\nu'} - \mathbf{R}_{p''\nu''}) \hat{c}_{p'\nu'\alpha'}^\dagger \hat{c}_{p''\nu''\alpha''} \\
&\quad + \delta_{p,p''} \delta_{\nu,\nu''} \partial_{p''\nu'' i} t_{\nu'\nu''}^{\alpha'\alpha''} (\mathbf{R}_{p'\nu'} - \mathbf{R}_{p''\nu''}) \hat{c}_{p'\nu'\alpha'}^\dagger \hat{c}_{p''\nu''\alpha''} \\
&= \sum_{p'\nu'\alpha'} \sum_{p''\nu''\alpha''} \partial_{p'\nu' i} t_{\nu'\nu''}^{\alpha'\alpha''} (\mathbf{R}_{p'\nu'} - \mathbf{R}_{p''\nu''}) + \partial_{p''\nu'' i} t_{\nu'\nu''}^{\alpha'\alpha''} (\mathbf{R}_{p'\nu'} - \mathbf{R}_{p''\nu''}) \hat{c}_{p'\nu'\alpha'}^\dagger \hat{c}_{p''\nu''\alpha''} \\
&= 0
\end{aligned} \tag{II4}$$

where we have used the fact that for any function $f(x - y)$

$$\partial_x f(x - y) + \partial_y f(x - y) = \partial_{(x-y)} f(x - y) - \partial_{(x-y)} f(x - y) = 0 \tag{II5}$$

Substituting Eq. (II4) into Eq. (15), we arrive to

$$\begin{aligned}
\sum_{p',\nu'} [\mathcal{C}^{(\text{el})}]_{p\nu i}^{p'\nu'} &= \sum_{p',\nu'} [\mathcal{C}^{(\text{el},1)}]_{p\nu i}^{p'\nu'} + \sum_{p',\nu'} [\mathcal{C}^{(\text{el},2)}]_{p\nu i}^{p'\nu'} \\
&= \sum_{m \neq 0} \frac{1}{\mathcal{E}_0 - \mathcal{E}_m} \left\langle \phi_{\{0\}}^{(m)} \left| \partial_{p\nu i} \hat{\mathcal{H}}_e \right| \phi_{\{0\}}^{(0)} \right\rangle \times \left\langle \phi_{\{0\}}^{(0)} \left| \sum_{p',\nu'} \partial_{p'\nu' j} \hat{\mathcal{H}}_e \right| \phi_{\{0\}}^{(m)} \right\rangle \\
&\quad + \frac{1}{\mathcal{E}_0 - \mathcal{E}_m} \left\langle \phi_{\{0\}}^{(m)} \left| \sum_{p',\nu'} \partial_{p'\nu' j} \hat{\mathcal{H}}_e \right| \phi_{\{0\}}^{(0)} \right\rangle \times \left\langle \phi_{\{0\}}^{(0)} \left| \partial_{p\nu i} \hat{\mathcal{H}}_e \right| \phi_{\{0\}}^{(m)} \right\rangle \\
&\quad + \left\langle \phi_{\{0\}}^{(0)} \left| \partial_{p\nu i} \left(\sum_{p',\nu'} \partial_{p'\nu' j} \hat{\mathcal{H}}_e \right) \right| \phi_{\{0\}}^{(0)} \right\rangle, \\
&= 0
\end{aligned} \tag{II6}$$

which is identical to Eq. (II3). This proof does not require the Gaussian approximation.

Only continuous translational symmetry is required for the acoustic sum rules. We consider a general Hamiltonian parameterized by the set of displacements $\{\mathbf{u}_{p\nu}\}$. Translational symmetry implies that if all atoms are uniformly displaced by an arbitrary vector $\Delta\mathbf{u}$, the Hamiltonian remains invariant.

$$\hat{\mathcal{H}}_e(\{\mathbf{u}_{p\nu}\}) = \hat{\mathcal{H}}_e(\{\mathbf{u}_{p\nu} + \Delta\mathbf{u}\}) \tag{II7}$$

We consider a infinitesimal $\Delta\mathbf{u}$ in i direction, we obtained

$$\begin{aligned}
\partial_{p\nu i} \hat{\mathcal{H}}_e(\{\mathbf{u}_{p\nu}\}) \Delta u_i &= 0 \\
\partial_{p\nu i} \hat{\mathcal{H}}_e(\{\mathbf{u}_{p\nu}\}) &= 0
\end{aligned} \tag{II8}$$

Eq. (II8) leads to sum rule as show in Eq. (II6). This is known as the Goldstone theorem.

Appendix III: The force constants in terms of Hamiltonian derivatives

To derive an explicit expression for the quantity $\mathcal{C}^{(\text{el})}$ as defined in Eq. (7), we use the Hellmann-Feynmann theorem [S6] carefully combined with the second-order derivative:

$$\begin{aligned}
[\mathcal{C}^{(\text{el})}]_{p\nu i}^{p'\nu'j} &= \frac{\partial^2}{\partial u_{p\nu i} \partial u_{p'\nu'j}} \left\langle \phi_{\{\mathbf{u}_{p\nu}\}}^{(0)} \left| \hat{\mathcal{H}}_e(\{\mathbf{u}_{p\nu}\}) \right| \phi_{\{\mathbf{u}_{p\nu}\}}^{(0)} \right\rangle \Big|_0 \\
&= \partial_{p\nu i} \left\langle \phi^{(0)} \left| \partial_{p'\nu'j} \hat{\mathcal{H}}_e \right| \phi^{(0)} \right\rangle \Big|_0 \\
&= \left\langle \partial_{p\nu i} \phi^{(0)} \left| \partial_{p'\nu'j} \hat{\mathcal{H}}_e \right| \phi^{(0)} \right\rangle \Big|_0 + \left\langle \phi^{(0)} \left| \partial_{p'\nu'j} \hat{\mathcal{H}}_e \right| \partial_{p\nu i} \phi^{(0)} \right\rangle \Big|_0 \\
&\quad + \left\langle \phi^{(0)} \left| \partial_{p\nu i} \partial_{p'\nu'j} \hat{\mathcal{H}}_e \right| \phi^{(0)} \right\rangle \Big|_0 .
\end{aligned} \tag{III1}$$

Here, we used the shorthand notation $\partial_{p\nu i} \equiv \partial/\partial u_{p\nu i}$ and omitted, starting from the second equality, the explicit parametric dependence of the Hamiltonian and its ground state on $\{\mathbf{u}_{p\nu}\}$.

The parametric derivatives of the many-body ground state in the previous expression are formally well-defined but impractical to compute directly. Consequently, we replace them with derivatives of the Hamiltonian. However, this substitution necessitates the introduction of the exact excited eigenstates of the Hamiltonian, which are determined by the Schrödinger equation:

$$\hat{\mathcal{H}}_e |\phi^{(m)}\rangle = \mathcal{E}_m |\phi^{(m)}\rangle . \tag{III2}$$

In the following, we simplify the parametric derivatives of the many-body ground state using the excited states. From

$$\begin{aligned}
\langle \phi^{(m)} | \hat{\mathcal{H}}_e | \phi^{(n)} \rangle &= \mathcal{E}_m \delta_{m,n} \\
\langle \partial_{p\nu i} \phi^{(m)} | \hat{\mathcal{H}}_e | \phi^{(n)} \rangle + \langle \phi^{(m)} | \partial_{p\nu i} \hat{\mathcal{H}}_e | \phi^{(n)} \rangle + \langle \phi^{(m)} | \hat{\mathcal{H}}_e | \partial_{p\nu i} \phi^{(n)} \rangle &= \partial_{p\nu i} \mathcal{E}_m \delta_{m,n}
\end{aligned} \tag{III3}$$

we arrive at the Epstein generalization [S1] of the Hellmann-Feynman theorem for $m \neq n$:

$$\left\langle \phi^{(m)} \left| \partial_{p\nu i} \phi^{(n)} \right\rangle = \frac{\left\langle \phi^{(m)} \left| \partial_{p\nu i} \hat{\mathcal{H}}_e \right| \phi^{(n)} \right\rangle}{\mathcal{E}_n - \mathcal{E}_m} , \quad (m \neq n) . \tag{III4}$$

For $m = n$ we get the Hellmann-Feynman theorem

$$\langle \phi^{(n)} | \partial_{p\nu i} \hat{\mathcal{H}}_e | \phi^{(n)} \rangle = \partial_{p\nu i} \mathcal{E}_n \tag{III5}$$

Using Eq. (III4) inside Eq. (III1), we get

$$\begin{aligned}
[\mathcal{C}^{(\text{el})}]_{p\nu i}^{p'\nu'j} &= \left\langle \partial_{p\nu i} \phi^{(0)} \left| \partial_{p'\nu'j} \hat{\mathcal{H}}_e \right| \phi^{(0)} \right\rangle \Big|_0 + \left\langle \phi^{(0)} \left| \partial_{p'\nu'j} \hat{\mathcal{H}}_e \right| \partial_{p\nu i} \phi^{(0)} \right\rangle \Big|_0 \\
&\quad + \left\langle \phi^{(0)} \left| \partial_{p\nu i} \partial_{p'\nu'j} \hat{\mathcal{H}}_e \right| \phi^{(0)} \right\rangle \Big|_0 . \\
&= \left\langle \partial_{p\nu i} \phi^{(0)} \left| \sum_m |\phi^{(m)}\rangle \left\langle \phi^{(m)} \right| \partial_{p'\nu'j} \hat{\mathcal{H}}_e \right| \phi^{(0)} \right\rangle \Big|_0 + \left\langle \phi^{(0)} \left| \partial_{p'\nu'j} \hat{\mathcal{H}}_e \sum_m |\phi^{(m)}\rangle \left\langle \phi^{(m)} \right| \partial_{p\nu i} \phi^{(0)} \right\rangle \Big|_0 \right. \\
&\quad \left. + \left\langle \phi^{(0)} \left| \partial_{p\nu i} \partial_{p'\nu'j} \hat{\mathcal{H}}_e \right| \phi^{(0)} \right\rangle \Big|_0 . \right. \\
&= \left\langle \partial_{p\nu i} \phi^{(0)} \left| \sum_{m \neq 0} |\phi^{(m)}\rangle \left\langle \phi^{(m)} \right| \partial_{p'\nu'j} \hat{\mathcal{H}}_e \right| \phi^{(0)} \right\rangle \Big|_0 + \left\langle \phi^{(0)} \left| \partial_{p'\nu'j} \hat{\mathcal{H}}_e \sum_{m \neq 0} |\phi^{(m)}\rangle \left\langle \phi^{(m)} \right| \partial_{p\nu i} \phi^{(0)} \right\rangle \Big|_0 \right. \\
&\quad \left. + \left\langle \phi^{(0)} \left| \partial_{p\nu i} \partial_{p'\nu'j} \hat{\mathcal{H}}_e \right| \phi^{(0)} \right\rangle \Big|_0 . \right. \\
&= \sum_{m \neq 0} \frac{1}{\mathcal{E}_0 - \mathcal{E}_m} \left\langle \phi_{\{\mathbf{0}\}}^{(m)} \left| \partial_{p\nu i} \hat{\mathcal{H}}_e \right| \phi_{\{\mathbf{0}\}}^{(0)} \right\rangle \times \left\langle \phi_{\{\mathbf{0}\}}^{(0)} \left| \partial_{p'\nu'j} \hat{\mathcal{H}}_e \right| \phi_{\{\mathbf{0}\}}^{(m)} \right\rangle \Big|_0 + \text{H.c.} \\
&\quad + \left\langle \phi^{(0)} \left| \partial_{p\nu i} \partial_{p'\nu'j} \hat{\mathcal{H}}_e \right| \phi^{(0)} \right\rangle \Big|_0 .
\end{aligned} \tag{III6}$$

In the derivation, we used the fact that

$$\left\langle \partial_{p\nu i} \phi^{(m)} \left| \phi^{(n)} \right\rangle + \left\langle \phi^{(m)} \left| \partial_{p\nu i} \phi^{(n)} \right\rangle = 0. \quad (\text{III7})$$

The two terms in Eq. (III6) are nothing but $\mathcal{C}^{(\text{el}, 1)}$ and $\mathcal{C}^{(\text{el}, 2)}$ defined in Eqs. (14)-(15) of the main text.

We remark that from Eq. (III4), one can also obtain

$$\begin{aligned} \left| \partial_{p\nu i} \phi^{(n)} \right\rangle &= \sum_m |\phi^{(m)}\rangle \left\langle \phi^{(m)} \left| \partial_{p\nu i} \phi^{(n)} \right\rangle \right. \\ &= \sum_{m \neq n} |\phi^{(m)}\rangle \left\langle \phi^{(m)} \left| \partial_{p\nu i} \phi^{(n)} \right\rangle \right. \\ &= \sum_{m \neq n} |\phi^{(m)}\rangle \frac{\left\langle \phi^{(m)} \left| \partial_{p\nu i} \hat{\mathcal{H}}_e \right| \phi^{(n)} \right\rangle}{\mathcal{E}_n - \mathcal{E}_m}. \end{aligned} \quad (\text{III8})$$

In the second equation of Eq. (III8), a parallel-transport gauge is assumed such that the Berry connection vanishes:

$$\left\langle \phi^{(n)} \left| \partial_{p\nu i} \phi^{(n)} \right\rangle = 0. \quad (\text{III9})$$

However, this gauge condition cannot be imposed globally if the system exhibits a nonzero Berry phase. We emphasize that the derivation of Eq. (III6) only requires the use of Eq. (III7), not the stricter condition in Eq. (III9).

Appendix IV: Formulas for the dynamical matrix

In this section, we derive the formulas for the dynamical matrix from the electronic contributions. We first present the main results and then show the detailed derivations.

The amplitudes $\left\langle \phi_{\{0\}}^{(m)} \left| \partial_{p\nu i} \hat{\mathcal{H}}_e \right| \phi_{\{0\}}^{(0)} \right\rangle$ appearing in Eq. (14) of the main text are nonzero only for the following class of states:

$$|\phi_{\{0\}}^{(n\mathbf{k}, n'\mathbf{k}')}\rangle = \hat{\gamma}_{n'\mathbf{k}'}^\dagger \hat{\gamma}_{n\mathbf{k}} |\phi_{\{0\}}^{(0)}\rangle, \quad \text{with} \quad \begin{cases} E_n(\mathbf{k}) < \mu \\ E_{n'}(\mathbf{k}') > \mu \end{cases}, \quad (\text{IV1})$$

where μ is the chemical potential, and $\hat{\gamma}_{n\mathbf{k}}^\dagger$ creates an electron in a Bloch state labeled by n, \mathbf{k} : $\hat{\gamma}_{n\mathbf{k}}^\dagger |0\rangle = e^{-i\mathbf{k}\cdot\hat{\mathbf{r}}} |u_{n\mathbf{k}}\rangle$.

The first derivatives of the Hamiltonian with respect to the displacements, which appear in Eq. (III6), can be calculated starting from the modified tight-binding Hamiltonian—see Eq. (4) of the main text. The evaluation of these derivatives on the states (IV1) allows us to get to an explicit form for the term $\mathcal{C}^{(\text{el}, 1)}$ as defined in Eq. (14). The expectation value on the Fermi sea that appears in the Eq. (15) for $[\mathcal{C}_{ij}^{(\text{el}, 2)}]_{\nu\nu'}^{pp'}$ in the main text is evaluated by explicit calculation of the second derivatives of the Hamiltonian with respect to the displacements. By taking the Fourier transform with respect to the ion positions, thereby defining

$$[\mathcal{D}^{(\text{el}, 1/2)}(\mathbf{q})]_{\nu i}^{\nu' j} \equiv \frac{1}{\sqrt{M_\nu M_{\nu'}}} \sum_p e^{-i\mathbf{q}\cdot(\mathbf{R}_p + \boldsymbol{\tau}_\nu - \boldsymbol{\tau}_{\nu'})} [\mathcal{C}_{ij}^{(\text{el}, 1/2)}]_{\nu\nu'}^{p, p'=0} \quad (\text{IV2})$$

so that $\mathcal{D}^{(\text{el})}(\mathbf{q}) = \mathcal{D}^{(\text{el}, 1)}(\mathbf{q}) + \mathcal{D}^{(\text{el}, 2)}(\mathbf{q})$, we obtain the following explicit formulas for the dynamical matrix:

$$[\mathcal{D}^{(\text{el}, 1)}(\mathbf{q})]_{\nu i}^{\nu' j} = \frac{1}{\sqrt{M_\nu M_{\nu'}}} \frac{2}{N} \sum_n \sum_{n'} \sum_{\mathbf{k}}^{\text{occ. unocc. FBZ}} \left\{ \frac{[F_i(n\mathbf{k}, n'\mathbf{k} + \mathbf{q})]_\nu [F_j(n'\mathbf{k} + \mathbf{q}, n\mathbf{k})]_{\nu'}}{E_n(\mathbf{k}) - E_{n'}(\mathbf{k} + \mathbf{q})} \right\} + \text{H.c.} \quad (\text{IV3})$$

and

$$[\mathcal{D}^{(\text{el}, 2)}(\mathbf{q})]_{\nu i}^{\nu' j} = \frac{1}{\sqrt{M_\nu M_{\nu'}}} \frac{2}{N} \sum_{\tilde{\nu}} \sum_n \sum_{\mathbf{k}\tilde{\mathbf{k}}}^{\text{occ. FBZ}} \sum_{\alpha\alpha'} [\delta_{\nu\nu'} \delta_{\tilde{\mathbf{k}}, \mathbf{0}} - \delta_{\tilde{\nu}\nu'} \delta_{\tilde{\mathbf{k}}, \mathbf{q}}] \left\{ [M_{ij}(\mathbf{k} + \tilde{\mathbf{k}})]_{\nu\alpha}^{\tilde{\nu}\alpha'} [P_n(\mathbf{k})]_{\tilde{\nu}\alpha'}^{\nu\alpha} \right\} + \text{H.c.}, \quad (\text{IV4})$$

Notice that here the hermitian conjugation accounts for taking the complex conjugate and exchanging the $\nu\nu'$ indices. The factor of two comes from the spin degrees of freedom. $P_n(\mathbf{k}) = U_n(\mathbf{k}) U_n^\dagger(\mathbf{k})$ is the projection matrix onto the

eigenvector $U_n(\mathbf{k})$ of the Bloch Hamiltonian $h(\mathbf{k})$, while N is the number of atoms in the Born-von Karman supercell, which is equal to the number of Bloch wave vectors involved in the sum over the first Brillouin zone (FBZ). In writing Eqs. (IV3)-(IV4) we employed the following shorthand notation for summations over the Fermi sea,

$$\sum_{nn'} \sum_{\mathbf{k}\mathbf{k}'}^{\text{FBZ}} \Theta(\mu - E_\nu(\mathbf{k})) \Theta(E_{n'}(\mathbf{k}') - \mu) = \sum_{\mathbf{k} \in \text{FBZ}}^{E_n(\mathbf{k}) < \mu} \sum_{\mathbf{k}' \in \text{FBZ}}^{E_{n'}(\mathbf{k}') > \mu} \equiv \sum_{n\mathbf{k}}^{\text{occ.}} \sum_{n'\mathbf{k}'}^{\text{unocc.}}, \quad (\text{IV5})$$

and defined the following quantity:

$$[F_i(n\mathbf{k}, n'\mathbf{k}')]_{\nu} \equiv \sum_{\tilde{\nu}} \sum_{\nu_1 \nu_2} \sum_{\alpha \alpha'} [U_n^\dagger(\mathbf{k})]_{\nu_1 \alpha} \left\{ \delta_{\nu \nu_1} \delta_{\tilde{\nu} \nu_2} [f_i(\mathbf{k}')]_{\nu \alpha'}^{\tilde{\nu} \alpha'} - \delta_{\nu \nu_2} \delta_{\tilde{\nu} \nu_1} [f_i(\mathbf{k})]_{\tilde{\nu} \alpha}^{\nu \alpha'} \right\} [U_{n'}(\mathbf{k}')]_{\nu_2 \alpha'} . \quad (\text{IV6})$$

We now turn to a detailed calculation of the Hamiltonian parametric derivatives. We start from the modified tight-binding (TB) form for the electron Hamiltonian:

$$\hat{\mathcal{H}}_e = \sum_{p, \nu, \alpha} \sum_{p', \nu', \alpha'} t_{\nu \nu'}^{\alpha \alpha'} (\mathbf{R}_{p\nu} - \mathbf{R}_{p'\nu'}) \hat{c}_{p\nu\alpha}^\dagger \hat{c}_{p'\nu'\alpha'} . \quad (\text{IV7})$$

where $\mathbf{R}_{p\nu} = \mathbf{R}_p + \boldsymbol{\tau}_\nu + \mathbf{u}_{p\nu}$, and $t_{\nu \nu'}^{\alpha \alpha'}(\mathbf{r})$ is supposed to be a real function of \mathbf{r} .

The parametric gradient of the TB Hamiltonian can be calculated component-wise by directly differentiating the form in Eq. (IV7):

$$\begin{aligned} \frac{\partial \hat{\mathcal{H}}_e}{\partial u_{p\nu i}} &= \sum_{\alpha' \alpha''} \sum_{p' \nu'} \sum_{p'' \nu''} \left\{ \partial_{p' \nu' i} t_{\nu' \nu''}^{\alpha' \alpha''} \Big|_0 \delta_{pp'} \delta_{\nu \nu'} + \partial_{p'' \nu'' i} t_{\nu' \nu''}^{\alpha' \alpha''} \Big|_0 \delta_{pp''} \delta_{\nu \nu''} \right\} \hat{c}_{p' \nu' \alpha'}^\dagger \hat{c}_{p'' \nu'' \alpha''} \\ &= \sum_{\alpha \alpha'} \sum_{p' \nu'} \left\{ [\partial_i t_{\nu \nu'}^{\alpha \alpha'}(\mathbf{r})] \Big|_{\mathbf{R}_{p\nu}^0 - \mathbf{R}_{p'\nu'}^0} c_{p\nu\alpha}^\dagger c_{p'\nu'\alpha'} - \partial_i t_{\nu' \nu}^{\alpha \alpha'}(\mathbf{r}) \Big|_{\mathbf{R}_{p'\nu'}^0 - \mathbf{R}_{p\nu}^0} c_{p'\nu'\alpha'}^\dagger c_{p\nu\alpha} \right\} \\ &= \sum_{\alpha \alpha'} \sum_{p' \nu'} \partial_i t_{\nu \nu'}^{\alpha \alpha'}(\mathbf{r}) \Big|_{\mathbf{R}_{p\nu}^0 - \mathbf{R}_{p'\nu'}^0} \hat{c}_{p\nu\alpha}^\dagger \hat{c}_{p'\nu'\alpha'} + \text{H.c.}, \end{aligned} \quad (\text{IV8})$$

where $\partial_i \equiv \partial / \partial r_i$.

Now, we Fourier-transform the electron operators

$$\hat{c}_{p\nu\alpha}^\dagger \hat{c}_{p'\nu'\alpha'} = \frac{1}{N} \sum_{\mathbf{k}\mathbf{k}'}^{\text{FBZ}} e^{-i\mathbf{k} \cdot \mathbf{R}_{p\nu}^0} e^{i\mathbf{k}' \cdot \mathbf{R}_{p'\nu'}^0} \hat{c}_{\mathbf{k}\nu\alpha}^\dagger \hat{c}_{\mathbf{k}'\nu'\alpha'} . \quad (\text{IV9})$$

According to the same convention, we define the Fourier transform of the gradient of the hopping function:

$$[f_i(\mathbf{k})]_{\nu \nu'}^{\alpha \alpha'} \equiv \sum_p e^{-i\mathbf{k} \cdot (\mathbf{R}_p + \boldsymbol{\tau}_\nu - \boldsymbol{\tau}_{\nu'})} \partial_i t_{\nu \nu'}^{\alpha \alpha'}(\mathbf{r}) \Big|_{\mathbf{R}_p + \boldsymbol{\tau}_\nu - \boldsymbol{\tau}_{\nu'}} . \quad (\text{IV10})$$

It is easy to prove that this object is anti-hermitian with respect to the exchange of sublattice indices:

$$\begin{aligned} [f_i^*(\mathbf{k})]_{\nu \nu'}^{\alpha \alpha'} &= \sum_p e^{i\mathbf{k} \cdot (\mathbf{R}_p + \boldsymbol{\tau}_\nu - \boldsymbol{\tau}_{\nu'})} \partial_i t_{\nu \nu'}^{\alpha \alpha'}(\mathbf{r}) \Big|_{\mathbf{R}_p + \boldsymbol{\tau}_\nu - \boldsymbol{\tau}_{\nu'}} \\ &= \sum_p e^{-i\mathbf{k} \cdot (-\mathbf{R}_p + \boldsymbol{\tau}_{\nu'} - \boldsymbol{\tau}_\nu)} \left(-\partial_i t_{\nu' \nu}^{\alpha \alpha'}(\mathbf{r}) \Big|_{-\mathbf{R}_p + \boldsymbol{\tau}_{\nu'} - \boldsymbol{\tau}_\nu} \right) \\ &= -\sum_p e^{-i\mathbf{k} \cdot (\mathbf{R}_p + \boldsymbol{\tau}_{\nu'} - \boldsymbol{\tau}_\nu)} \partial_i t_{\nu' \nu}^{\alpha \alpha'}(\mathbf{r}) \Big|_{\mathbf{R}_p + \boldsymbol{\tau}_{\nu'} - \boldsymbol{\tau}_\nu} \\ &= -[f_i(\mathbf{k})]_{\nu' \nu}^{\alpha \alpha'} . \end{aligned} \quad (\text{IV11})$$

Here, we exploit invariance under inversion of the Bravais vectors set $\{\mathbf{R}_p\}$. Moreover, by virtue of $t_{\nu \nu'}^{\alpha \alpha'}(\mathbf{r})$ being a

real number, we have $[f_i(-\kappa)]_{\nu\nu'}^{\alpha\alpha'} = [f_i^*(\kappa)]_{\nu\nu'}^{\alpha\alpha'}$. Exploiting both these properties, we thus obtain

$$\begin{aligned}
\frac{\partial \hat{\mathcal{H}}_e}{\partial u_{p\nu i}} &= \frac{1}{N^2} \sum_{\alpha\alpha'} \sum_{p'\nu'} \sum_{\kappa\mathbf{k}\mathbf{k}'}^{\text{FBZ}} e^{i\kappa \cdot (\mathbf{R}_{p\nu}^0 - \mathbf{R}_{p'\nu'}^0)} [f_i(\kappa)]_{\nu\nu'}^{\alpha\alpha'} \left\{ e^{-i\mathbf{k} \cdot \mathbf{R}_{p\nu}^0} e^{i\mathbf{k}' \cdot \mathbf{R}_{p'\nu'}^0} c_{\mathbf{k}\nu\alpha}^\dagger c_{\mathbf{k}'\nu'\alpha'} \right\} + \text{H.c.} \\
&= \frac{1}{N} \sum_{\alpha\alpha'} \sum_{\nu'} \sum_{\kappa\mathbf{k}\mathbf{k}'}^{\text{FBZ}} [f_i(\kappa)]_{\nu\nu'}^{\alpha\alpha'} \left\{ e^{i(\kappa-\mathbf{k}) \cdot \mathbf{R}_{p\nu}^0} \delta_{\kappa,\mathbf{k}'} c_{\mathbf{k}\nu\alpha}^\dagger c_{\mathbf{k}'\nu'\alpha'} + e^{i(\kappa+\mathbf{k}) \cdot \mathbf{R}_{p\nu}^0} \delta_{\kappa,-\mathbf{k}'} c_{\mathbf{k}'\nu'\alpha'}^\dagger c_{\mathbf{k}\nu\alpha} \right\} \\
&= \frac{1}{N} \sum_{\alpha\alpha'} \sum_{\nu'} \sum_{\mathbf{k}\mathbf{k}'}^{\text{FBZ}} \left\{ e^{i(\mathbf{k}'-\mathbf{k}) \cdot \mathbf{R}_{p\nu}^0} c_{\mathbf{k}\nu\alpha}^\dagger [f_i(\kappa)]_{\nu\nu'}^{\alpha\alpha'} c_{\mathbf{k}'\nu'\alpha'} - e^{i(\mathbf{k}-\mathbf{k}') \cdot \mathbf{R}_{p\nu}^0} c_{\mathbf{k}'\nu'\alpha'}^\dagger [f_i(\kappa)]_{\nu\nu'}^{\alpha'\alpha} c_{\mathbf{k}\nu\alpha} \right\} \\
&= \frac{1}{N} \sum_{\alpha\alpha'} \sum_{\nu'} \sum_{\mathbf{k}\mathbf{k}'}^{\text{FBZ}} \left\{ e^{i(\mathbf{k}'-\mathbf{k}) \cdot \mathbf{R}_{p\nu}^0} c_{\mathbf{k}\nu\alpha}^\dagger [f_i(\kappa)]_{\nu\nu'}^{\alpha\alpha'} c_{\mathbf{k}'\nu'\alpha'} \right\} + \text{H.c.} .
\end{aligned} \tag{IV12}$$

Now, we rotate the creation and annihilation operators in the diagonal basis $\hat{\gamma}_{n\mathbf{k}\alpha}$, i.e.

$$\hat{c}_{\mathbf{k}\nu\alpha}^\dagger \hat{c}_{\mathbf{k}'\nu'\alpha'} = \sum_{nn'} [U_n^\dagger(\mathbf{k})]_{\nu\alpha} [U_{n'}(\mathbf{k}')]_{\nu'\alpha'} \hat{\gamma}_{n\mathbf{k}}^\dagger \hat{\gamma}_{n'\mathbf{k}'} . \tag{IV13}$$

Our final expression for the Hamiltonian first-order parametric derivative is thus

$$\frac{\partial \hat{\mathcal{H}}_e}{\partial u_{p\nu i}} = \frac{1}{N} \sum_{\alpha\alpha'} \sum_{\nu'} \sum_{nn'} \sum_{\mathbf{k}\mathbf{k}'}^{\text{FBZ}} \left\{ e^{i(\mathbf{k}'-\mathbf{k}) \cdot \mathbf{R}_{p\nu}^0} [U_n^\dagger(\mathbf{k})]_{\nu\alpha} [f_i(\kappa)]_{\nu\nu'}^{\alpha\alpha'} [U_{n'}(\mathbf{k}')]_{\nu'\alpha'} \hat{\gamma}_{n\mathbf{k}}^\dagger \hat{\gamma}_{n'\mathbf{k}'} \right\} + \text{H.c.} . \tag{IV14}$$

We shall now calculate the second-order parametric derivative of the Hamiltonian (IV7). We proceed in the exact same way as above, omitting orbital indices for the sake of simplicity:

$$\begin{aligned}
\partial_{p\nu i} \partial_{p'\nu' j} \mathcal{H}_e|_0 &= \partial_{p\nu i} \sum_{p_1\nu_1} \sum_{p_2\nu_2} \left\{ \partial_{p_1\nu_1 j} t_{\nu_1\nu_2} \delta_{pp_1} \delta_{\nu\nu_1} + \partial_{p_2\nu_2 j} t_{\nu_1\nu_2} \delta_{pp_2} \delta_{\nu\nu_2} \right\} \hat{c}_{p_1\nu_1}^\dagger \hat{c}_{p_2\nu_2} \Big|_0 \\
&= \sum_{p_1\nu_1} \sum_{p_2\nu_2} \left\{ \partial_{p_1\nu_1 i} \partial_{p_1\nu_1 j} t_{\nu_1\nu_2} \Big|_0 \delta_{pp_1} \delta_{\nu\nu_1} \delta_{p'p_1} \delta_{\nu'\nu_1} \right. \\
&\quad + \partial_{p_2\nu_2 i} \partial_{p_2\nu_2 j} t_{\nu_1\nu_2} \Big|_0 \delta_{pp_2} \delta_{\nu\nu_2} \delta_{p'p_2} \delta_{\nu'\nu_2} \\
&\quad + \partial_{p_1\nu_1 i} \partial_{p_2\nu_2 j} t_{\nu_1\nu_2} \Big|_0 \delta_{p'p_1} \delta_{\nu'\nu_1} \delta_{pp_2} \delta_{\nu\nu_2} \\
&\quad \left. + \partial_{p_2\nu_2 i} \partial_{p_1\nu_1 j} t_{\nu_1\nu_2} \Big|_0 \delta_{pp_1} \delta_{\nu\nu_1} \delta_{p'p_2} \delta_{\nu'\nu_2} \right\} \hat{c}_{p_1\nu_1}^\dagger \hat{c}_{p_2\nu_2} \\
&= \delta_{pp'} \delta_{\nu\nu'} \sum_{p_2\nu_2} \partial_i \partial_j t_{\nu\nu_2}(\mathbf{r})|_{\mathbf{R}_{p\nu}^0 - \mathbf{R}_{p_2\nu_2}^0} \hat{c}_{p\nu}^\dagger \hat{c}_{p_2\nu_2} \\
&\quad + \delta_{pp'} \delta_{\nu\nu'} \sum_{p_1\nu_1} \partial_i \partial_j t_{\nu_1\nu}(\mathbf{r})|_{\mathbf{R}_{p_1\nu_1}^0 - \mathbf{R}_{p\nu}^0} \hat{c}_{p_1\nu_1}^\dagger \hat{c}_{p\nu} \\
&\quad - \partial_i \partial_j t_{\nu\nu'}(\mathbf{r})|_{\mathbf{R}_{p\nu}^0 - \mathbf{R}_{p'\nu'}^0} \hat{c}_{p\nu}^\dagger \hat{c}_{p'\nu'} \\
&\quad - \partial_i \partial_j t_{\nu'\nu}(\mathbf{r})|_{\mathbf{R}_{p'\nu'}^0 - \mathbf{R}_{p\nu}^0} \hat{c}_{p'\nu'}^\dagger \hat{c}_{p\nu} \\
&= \sum_{p''\nu''} (\delta_{pp'} \delta_{\nu\nu'} - \delta_{p'p''} \delta_{\nu'\nu''}) \partial_i \partial_j t_{\nu\nu''}(\mathbf{r})|_{\mathbf{R}_{p\nu}^0 - \mathbf{R}_{p''\nu''}^0} \hat{c}_{p\nu}^\dagger \hat{c}_{p''\nu''} + \text{H.c.} .
\end{aligned} \tag{IV15}$$

In calculating this form, we exploited the parity properties of the second derivatives of the hopping functions, and arbitrarily relabeled some dummy indices. We define the Fourier transform of the Hessian of the hopping function as

$$[M_{ij}(\kappa)]_{\nu\nu'} \equiv \sum_p e^{-i\kappa \cdot (\mathbf{R}_p + \boldsymbol{\tau}_\nu - \boldsymbol{\tau}_{\nu'})} \partial_i \partial_j t_{\nu\nu'}(\mathbf{r})|_{\mathbf{R}_p + \boldsymbol{\tau}_\nu - \boldsymbol{\tau}_{\nu'}} . \tag{IV16}$$

This object can be easily proven to be hermitian, following the same line of reasoning as above. The following constraints are easy to prove:

$$[M_{ij}(\boldsymbol{\kappa})]_{\nu\nu'} = [M_{ij}^*(\boldsymbol{\kappa})]_{\nu'\nu} \quad \text{and} \quad [M_{ij}(-\boldsymbol{\kappa})]_{\nu\nu'} = [M_{ij}^*(\boldsymbol{\kappa})]_{\nu\nu'}. \quad (\text{IV17})$$

We obtain the following form:

$$\begin{aligned} \partial_{p\nu i} \partial_{p'\nu' j} \mathcal{H}_e|_0 &= \frac{1}{N^2} \sum_{p''\nu''} \sum_{\boldsymbol{\kappa} \mathbf{k} \mathbf{k}'}^{\text{FBZ}} (\delta_{pp'} \delta_{\nu\nu'} - \delta_{p'p''} \delta_{\nu'\nu''}) [M_{ij}(\boldsymbol{\kappa})]_{\nu\nu''} \times \\ &\quad \times e^{i\boldsymbol{\kappa} \cdot (\mathbf{R}_{p\nu}^0 - \mathbf{R}_{p''\nu''}^0)} \left\{ e^{-i\mathbf{k} \cdot \mathbf{R}_{p\nu}^0} e^{i\mathbf{k}' \cdot \mathbf{R}_{p''\nu''}^0} c_{\mathbf{k}\nu}^\dagger c_{\mathbf{k}'\nu''} \right\} + \text{H.c.} \\ &= \frac{1}{N^2} \sum_{p''\nu''} \sum_{\boldsymbol{\kappa} \mathbf{k} \mathbf{k}'}^{\text{FBZ}} (\delta_{pp'} \delta_{\nu\nu'} - \delta_{p'p''} \delta_{\nu'\nu''}) [M_{ij}(\boldsymbol{\kappa})]_{\nu\nu''} \times \\ &\quad \times \left\{ e^{i(\boldsymbol{\kappa} - \mathbf{k}) \cdot \mathbf{R}_{p\nu}^0} e^{-i(\boldsymbol{\kappa} - \mathbf{k}') \cdot \mathbf{R}_{p''\nu''}^0} c_{\mathbf{k}\nu}^\dagger c_{\mathbf{k}'\nu''} \right. \\ &\quad \left. + e^{i(\boldsymbol{\kappa} + \mathbf{k}) \cdot \mathbf{R}_{p\nu}^0} e^{-i(\boldsymbol{\kappa} + \mathbf{k}') \cdot \mathbf{R}_{p''\nu''}^0} c_{\mathbf{k}'\nu''}^\dagger c_{\mathbf{k}\nu} \right\} \\ &= \delta_{pp'} \delta_{\nu\nu'} \frac{1}{N} \sum_{\nu''} \sum_{\mathbf{k} \mathbf{k}'}^{\text{FBZ}} \left\{ e^{i(\mathbf{k}' - \mathbf{k}) \cdot \mathbf{R}_{p\nu}^0} c_{\mathbf{k}\nu}^\dagger [M_{ij}(\mathbf{k}')]_{\nu\nu''} c_{\mathbf{k}'\nu''} \right\} + \text{H.c.} \\ &\quad - \frac{1}{N^2} \sum_{\boldsymbol{\kappa} \mathbf{k} \mathbf{k}'}^{\text{FBZ}} e^{i\boldsymbol{\kappa} \cdot (\mathbf{R}_{p\nu}^0 - \mathbf{R}_{p'\nu'}^0)} \left\{ e^{-i\mathbf{k} \cdot \mathbf{R}_{p\nu}^0} e^{i\mathbf{k}' \cdot \mathbf{R}_{p'\nu'}^0} c_{\mathbf{k}\nu}^\dagger [M_{ij}(\boldsymbol{\kappa})]_{\nu\nu'} c_{\mathbf{k}'\nu'} \right\} + \text{H.c.} \end{aligned} \quad (\text{IV18})$$

Expectation values will be taken by once again rotating the annihilation and creation operators in the diagonal basis.

We now take the expectation values on states of the form (IV1). The state with $n\mathbf{k} = n'\mathbf{k}'$ is nothing but the ground state itself, and it is therefore excluded from the sum in Eq. (III6). The relevant expectation values can be recasted into ground-state averages:

$$\left\langle \Omega \left| \gamma_{n''\mathbf{k}''}^\dagger \gamma_{n'''\mathbf{k}'''} \right| \phi^{(n\mathbf{k}, n'\mathbf{k}')} \right\rangle = \delta_{nn''} \delta_{\mathbf{k}\mathbf{k}''} \delta_{n''n'''} \delta_{\mathbf{k}'\mathbf{k}'''} \left\langle \gamma_{n\mathbf{k}}^\dagger \gamma_{n'\mathbf{k}'} \gamma_{n'\mathbf{k}'}^\dagger \gamma_{n\mathbf{k}} \right\rangle_0; \quad (\text{IV19})$$

$$\left\langle \phi^{(n\mathbf{k}, n'\mathbf{k}')} \left| \gamma_{n''\mathbf{k}''}^\dagger \gamma_{n'''\mathbf{k}'''} \right| \Omega \right\rangle = \delta_{nn'''} \delta_{\mathbf{k}\mathbf{k}'''} \delta_{n'n''} \delta_{\mathbf{k}'\mathbf{k}''} \left\langle \gamma_{n\mathbf{k}}^\dagger \gamma_{n'\mathbf{k}'} \gamma_{n'\mathbf{k}'}^\dagger \gamma_{n\mathbf{k}} \right\rangle_0. \quad (\text{IV20})$$

The resulting two-body ground-state average is easily evaluated

$$\begin{aligned} \left\langle \gamma_{n\mathbf{k}}^\dagger \gamma_{n'\mathbf{k}'} \gamma_{n'\mathbf{k}'}^\dagger \gamma_{n\mathbf{k}} \right\rangle_0 &= \left\langle \gamma_{n\mathbf{k}}^\dagger \left(1 - \gamma_{n'\mathbf{k}'}^\dagger \gamma_{n'\mathbf{k}'} \right) \gamma_{n\mathbf{k}} \right\rangle_0 \\ &= \left\langle \gamma_{n\mathbf{k}}^\dagger \gamma_{n\mathbf{k}} \right\rangle - \left\langle \gamma_{n\mathbf{k}}^\dagger \gamma_{n\mathbf{k}} \gamma_{n'\mathbf{k}'}^\dagger \gamma_{n'\mathbf{k}'} \right\rangle_0 \\ &= n_{n\mathbf{k}} (1 - n_{n'\mathbf{k}'}) \\ &= \Theta[\mu - E_n(\mathbf{k})] \Theta[E_{n'}(\mathbf{k}') - \mu]. \end{aligned} \quad (\text{IV21})$$

It is immediate to see that, under the restrictions in Eq. (IV1), this counting factor is just unity. Moreover, the energy denominator appearing in Eq. (III6) is just the difference between the hole energy and the above-the-surface electron energy:

$$\mathcal{E}_0 - \mathcal{E}_{n\mathbf{k}, n'\mathbf{k}'} = E_n(\mathbf{k}) - E_{n'}(\mathbf{k}'). \quad (\text{IV22})$$

Plugging the expectation values in formula (III6), we immediately arrive via Fourier transform to expressions (IV3)

and (IV4) for the dynamical matrix:

$$\begin{aligned}
\mathcal{D}_{\nu\nu';ij}^{(\text{el}, 1)}(\mathbf{q}) &= \frac{1}{\sqrt{M_\nu M_{\nu'}}} \sum_p e^{-i\mathbf{q}\cdot(\mathbf{R}_p+\boldsymbol{\tau}_\nu-\boldsymbol{\tau}_{\nu'})} \left\{ [\mathcal{C}_{ij}^{(\text{el}, 1)}]_{\nu\nu'}^{p,p'=0} + [\mathcal{C}_{ji}^{(\text{el}, 1)}]_{\nu'\nu}^{p'=0,p} \right\} \\
&= \frac{1}{\sqrt{M_\nu M_{\nu'}}} \frac{2}{N} \sum_{n\mathbf{k}}^{\text{occ.}} \sum_{n'\mathbf{k}'}^{\text{unocc.}} \left\{ \delta_{\mathbf{k}', \mathbf{k}+\mathbf{q}} \frac{[F_i(n\mathbf{k}, n'\mathbf{k}')]_\nu [F_j(n'\mathbf{k}', n\mathbf{k})]_{\nu'}}{E_n(\mathbf{k}) - E_{n'}(\mathbf{k}')} \right. \\
&\quad \left. + \delta_{\mathbf{k}', \mathbf{k}-\mathbf{q}} \frac{[F_j(n\mathbf{k}, n'\mathbf{k}')]_{\nu'} [F_i(n'\mathbf{k}', n\mathbf{k})]_\nu}{E_n(\mathbf{k}) - E_{n'}(\mathbf{k}')} \right\} \\
&= \frac{1}{\sqrt{M_\nu M_{\nu'}}} \frac{2}{N} \sum_n^{\text{occ.}} \sum_{n'}^{\text{unocc.}} \sum_{\mathbf{k}}^{\text{FBZ}} \left\{ \frac{[F_i(n\mathbf{k}, n'\mathbf{k}+\mathbf{q})]_\nu [F_j(n'\mathbf{k}+\mathbf{q}, n\mathbf{k})]_{\nu'}}{E_n(\mathbf{k}) - E_{n'}(\mathbf{k}+\mathbf{q})} \right\} + \text{H.c.} , \tag{IV23}
\end{aligned}$$

$$\begin{aligned}
\mathcal{D}_{\nu\nu';ij}^{(\text{el}, 2)}(\mathbf{q}) &= \frac{1}{\sqrt{M_\nu M_{\nu'}}} \sum_p e^{-i\mathbf{q}\cdot(\mathbf{R}_p+\boldsymbol{\tau}_\nu-\boldsymbol{\tau}_{\nu'})} [\mathcal{C}_{ij}^{(\text{el}, 2)}]_{\nu\nu'}^{p,p'=0} \\
&= \frac{1}{M_\nu} \frac{2}{N} \delta_{\nu\nu'} \sum_{\tilde{\nu}}^{\text{occ.}} \sum_n^{\text{FBZ}} \{ M_{\nu\tilde{\nu};ij}(\mathbf{k}) [P_n(\mathbf{k})]_{\tilde{\nu}\nu} \} + \text{H.c.} \\
&\quad - \frac{1}{\sqrt{M_\nu M_{\nu'}}} \frac{2}{N} \sum_n^{\text{occ.}} \sum_{\mathbf{k}}^{\text{FBZ}} \{ M_{\nu\nu';ij}(\mathbf{k}+\mathbf{q}) [P_n(\mathbf{k})]_{\nu'\nu} \} + \text{H.c.} . \tag{IV24}
\end{aligned}$$

Appendix V: Formal analogy with linear response theory

The analogy with linear response theory is built as follows. The small-displacement expansion of the electronic Hamiltonian (Eq. (4) in the main text) is

$$\hat{\mathcal{H}}_{\mathbf{u}} = \hat{\mathcal{H}}_{\mathbf{u}}|_0 + \sum_{p,\nu,i} \left. \frac{\partial \hat{\mathcal{H}}_{\mathbf{u}}}{\partial u_{p\nu i}} \right|_0 u_{p\nu i} + \frac{1}{2} \sum_{p,\nu,i} \sum_{p',\nu',j} \left. \frac{\partial^2 \hat{\mathcal{H}}_{\mathbf{u}}}{\partial u_{p\nu i} \partial u_{p'\nu'j}} \right|_0 u_{p\nu i} u_{p'\nu'j} , \tag{V1}$$

where we introduced the shorthand notation $\hat{\mathcal{H}}_{\mathbf{u}} \equiv \hat{\mathcal{H}}_{\text{e}}(\{\mathbf{u}_{p\nu}\})$, and the $|_0$ subscript once again denotes the evaluation on the mechanical equilibrium configuration. The most general Hamiltonian of an electron system electron which has been minimally coupled to a time-independent gauge field $\mathbf{A}(\mathbf{r}, t) = \mathbf{A}(\mathbf{r})$ is

$$\hat{\mathcal{H}}_{\mathbf{A}} = \hat{\mathcal{H}}_{\mathbf{A}}|_0 + \sum_i \int d^D \mathbf{r} \left. \frac{\delta \hat{\mathcal{H}}_{\mathbf{A}}}{\delta A_i(\mathbf{r})} \right|_0 A_i(\mathbf{r}) + \frac{1}{2} \sum_{i,j} \iint d^D \mathbf{r} d^D \mathbf{r}' \left. \frac{\delta^2 \hat{\mathcal{H}}_{\mathbf{A}}}{\delta A_i(\mathbf{r}) \delta A_j(\mathbf{r}')} \right|_0 A_i(\mathbf{r}) A_j(\mathbf{r}') , \tag{V2}$$

where δ denotes a functional derivative, and the $|_0$ subscript means $\mathbf{A} = 0$. Considering a time-independent vector field parallels the Born-Oppenheimer approximation. The two expressions (V1) and (V2) are formally equivalent under exchange of

$$\mathbf{r} \leftrightarrow \mathbf{R}_{p\nu} , \quad \sum_i \int d^D \mathbf{r} \leftrightarrow \sum_i \sum_{p,\nu} , \quad \hat{\mathcal{H}}_{\mathbf{A}} \leftrightarrow \hat{\mathcal{H}}_{\mathbf{u}} , \quad \mathbf{A}(\mathbf{r}) \leftrightarrow \mathbf{u}_{p\nu} , \tag{V3}$$

Identifying $\mathbf{A}(\mathbf{r})$ with an electromagnetic vector potential, we can define the paramagnetic current operator $\hat{j}_i(\mathbf{r})$ and the diamagnetic operator $\hat{\mathcal{T}}_{ij}(\mathbf{r}, \mathbf{r}')$ respectively as

$$\hat{j}_i(\mathbf{r}) \equiv \frac{c}{e} \left. \frac{\delta \hat{\mathcal{H}}_{\mathbf{A}}}{\delta A_i(\mathbf{r})} \right|_0 , \tag{V4}$$

and

$$\hat{\mathcal{T}}_{ij}(\mathbf{r}, \mathbf{r}') \equiv \frac{c^2}{e^2} \left. \frac{\delta^2 \hat{\mathcal{H}}_{\mathbf{A}}}{\delta A_i(\mathbf{r}) \delta A_j(\mathbf{r}')} \right|_0 . \tag{V5}$$

The *physical* current operator for the Hamiltonian in Eq. (V2) can be thus written as

$$\hat{J}_i(\mathbf{r}) \equiv \frac{c}{e} \frac{\delta \hat{\mathcal{H}}_{\mathbf{A}}}{\delta A_i(\mathbf{r})} = \hat{j}_{p,i}(\mathbf{r}) + \frac{e}{c} \sum_j \int d^D \mathbf{r}' \hat{\mathcal{T}}_{ij}(\mathbf{r}, \mathbf{r}') A_j(\mathbf{r}') . \quad (\text{V6})$$

By formal analogy, we can build the same operators for the theory described by the Hamiltonian (V1):

$$\hat{j}_{p\nu i} \equiv \left. \frac{\partial \hat{\mathcal{H}}_{\mathbf{u}}}{\partial u_{p\nu i}} \right|_0 , \quad (\text{V7})$$

$$\hat{\mathcal{T}}_{p\nu i}^{p'\nu'j} \equiv \left. \frac{\partial^2 \hat{\mathcal{H}}_{\mathbf{u}}}{\partial u_{p\nu i} \partial u_{p'\nu'j}} \right|_0 , \quad (\text{V8})$$

$$\hat{J}_{p\nu i} \equiv \hat{j}_{p\nu i} + \sum_{p',\nu',j} \hat{\mathcal{T}}_{p\nu i}^{p'\nu'j} u_{p'\nu'j} . \quad (\text{V9})$$

For each of the two theories, we can build a zero-temperature, static, paramagnetic current-current response function, which can be written as follows in the Lehmann representation :

$$\chi_{j_i j_j}(\mathbf{r}, \mathbf{r}') = \sum_{m \neq 0} \frac{\langle \phi_{\mathbf{A}=0}^{(m)} | \hat{J}_i(\mathbf{r}) | \phi_{\mathbf{A}=0}^{(0)} \rangle \langle \phi_{\mathbf{A}=0}^{(0)} | \hat{J}_j(\mathbf{r}') | \phi_{\mathbf{A}=0}^{(m)} \rangle}{\mathcal{E}_0 - \mathcal{E}_m} + \text{H.c.} , \quad (\text{V10})$$

$$\chi_{j_{p\nu i} j_{p'\nu'j}} = \sum_{m \neq 0} \frac{\langle \phi_{\{\mathbf{0}\}}^{(m)} | \hat{j}_{p\nu i} | \phi_{\{\mathbf{0}\}}^{(0)} \rangle \langle \phi_{\{\mathbf{0}\}}^{(0)} | \hat{j}_{p'\nu'j} | \phi_{\{\mathbf{0}\}}^{(m)} \rangle}{\mathcal{E}_0 - \mathcal{E}_m} + \text{H.c.} , \quad (\text{V11})$$

with the same notation for excited states of the Hamiltonian as in the main text. To obtain the electronic force constants, we start from Eq. (III1), which states the following:

$$[\mathcal{C}^{(\text{el})}]_{p\nu i}^{p'\nu'j} = \left[\frac{\partial}{\partial u_{p'\nu'j}} \left\langle \phi_{\{\mathbf{u}_{p\nu}\}}^{(0)} \left| \frac{\partial \hat{\mathcal{H}}_{\mathbf{u}}}{\partial u_{p\nu i}} \right| \phi_{\{\mathbf{u}_{p\nu}\}}^{(0)} \right\rangle \right]_0 \equiv \left[\frac{\partial}{\partial u_{p'\nu'j}} \langle \hat{J}_{p\nu i} \rangle \right]_0 , \quad (\text{V12})$$

where we introduced the shorthand notation $\langle \cdot \rangle \equiv \langle \phi_{\{\mathbf{u}_{p\nu}\}}^{(0)} | \cdot | \phi_{\{\mathbf{u}_{p\nu}\}}^{(0)} \rangle$. This equation parallels the definition of the physical current-current response function [S6], i.e.

$$\chi_{ij}^J(\mathbf{r}, \mathbf{r}') \equiv \left[\frac{\delta}{\delta A_j(\mathbf{r}')} \left\langle \phi_{\mathbf{A}}^{(0)} \left| \frac{\delta \hat{\mathcal{H}}_{\mathbf{A}}}{\delta A_i(\mathbf{r})} \right| \phi_{\mathbf{A}}^{(0)} \right\rangle \right]_0 \equiv \left[\frac{\delta}{\delta A_j(\mathbf{r}')} \langle \hat{J}_i(\mathbf{r}) \rangle \right]_0 . \quad (\text{V13})$$

The expectation value of the physical current operator to first order in the gauge field amplitude is obtained as

$$\langle \hat{J}_i(\mathbf{r}) \rangle = \frac{e}{c} \sum_l \int d^D \mathbf{r}' \left[\chi_{j_i j_l}(\mathbf{r}, \mathbf{r}') + \frac{e}{c} \langle \hat{\mathcal{T}}_{il}(\mathbf{r}, \mathbf{r}') \rangle \right] A_l(\mathbf{r}') + \mathcal{O}(A^2) , \quad (\text{V14})$$

so we obtain

$$\chi_{ij}^J(\mathbf{r}, \mathbf{r}') = \chi_{j_i j_j}(\mathbf{r}, \mathbf{r}') + \frac{e}{c} \langle \hat{\mathcal{T}}_{ij}(\mathbf{r}, \mathbf{r}') \rangle , \quad (\text{V15})$$

$$[\mathcal{C}^{(\text{el})}]_{p\nu i}^{p'\nu'j} = \chi_{j_{p\nu i} j_{p'\nu'j}} + \langle \hat{\mathcal{T}}_{p\nu i}^{p'\nu'j} \rangle \quad (\text{V16})$$

We can therefore identify the linear contribution $\mathcal{C}^{(\text{el},1)}$ to the force constants, Eq. (14), as a paramagnetic current-current response function, through the formal substitution (V4). The second-order contribution $\mathcal{C}^{(\text{el},2)}$, Eq. (15), is therefore the parallel of the diamagnetic operator ground-state expectation value.

Via this identification, the acoustic sum rule restricted to $\mathcal{D}^{(\text{el})}(\mathbf{q})$ can be inferred as follows. Since a static, uniform field $\mathbf{A}(\mathbf{r}, t) \equiv \mathbf{A}$ can be gauged away by a unitary transformation of the Hamiltonian, the system cannot respond with a physical current to such a potential. Therefore, imposing that the physical current expectation value (Eq. (V14)) vanishes at every order in A , i.e.

$$\sum_j \int d^D \mathbf{r}' \chi_{ij}^J(\mathbf{r}, \mathbf{r}') A_j(\mathbf{r}) = \sum_j A_j \int d^D \mathbf{r}' \chi_{ij}^J(\mathbf{r}, \mathbf{r}') = 0 \quad \forall \mathbf{A} \in \mathbb{R}^D , \quad (\text{V17})$$

we find the real-space TRK sum rule [S7, S8]:

$$\int d^D \mathbf{r}' \chi_{ij}^J(\mathbf{r}, \mathbf{r}') = \int d^D \mathbf{r}' \left[\chi_{j_i j_j}(\mathbf{r}, \mathbf{r}') + \frac{e}{c} \left\langle \hat{T}_{ij}(\mathbf{r}, \mathbf{r}') \right\rangle \right] = 0 \quad \forall \mathbf{r} \in \mathbb{R}^D, i, j. \quad (\text{V18})$$

In App. VIII, we prove the TRK sum rule explicitly for a 1D toy model. By formal analogy, we can apply the same procedure to the parallel theory described by the Hamiltonian (V1), for a static and uniform displacement $\mathbf{u}_{p\nu} \equiv \mathbf{u} \forall p, \nu$ of all the atoms. We impose

$$\sum_{p', \nu', j} [\mathcal{C}^{(\text{el})}]_{p\nu i}^{p' \nu' j} u_{p' \nu' j} = \sum_j u_j \sum_{p', \nu'} [\mathcal{C}^{(\text{el})}]_{p\nu i}^{p' \nu' j} = 0 \quad \forall \mathbf{u} \in \mathbb{R}^D, \quad (\text{V19})$$

thus obtaining the real-space version of the acoustic sum rule (Eq. (12) in the main text) as the counterpart of the TRK sum rule:

$$\sum_{p', \nu'} [\mathcal{C}^{(\text{el})}]_{p\nu i}^{p' \nu' j} = \sum_{p', \nu'} \left[\chi_{j_{p\nu i} j_{p' \nu' j}} + \left\langle \hat{T}_{p\nu i}^{p' \nu' j} \right\rangle \right] = 0 \quad \forall p, \nu, i, j. \quad (\text{V20})$$

Appendix VI: Proof of the TRK sum rule in a simple case

We will now explicitly prove the TRK sum rule for a simple 1D toy model, the so-called *extended Falikov-Kimball (EFK) model* (see e.g. Ref. [S8] and references therein to earlier work), which describes a 1D chain of identical atoms. EFK models are often used in the literature to describe excitonic insulators provided that interactions are added to the noninteracting Hamiltonian below (for a complete list of references see Ref. [S8]). Each atom has an orbital degree of freedom $\alpha = \{s, p\}$, which may correspond to the s and p orbitals of a hydrogenoid atom. In the following, we will consider nearest neighbors (NN) interactions only. The first Brillouin zone (FBZ) for a monopartite 1D lattice of lattice spacing a is just the ring $(-\pi/a, \pi/a]$.

We begin by explicitly writing the EFK Hamiltonian, including only NN terms, as defined in Ref. [S8]:

$$\hat{\mathcal{H}} = \sum_{k \in \text{FBZ}} \left(\hat{c}_{k,s}^\dagger, \hat{c}_{k,p}^\dagger \right) \begin{pmatrix} \varepsilon_s - 2t_s \cos ka & 2i\tilde{t} \sin ka \\ -2i\tilde{t} \sin ka & \varepsilon_p + 2t_p \cos ka \end{pmatrix} \begin{pmatrix} \hat{c}_{k,s} \\ \hat{c}_{k,p} \end{pmatrix} \equiv \sum_{k \in \text{FBZ}} \sum_{\alpha, \beta} \hat{c}_{k,\alpha}^\dagger H_{\alpha\beta}(k) \hat{c}_{k,\beta}, \quad (\text{VI1})$$

where $\hat{c}_{k,\alpha}^\dagger$ creates an electron in a Bloch state with momentum k and orbital flavor $\alpha \in \{s, p\}$. In Eq. (VI1) we introduce on-site energies ε_α , intra-orbital hopping amplitudes t_α , and an inter-orbital amplitude $\tilde{t} \equiv t_{sp} = t_{ps}$, which is real by gauge choice. To simplify the model, we shift the zero-point energy by setting $\delta \equiv (\varepsilon_s - \varepsilon_p)/2$, and assume $t_s = t_p \equiv t$. The Hamiltonian can therefore be written in the following pseudospin form:

$$\underline{H}(k) = \begin{pmatrix} \delta - 2t \cos ka & 2i\tilde{t} \sin ka \\ -2i\tilde{t} \sin ka & -\delta + 2t \cos ka \end{pmatrix} = \mathbf{d}_k \cdot \boldsymbol{\sigma}, \quad (\text{VI2})$$

where $\boldsymbol{\sigma} = (\sigma_x, \sigma_y, \sigma_z)$ is the usual vector of spin-1/2 Pauli matrices and $\mathbf{d}_k = (0, -2\tilde{t} \sin ka, \delta - 2t \cos ka)$.

The energy bands of the noninteracting 1D EFK model can be readily obtained using the straightforward procedure outlined in Ref. [S2]:

$$\varepsilon_{\pm, k} = \pm \varepsilon_k = \pm \sqrt{4\tilde{t}^2 \sin^2 ka + (\delta - 2t \cos ka)^2}, \quad (\text{VI3})$$

together with the Bloch eigenvectors

$$U_{+, k} = \frac{1}{\sqrt{2\varepsilon_k(\varepsilon_k + \delta - 2t \cos ka)}} \begin{pmatrix} \varepsilon_k + \delta - 2t \cos ka \\ -2i\tilde{t} \sin ka \end{pmatrix}, \quad (\text{VI4})$$

$$U_{-, k} = \frac{1}{\sqrt{2\varepsilon_k(\varepsilon_k + \delta - 2t \cos ka)}} \begin{pmatrix} -2i\tilde{t} \sin ka \\ \varepsilon_k + \delta - 2t \cos ka \end{pmatrix}. \quad (\text{VI5})$$

We impose $\delta \neq 2t$ to avoid accidental band crossing. The Bloch states of the system are defined by the contraction of the Bloch eigenvectors with the orbital basis operators, i.e.

$$|\psi_{\pm, k}\rangle = \hat{\gamma}_{\pm, k}^\dagger |0\rangle = \sum_{\alpha} [U_{\pm, k}]_{\alpha} \hat{c}_{k,\alpha}^\dagger |0\rangle \equiv \sum_{\alpha} [U_{\pm, k}]_{\alpha} |k, \alpha\rangle, \quad (\text{VI6})$$

where $\hat{\gamma}_{\pm,k}^\dagger$ is the fermionic creation operator in the band basis.

The static $\omega = 0$, $q = 0$ paramagnetic current operator can be presented as

$$\hat{j}_p \equiv \sum_{k \in \text{FBZ}} \sum_{\alpha, \beta} \hat{c}_{k,\alpha}^\dagger j_{p;\alpha\beta}(k) \hat{c}_{k,\beta} = \frac{2a}{\hbar} \sum_{k \in \text{FBZ}} \left(\hat{c}_{k,s}^\dagger, \hat{c}_{k,p}^\dagger \right) \begin{pmatrix} t \sin ka & i\tilde{t} \cos ka \\ -i\tilde{t} \cos ka & -t \sin ka \end{pmatrix} \begin{pmatrix} \hat{c}_{k,s} \\ \hat{c}_{k,p} \end{pmatrix}, \quad (\text{VI7})$$

where we have introduced the following first derivative of the Hamiltonian with respect to k :

$$j_{p;\alpha\beta}(k) \equiv \frac{1}{\hbar} \frac{\partial H_{\alpha\beta}(k)}{\partial k_p}. \quad (\text{VI8})$$

This current operator finds a more convenient representation in the band basis:

$$\sum_{k \in \text{FBZ}} \sum_{\alpha, \beta} \hat{c}_{k,\alpha}^\dagger j_{p;\alpha\beta}(k) \hat{c}_{k,\beta} = \sum_{k \in \text{FBZ}} \sum_{\alpha, \beta} \sum_{n, m = \pm} \hat{\gamma}_{n,k}^\dagger [U_{n,k}^\dagger]_\alpha j_{p;\alpha\beta}(k) [U_{n,k}]_\beta \hat{\gamma}_{n,k} \equiv \sum_{k \in \text{FBZ}} \sum_{n, m = \pm} \hat{\gamma}_{n,k}^\dagger j_{p;nm}(k) \hat{\gamma}_{n,k}, \quad (\text{VI9})$$

with

$$j_{p;nm}(k) = \sum_{\alpha, \beta} [U_{n,k}^\dagger]_\alpha j_{p;\alpha\beta}(k) [U_{m,k}]_\beta. \quad (\text{VI10})$$

The current vector is parallel to the Bravais lattice vector $\hat{\mathbf{u}}$, i.e. $\hat{\mathbf{j}}_p = \hat{j}_p \hat{\mathbf{u}}$, where \hat{j}_p is defined above in Eq. (VI7). The total (i.e. physical) macroscopic (i.e. $q = 0$) current operator, which measures the linear response of the system to a static and uniform vector potential $\mathbf{A}_0 = A_0 \hat{\mathbf{u}}$, contains the above paramagnetic contribution but also a *diamagnetic* one. This can be easily seen by coupling the 1D EFK model to \mathbf{A}_0 on the lattice via the Peierls substitution. The linear response of the system to \mathbf{A}_0 requires to expand the Peierls-coupled EFK model up to the second order in A_0 :

$$\hat{J}_{\text{phys}} = \hat{j}_p - \frac{e}{c} A_0 \frac{a^2}{\hbar^2} \hat{\mathcal{T}}. \quad (\text{VI11})$$

Here we have introduced the “kinetic” operator:

$$\hat{\mathcal{T}} \equiv \sum_{k \in \text{FBZ}} \sum_{\alpha, \beta} \hat{c}_{k,\alpha}^\dagger \mathcal{T}_{\alpha\beta}(k) \hat{c}_{k,\beta} = 2 \sum_{k \in \text{FBZ}} \left(\hat{c}_{k,s}^\dagger, \hat{c}_{k,p}^\dagger \right) \begin{pmatrix} -t \cos ka & i\tilde{t} \sin ka \\ -i\tilde{t} \sin ka & t \cos ka \end{pmatrix} \begin{pmatrix} \hat{c}_{k,s} \\ \hat{c}_{k,p} \end{pmatrix}, \quad (\text{VI12})$$

where we have introduced the following second derivative of the Hamiltonian with respect to k :

$$\mathcal{T}_{\alpha\beta}(k) \equiv -\frac{1}{a^2} \frac{\partial^2 H_{\alpha\beta}(k)}{\partial k^2}. \quad (\text{VI13})$$

As discussed, for example, in the Supplemental Material of Ref. [S8], gauge invariance ensures that the system cannot generate a finite physical current in response to a static and spatially uniform vector potential, i.e.,

$$\langle \hat{J}_{\text{phys}} \rangle = \frac{e}{c} \chi_{j_p j_p} A_0 - \frac{e}{c} A_0 \frac{a^2}{\hbar^2} \langle \hat{\mathcal{T}} \rangle = \frac{e}{c} \left(\chi_{j_p j_p} - \frac{a^2}{\hbar^2} \langle \hat{\mathcal{T}} \rangle \right) A_0 = 0 \quad \forall A_0, \quad (\text{VI14})$$

where $\chi_{j_p j_p}$ is the $\omega = 0$ and $q \rightarrow 0$ limit of the paramagnetic current-current response function, explicitly given by:

$$\begin{aligned} \chi_{j_p j_p} &\equiv \lim_{q \rightarrow 0} \chi_{j_p; q, j_p; -q}(\omega = 0) = \lim_{q \rightarrow 0} \frac{1}{L} \sum_{n, m} \sum_{k \in \text{FBZ}} \frac{f_{n,k} - f_{m,k+q}}{\varepsilon_{n,k} - \varepsilon_{m,k+q}} \langle \psi_{n,k} | \hat{\mathbf{j}}_{p; q} \cdot \hat{\mathbf{u}} | \psi_{m,k+q} \rangle \langle \psi_{m,k+q} | \hat{\mathbf{j}}_{p; -q} \cdot \hat{\mathbf{u}} | \psi_{n,k} \rangle \\ &= -\frac{1}{L} \sum_n \sum_{k \in \text{FBZ}} \delta(\varepsilon_{n,k}) |\langle \psi_{n,k} | \hat{\mathbf{j}}_p | \psi_{n,k} \rangle|^2 \\ &\quad + \sum_{n \neq m} \frac{1}{L} \sum_{k \in \text{FBZ}} \frac{f_{n,k} - f_{m,k}}{\varepsilon_{n,k} - \varepsilon_{m,k}} |\langle \psi_{n,k} | \hat{\mathbf{j}}_p | \psi_{m,k} \rangle|^2 = -\frac{2}{L} \sum_{k \in \text{FBZ}} \frac{|\langle \psi_{+,k} | \hat{\mathbf{j}}_p | \psi_{-,k} \rangle|^2}{\varepsilon_{+,k} - \varepsilon_{-,k}}, \end{aligned} \quad (\text{VI15})$$

where $L = Na$ is the lattice length and N is the number of unit cells in the lattice. We have also employed the zero-temperature limit of the Fermi-Dirac distribution, i.e., $f_{n,k} \rightarrow \Theta(\mu - \varepsilon_{n,k})$. The first term in the second line of

Eq. (VI15) is zero when the chemical potential $\mu = 0$ is chosen to lie within the insulating gap. On the other hand, the zero-temperature expectation value of the kinetic operator is given by

$$\langle \hat{T} \rangle = \frac{1}{N} \sum_{n=\pm} \sum_{k \in \text{FBZ}} \Theta(-\varepsilon_{n,k}) \langle \psi_{n,k} | \hat{T} | \psi_{n,k} \rangle = \frac{1}{N} \sum_{k \in \text{FBZ}} \langle \psi_{-,k} | \hat{T} | \psi_{-,k} \rangle . \quad (\text{VI16})$$

The TRK sum rule (VI14) at temperature $T = 0$ for the 1D EFK model can thus be written as:

$$-\frac{2}{L} \sum_{k \in \text{FBZ}} \frac{|\langle \psi_{+,k} | \hat{j}_p | \psi_{-,k} \rangle|^2}{\varepsilon_{+,k} - \varepsilon_{-,k}} = \frac{a^2}{N \hbar^2} \sum_{k \in \text{FBZ}} \langle \psi_{-,k} | \hat{T} | \psi_{-,k} \rangle . \quad (\text{VI17})$$

We start by evaluating the relevant current operator matrix element:

$$\langle \psi_{+,k} | \hat{j}_p | \psi_{-,k} \rangle = j_{p;+-}(k) = \sum_{\alpha, \beta} [U_{+,k}^\dagger]_\alpha j_{p;\alpha\beta}(k) [U_{-,k}]_\beta . \quad (\text{VI18})$$

The argument of the FBZ sum in Eq. (VI14) is therefore

$$\frac{|\langle \psi_{+,k} | \hat{j}_p | \psi_{-,k} \rangle|^2}{\varepsilon_{+,k} - \varepsilon_{-,k}} = \frac{2a^2 \tilde{t}^2 (\delta \cos ka - 2t)^2}{\hbar^2 \varepsilon_k^3} . \quad (\text{VI19})$$

We take the thermodynamic limit,

$$\frac{1}{N} \sum_{k \in \text{FBZ}} \rightarrow \frac{1}{2\pi} \int_{-\pi}^{\pi} d(ka) , \quad (\text{VI20})$$

and find

$$-\frac{\hbar^2}{a^2} \frac{2}{L} \sum_{k \in \text{FBZ}} \frac{|\langle \psi_{+,k} | \hat{j}_p | \psi_{-,k} \rangle|^2}{\varepsilon_{+,k} - \varepsilon_{-,k}} \rightarrow -\frac{2}{\pi} \int_0^\pi d(ka) \frac{2(\delta \cos ka - 2t)^2}{\tilde{t} (4 \sin^2 ka + (\delta - 2t \cos ka)^2 / \tilde{t}^2)^{3/2}} , \quad (\text{VI21})$$

where the integration domain was reduced due to parity of the integrand. We proceed to explicitly evaluate the kinetic operator expectation value, i.e.

$$\begin{aligned} \langle \hat{T} \rangle &= \frac{1}{N} \sum_{\alpha, \beta} \sum_{k \in \text{FBZ}} [U_{-,k}^\dagger]_\alpha \mathcal{T}_{\alpha\beta}(k) [U_{-,k}]_\beta \\ &= \frac{1}{N} \sum_{k \in \text{FBZ}} \frac{2[t \cos ka (\delta - 2t \cos ka) - 2\tilde{t}^2 \sin^2 ka]}{\tilde{t} (4 \sin^2 ka + (\delta - 2t \cos ka)^2 / \tilde{t}^2)^{1/2}} \\ &\rightarrow \frac{2}{\pi} \int_0^\pi d(ka) \frac{t \cos ka (\delta - 2t \cos ka) - 2\tilde{t}^2 \sin^2 ka}{\tilde{t} (4 \sin^2 ka + (\delta - 2t \cos ka)^2 / \tilde{t}^2)^{1/2}} . \end{aligned} \quad (\text{VI22})$$

The TRK sum rule

$$\chi_{j_p j_p} = \frac{a^2}{\hbar^2} \langle \hat{T} \rangle \quad (\text{VI23})$$

thus reduces to an identity between two integrals:

$$\int_0^\pi dx \frac{2(\delta \cos x - 2t)^2}{(4 \sin^2 x + (\delta - 2t \cos x)^2 / \tilde{t}^2)^{3/2}} = \int_0^\pi dx \frac{2\tilde{t}^2 \sin^2 x - t \cos x (\delta - 2t \cos x)}{(4 \sin^2 x + (\delta - 2t \cos x)^2 / \tilde{t}^2)^{1/2}} . \quad (\text{VI24})$$

The correctness of the previous equality can be easily verified by evaluating the integral of the difference between the two integrand functions. Defining:

$$F(x) \equiv \frac{2(\delta \cos x - 2t)^2}{(4 \sin^2 x + (\delta - 2t \cos x)^2 / \tilde{t}^2)^{3/2}} , \quad (\text{VI25})$$

$$G(x) \equiv \frac{2\tilde{t}^2 \sin^2 x - t \cos x (\delta - 2t \cos x)}{(4 \sin^2 x + (\delta - 2t \cos x)^2 / \tilde{t}^2)^{1/2}} , \quad (\text{VI26})$$

we obtain

$$\int_0^\pi dx \left[F(x) - G(x) \right] = \frac{[2(t^2 - \tilde{t}^2) \cos x - \delta t]}{[\delta^2 + 2(t^2 + \tilde{t}^2) - 4\delta t \cos x + 2(t^2 - \tilde{t}^2) \cos 2x]^{1/2}} \sin x \Big|_0^\pi = 0, \quad (\text{VI27})$$

thus proving the TRK sum rule for the noninteracting 1D EFK model.

Appendix VII: Isolation of the non-trivial geometric terms

The Gaussian approximation introduced in Eq. (22) of the main text allows us to decompose the \mathbf{k} -space hopping gradient $f_i(\mathbf{k})$, effectively isolating non-trivial quantum geometric terms, as demonstrated in Eqs. (25) and (26) of the main text:

$$M_{ij}(\mathbf{k}) = M_{ij}^{\text{H}}(\mathbf{k}) + M_{ij}^{\text{E}}(\mathbf{k}) + M_{ij}^{\text{E-g}}(\mathbf{k}) + M_{ij}^{\text{g}}(\mathbf{k}), \quad (\text{VII1})$$

where we introduced the following quantities:

$$M_{ij}^{\text{H}}(\mathbf{k}) \equiv \delta_{ij} \gamma h(\mathbf{k}), \quad (\text{VII2})$$

$$M_{ij}^{\text{E}}(\mathbf{k}) \equiv -\gamma^2 \sum_n \partial_i \partial_j E_n(\mathbf{k}) P_n(\mathbf{k}), \quad (\text{VII3})$$

$$M_{ij}^{\text{E-g}}(\mathbf{k}) \equiv -\gamma^2 \sum_n \partial_i E_n(\mathbf{k}) \partial_j P_n(\mathbf{k}) + (i \leftrightarrow j), \quad (\text{VII4})$$

$$M_{ij}^{\text{g}}(\mathbf{k}) \equiv -\gamma^2 \sum_n E_n(\mathbf{k}) \partial_i \partial_j P_n(\mathbf{k}). \quad (\text{VII5})$$

Here, $M_{ij}^{\text{H}}(\mathbf{k})$ is directly proportional to the Hamiltonian $h(\mathbf{k})$ and $M_{ij}^{\text{E-g}}(\mathbf{k})$ is a cross term, which depends on both energy dispersion and quantum geometry. Therefore, using Eqs. (IV3) and (IV4), together with the decomposition $f_i(\mathbf{k}) = f_i^{\text{E}}(\mathbf{k}) + f_i^{\text{g}}(\mathbf{k})$ of the \mathbf{k} -space hopping gradient provided in the main text and the analogous decomposition for the Hessian tensor given in Eqs. (VII1)-(VII5), we obtain the following explicit formulas for the geometric term $\mathcal{D}_{\text{g}}(\mathbf{q}) \equiv \mathcal{D}_{\text{g}}^{(1)}(\mathbf{q}) + \mathcal{D}_{\text{g}}^{(2)}(\mathbf{q})$:

$$[\mathcal{D}_{\text{g}}^{(1)}(\mathbf{q})]_{\nu i}^{\nu' j} = \frac{1}{\sqrt{M_\nu M_{\nu'}}} \frac{2}{N} \sum_n \sum_{n'} \sum_{\mathbf{k}}^{\text{occ. unocc. FBZ}} \left\{ \frac{[F_i(n\mathbf{k}, n'\mathbf{k} + \mathbf{q})]_\nu [F_j(n'\mathbf{k} + \mathbf{q}, n\mathbf{k})]_{\nu'}}{E_n(\mathbf{k}) - E_{n'}(\mathbf{k} + \mathbf{q})} + \right. \\ \left. - \frac{[F_i^{\text{E}}(n\mathbf{k}, n'\mathbf{k} + \mathbf{q})]_\nu [F_j^{\text{E}}(n'\mathbf{k} + \mathbf{q}, n\mathbf{k})]_{\nu'}}{E_n(\mathbf{k}) - E_{n'}(\mathbf{k} + \mathbf{q})} \right\} + \text{H.c.}, \quad (\text{VII6})$$

$$[\mathcal{D}_{\text{g}}^{(2)}(\mathbf{q})]_{\nu i}^{\nu' j} = \frac{1}{\sqrt{M_\nu M_{\nu'}}} \frac{2}{N} \sum_{\tilde{\nu}} \sum_n \sum_{\mathbf{k}, \tilde{\mathbf{k}}}^{\text{occ. FBZ}} \sum_{\alpha \alpha'} \left[\delta_{\nu \nu'} \delta_{\tilde{\mathbf{k}}, \mathbf{0}} - \delta_{\tilde{\nu} \nu'} \delta_{\tilde{\mathbf{k}}, \mathbf{q}} \right] \times \\ \times \left\{ \left[M_{ij}^{\text{g}}(\mathbf{k} + \tilde{\mathbf{k}}) \right]_{\nu \alpha}^{\tilde{\nu} \alpha'} + \left[M_{ij}^{\text{E-g}}(\mathbf{k} + \tilde{\mathbf{k}}) \right]_{\nu \alpha}^{\tilde{\nu} \alpha'} \right\} [P_n(\mathbf{k})]_{\tilde{\nu} \alpha'}^{\nu \alpha} + \text{H.c.}, \quad (\text{VII7})$$

where we have introduced the following quantities:

$$[F_i^{\text{E}}(n\mathbf{k}, n'\mathbf{k}')]_{\nu} = \sum_{\tilde{\nu}} \sum_{\nu_1 \nu_2} \sum_{\alpha \alpha'} [U_n^\dagger(\mathbf{k})]_{\nu_1 \alpha} \left\{ \delta_{\nu \nu_1} \delta_{\tilde{\nu} \nu_2} [f_i^{\text{E}}(\mathbf{k}')]_{\nu \alpha}^{\tilde{\nu} \alpha'} - \delta_{\nu \nu_2} \delta_{\tilde{\nu} \nu_1} [f_i^{\text{E}}(\mathbf{k})]_{\tilde{\nu} \alpha}^{\nu \alpha'} \right\} [U_{n'}(\mathbf{k}')]_{\nu_2 \alpha'}, \quad (\text{VII8})$$

$$[F_i^{\text{g}}(n\mathbf{k}, n'\mathbf{k}')]_{\nu} = \sum_{\tilde{\nu}} \sum_{\nu_1 \nu_2} \sum_{\alpha \alpha'} [U_n^\dagger(\mathbf{k})]_{\nu_1 \alpha} \left\{ \delta_{\nu \nu_1} \delta_{\tilde{\nu} \nu_2} [f_i^{\text{g}}(\mathbf{k}')]_{\nu \alpha}^{\tilde{\nu} \alpha'} - \delta_{\nu \nu_2} \delta_{\tilde{\nu} \nu_1} [f_i^{\text{g}}(\mathbf{k})]_{\tilde{\nu} \alpha}^{\nu \alpha'} \right\} [U_{n'}(\mathbf{k}')]_{\nu_2 \alpha'}, \quad (\text{VII9})$$

$$[F_i(n\mathbf{k}, n'\mathbf{k}')]_{\nu} = [F_i^{\text{E}}(n\mathbf{k}, n'\mathbf{k}')]_{\nu} + [F_i^{\text{g}}(n\mathbf{k}, n'\mathbf{k}')]_{\nu} \quad (\text{VII10})$$

Notice here the hermitian conjugate is taking the conjugate and transposing the ν index.

We now show that also $\mathcal{D}_g(\mathbf{q})$ alone satisfies the acoustic sum rule. In fact, the sum rule can be shown to hold separately for $\mathcal{D}_g^{(1)}$ and $\mathcal{D}_g^{(2)}$. First we have, starting from formula (VII6) given below:

$$\sum_{\nu'} \sqrt{M_{\nu'}} [\mathcal{D}_g^{(1)}(\mathbf{0})]_{\nu i}^{\nu' j} = \frac{1}{\sqrt{M_{\nu}}} \frac{2}{N} \sum_n \sum_{n'} \sum_{\mathbf{k}}^{\text{occ. FBZ}} \left\{ \frac{[F_i(n\mathbf{k}, n'\mathbf{k})]_{\nu} \sum_{\nu'} [F_j(n'\mathbf{k}, n\mathbf{k})]_{\nu'}}{E_n(\mathbf{k}) - E_{n'}(\mathbf{k})} + \right. \\ \left. - \frac{[F_i^E(n\mathbf{k}, n'\mathbf{k})]_{\nu} \sum_{\nu'} [F_j^E(n'\mathbf{k}, n\mathbf{k})]_{\nu'}}{E_n(\mathbf{k}) - E_{n'}(\mathbf{k})} \right\} + \text{H.c.} \quad (\text{VII11})$$

Using expression (VII9), we get

$$\sum_{\nu} [F_i(n\mathbf{k}, n'\mathbf{k})]_{\nu} = \sum_{\nu\bar{\nu}} \sum_{\nu_1\nu_2} \sum_{\alpha\alpha'} [U_n^\dagger(\mathbf{k})]_{\nu_1\alpha} \left\{ \delta_{\nu\nu_1} \delta_{\bar{\nu}\nu_2} [f_i(\mathbf{k})]_{\nu\alpha}^{\bar{\nu}\alpha'} - \delta_{\nu\nu_2} \delta_{\bar{\nu}\nu_1} [f_i(\mathbf{k})]_{\nu\alpha}^{\bar{\nu}\alpha'} \right\} [U_{n'}(\mathbf{k})]_{\nu_2\alpha'} \\ = \sum_{\nu\bar{\nu}} \sum_{\alpha\alpha'} \left\{ [U_n^\dagger(\mathbf{k})]_{\nu\alpha} [f_i(\mathbf{k})]_{\nu\alpha}^{\bar{\nu}\alpha'} [U_{n'}(\mathbf{k})]_{\bar{\nu}\alpha'} - [U_n^\dagger(\mathbf{k})]_{\bar{\nu}\alpha} [f_i(\mathbf{k})]_{\bar{\nu}\alpha}^{\nu\alpha'} [U_{n'}(\mathbf{k})]_{\nu\alpha'} \right\} \\ = 0, \quad (\text{VII12})$$

and identically we can show that $\sum_{\nu} [F_i^E(n\mathbf{k}, n'\mathbf{k})]_{\nu} = 0$, thus proving $\sum_{\nu'} [\mathcal{D}_g^{(1)}(\mathbf{0})]_{\nu i}^{\nu' j} = 0$.

For the second-order term, the calculation is straightforward:

$$\sum_{\nu'} \sqrt{M_{\nu'}} [\mathcal{D}_g^{(2)}(\mathbf{0})]_{\nu i}^{\nu' j} = \frac{1}{\sqrt{M_{\nu}}} \frac{2}{N} \sum_{\nu'\bar{\nu}} \sum_n \sum_{\mathbf{k}\tilde{\mathbf{k}}}^{\text{occ. FBZ}} \sum_{\alpha\alpha'} \left[\delta_{\nu\nu'} \delta_{\tilde{\mathbf{k}}, \mathbf{0}} - \delta_{\bar{\nu}\nu'} \delta_{\tilde{\mathbf{k}}, \mathbf{0}} \right] \times \\ \times \left\{ \left[[M_{ij}^g(\mathbf{k} + \tilde{\mathbf{k}})]_{\nu\alpha}^{\bar{\nu}\alpha'} + [M_{ij}^{E-g}(\mathbf{k} + \tilde{\mathbf{k}})]_{\nu\alpha}^{\bar{\nu}\alpha'} \right] [P_n(\mathbf{k})]_{\bar{\nu}\alpha'}^{\nu\alpha} \right\} + \text{H.c.} \quad (\text{VII13}) \\ = \frac{1}{\sqrt{M_{\nu}}} \frac{2}{N} \sum_{\nu'\bar{\nu}} \sum_n \sum_{\mathbf{k}}^{\text{occ. FBZ}} \sum_{\alpha\alpha'} [\delta_{\nu\nu'} - \delta_{\bar{\nu}\nu'}] \times \\ \times \left\{ \left[[M_{ij}^g(\mathbf{k})]_{\nu\alpha}^{\bar{\nu}\alpha'} + [M_{ij}^{E-g}(\mathbf{k})]_{\nu\alpha}^{\bar{\nu}\alpha'} \right] [P_n(\mathbf{k})]_{\bar{\nu}\alpha'}^{\nu\alpha} \right\} + \text{H.c.} .$$

Since the quantity inside the braces does not depend on ν' , we immediately get $\sum_{\nu'} [\delta_{\nu\nu'} - \delta_{\bar{\nu}\nu'}] = 1 - 1 = 0$, thus proving the sum rule $\sum_{\nu'} \sqrt{M_{\nu'}} [\mathcal{D}_g^{(2)}(\mathbf{0})]_{\nu i}^{\nu' j}$. Therefore, the entire geometric contribution satisfies

$$\sum_{\nu'} \sqrt{M_{\nu'}} [\mathcal{D}_g(\mathbf{q} = \mathbf{0})]_{\nu i}^{\nu' j} = 0, \quad (\text{VII14})$$

thus enforcing the presence of two massless acoustic modes.

Appendix VIII: Further details on the case of graphene

In order to obtain a complete description of electrons and phonons in graphene, as well as extract the relevant parameters of the hopping function within the Gaussian approximation, we have carried out *ab initio* density functional theory (DFT) and density-functional perturbation theory (DFPT) [S9] calculations using Quantum ESPRESSO (QE) [S10, S11].

The necessary pseudopotentials were taken from the standard solid-state pseudopotential (SSSP) accuracy library [S12, S13]. The exchange-correlation potential was treated in the Generalized Gradient Approximation (GGA), as parametrized by the Perdew-Burke-Ernzerhof (PBE) formula [S14], with the vdW-D2 correction proposed by Grimme [S15]. For integrations over the FBZ, we employed a Methfessel-Paxton smearing function [S16] of 10^{-2} Ryd. A dense Monkhorst-Pack (MP) [S17] \mathbf{k} -point grid with $96 \times 96 \times 1$ points is chosen to sample for self-consistent calculations of the charge density. The equilibrium lattice parameter of graphene is $a = 2.467$ Å. We considered a simulation cell with approximately 22 Å of vacuum between periodic images along the c -direction. We also introduced a 2D Coulomb cutoff for a better description of phonons at small wave vectors [S18].

The next-nearest-neighbor (NNN) Born-von Karman model for in-plane phonon dispersion has four force constants $\alpha, \beta, \gamma, \delta$ as free parameters. These parameters are optimized via least absolute deviations fitting to DFPT results.

The electronic dispersion in graphene is described by a next-next-nearest-neighbor (NNNN) tight-binding model [S19], which depends on seven parameters: three hopping integrals $t^{(i)}$, three overlap integrals $s^{(i)}$ with $i = 1, 2, 3$, and an on-site energy ε_{p_z} . The latter parameter can be set equal to zero due to gauge freedom. The remaining six physical parameters are determined via a least-squares procedure applied to the results of our DFT calculations. The results of this procedure are reported in Fig. 1(a). Fixing the six above-mentioned parameters allows us to reconstruct the Bloch Hamiltonian $h(\mathbf{k})$ on the entire FBZ, thus obtaining the Bloch eigenvectors $U_n(\mathbf{k})$ and the electron bands $E_n(\mathbf{k})$ with $\mathbf{k} \in \text{FBZ}$. The reconstructed Hamiltonian is then regularized following the standard prescription [S20]

$$h(\mathbf{k}) \rightarrow h(\mathbf{k}) + \begin{pmatrix} \Delta/2 & 0 \\ 0 & -\Delta/2 \end{pmatrix}, \quad (\text{VIII1})$$

fixing a gap Δ at the Dirac point. The effect of the gap size is discussed in the main text. The regularized Fubini-Study metric and Berry curvature are shown in Fig. 2(a)-(d). We note that the overlap matrix is close to unity, and the parameters $s^{(i)}$ can thus be set to zero without significantly affecting the numerical results.

The hopping functions in graphene are modeled within the Gaussian approximation (Eq. (22) in the main text):

$$t_{AB}^{p_z p_z}(r) = t_{AB}^{p_z p_z}(0) \exp\left(\frac{1}{2}\gamma_{AB}r^2\right), \quad t_{AA}^{p_z p_z}(r) = t_{AA}^{p_z p_z}(0) \exp\left(\frac{1}{2}\gamma_{AA}r^2\right). \quad (\text{VIII2})$$

Clearly, NN- and NNNN-type hopping integrals are parametrized by the first of the two equations above, while NNN-type hopping integrals are parametrized by the second one. The spatial dependence of the hopping integrals is determined as follows: after calculating the hopping integrals $t^{(1,2,3)}$ for a relaxed graphene lattice with lattice constant a , starting from the band structure as discussed above, the procedure is repeated by calculating electron bands on strained graphene lattices, i.e. graphene lattices whose lattice spacing a^* is imposed to be $a^* \neq a$. This approach allows us to extract sufficient information about the spatial dependence of $t^{(1,2,3)}(r)$ to perform a Gaussian interpolation, as shown in Fig. 1(b). From this interpolation, the relevant parameters are estimated to be $\gamma_{AA} = -1.37 \text{ \AA}^{-2}$ and $\gamma_{AB} = -1.10 \text{ \AA}^{-2}$. In calculating the numeric result, for simplicity, a single effective parameter $\gamma_{\text{eff}} = -1.18 \text{ \AA}^{-2}$ was employed to parametrize both $t_{AA}(\mathbf{r})$ and $t_{AB}(\mathbf{r})$, changing the sign of the amplitude accordingly, with $t_{AB}^{p_z p_z}(0) = -t_{AA}^{p_z p_z}(0) = -9.462 \text{ eV}$.

Summations over electron wave vectors $\mathbf{k} \in \text{FBZ}$ appearing in Eqs. (IV3)-(IV4) have been carried out on a $N = 600 \times 600$ -dense partition of the FBZ. The evaluation of $\mathcal{D}_g(\mathbf{q})$ at fixed \mathbf{q} was repeated for each phonon wave vector $\mathbf{q} \in \Gamma\text{K}\Gamma$. We note that, as shown by comparing Fig. 4(a)-(b) in the main text with Fig. 1(c)-(d), the behavior of the acoustic modes for $\mathbf{q} \rightarrow \Gamma$ is invariant under rotations.

Appendix IX: Analytical results of the gapless and gapped Dirac fermions

In this section, we consider the contribution of a single Dirac node of the graphene to $\mathcal{D}_g(\mathbf{q})$ in the long-wavelength limit. To this end, we consider the following effective Hamiltonian, which characterizes a single Dirac node in graphene

$$h(\mathbf{k}) = v_F \begin{pmatrix} 0 & k_x - ik_y \\ k_x + ik_y & 0 \end{pmatrix} \quad (\text{IX1})$$

We restrict our analysis to electrons near the Dirac node with momenta satisfying $|\mathbf{k}| < \Lambda$, where Λ is an ultraviolet cutoff. The eigenvalues and eigenfunctions of the Dirac Hamiltonian are given by

$$\epsilon_{\pm, \mathbf{k}} = \pm v_F |\mathbf{k}|, \quad U_+(\mathbf{k}) = \frac{1}{\sqrt{2}|\mathbf{k}|} \begin{pmatrix} |\mathbf{k}| \\ k_x + ik_y \end{pmatrix}, \quad U_-(\mathbf{k}) = \frac{1}{\sqrt{2}|\mathbf{k}|} \begin{pmatrix} ik_y - k_x \\ |\mathbf{k}| \end{pmatrix}. \quad (\text{IX2})$$

Our primary focus is on the behavior of the acoustic mode. To this end, we project the force constant matrix onto the acoustic mode, which is characterized by the eigenvector $[v^{\text{ac}}]_\nu = \frac{1}{\sqrt{2}}$. Since there are only two atoms with the same mass within the unit cell of the graphene, the vector v^{ac} takes the same value for all its components. The force constant matrix elements after projection onto the acoustic mode are given by

$$\begin{aligned} [\mathcal{D}_g^{\text{ac}}(\mathbf{q})]_i^j &= \sum_{\nu\nu'} [v^{\text{ac}}]_\nu^* [\mathcal{D}_g(\mathbf{q})]_{\nu i}^{\nu' j} [v^{\text{ac}}]_{\nu'} \\ [\mathcal{D}_{\text{el}}^{\text{ac}}(\mathbf{q})]_i^j &= \sum_{\nu\nu'} [v^{\text{ac}}]_\nu^* [\mathcal{D}^{(\text{el})}(\mathbf{q})]_{\nu i}^{\nu' j} [v^{\text{ac}}]_{\nu'} \end{aligned} \quad (\text{IX3})$$

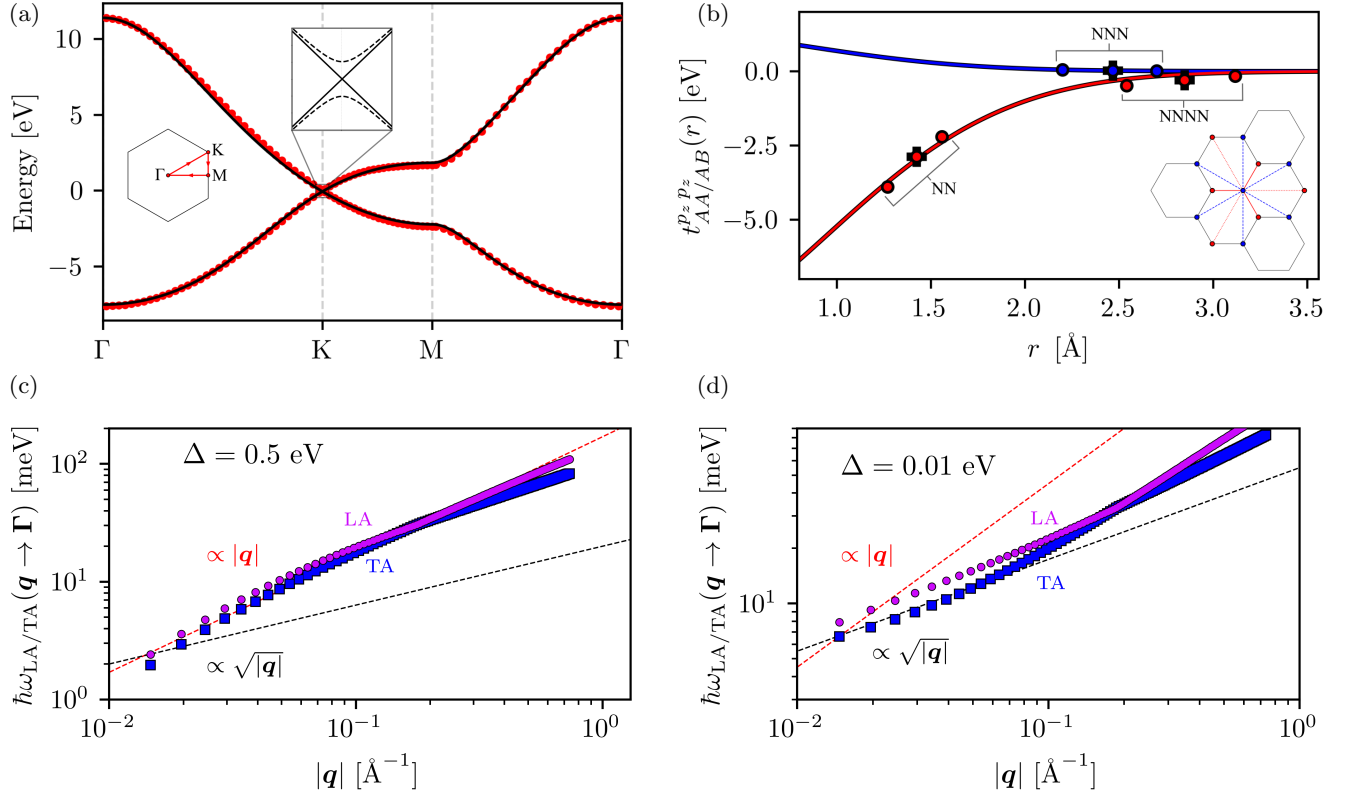


FIG. 1. (Color online) (a) Plot of the π bands of graphene along the high-symmetry $\Gamma\text{K}\text{M}\Gamma$ path in the first Brillouin zone. Red circles: Results of the *ab initio* DFT calculations. Black line: best fit based on our analytical overlap-inclusive NNNN model. Inset shows the low-energy electron dispersion near the Dirac point for $\Delta = 0$ (solid black line) and $\Delta = 10$ meV (dotted black line), corresponding respectively to massless and massive Dirac fermions. (b) Hopping integrals generating the graphene's π bands, obtained via the strained-lattice method. Red circles: inter-sublattice (AB) hopping integrals. Blue dots: intra-sublattice (AA) hopping integrals. Both are obtained as optimal parameters from a least-square best-fit procedure on the *ab initio* bands of strained lattices. Black crosses: hopping integrals in a relaxed graphene lattice. Red (blue) lines: Gaussian best fit to the inter- (intra-) sublattice hopping integral as a function of the inter-atomic distance r . The inset shows the hierarchy of nearest neighbors in a honeycomb lattice. (c)-(d) Behavior of the acoustic modes near Γ for (c) $|\mathbf{q}| \lesssim q_{\text{thr}} = \Delta/\hbar v_F$ and (d) $|\mathbf{q}| \gtrsim q_{\text{thr}}$, as illustrated in Fig. 4 of the main text; here, \mathbf{q} is on the $\text{M} \rightarrow \Gamma$ portion of the high-symmetry contour.

where $i, j \in \{x, y\}$. $[\mathcal{D}_{\text{g}}^{\text{ac}}(\mathbf{q})]$ and $[\mathcal{D}_{\text{el}}^{\text{ac}}(\mathbf{q})]$ denote the geometric contribution and total electronic contribution respectively. $[\mathcal{D}_{\text{g}}^{\text{ac}}(\mathbf{q})]$ and $[\mathcal{D}_{\text{el}}^{\text{ac}}(\mathbf{q})]$ can be calculated directly via Eq. (VII6) and Eq. (IV2).

We now aim to evaluate the behaviors of $[\mathcal{D}_{\text{g}}^{\text{ac}}(\mathbf{q})]$, $[\mathcal{D}_{\text{el}}^{\text{ac}}(\mathbf{q})]$ in the long-wavelength limit $\mathbf{q} \rightarrow \mathbf{0}$. We first show that the total electronic contribution vanishes: $[\mathcal{D}_{\text{el}}^{\text{ac}}(\mathbf{q})]_i^j = 0$. As in Eqs. (IV3) and (IV4), we introduce

$$[\mathcal{D}_{\text{el},1}^{\text{ac}}(\mathbf{q})] = \sum_{\nu\nu'} [v^{\text{ac}}]_{\nu}^* [\mathcal{D}^{(\text{el},1)}(\mathbf{q})]_{\nu i}^{\nu' j} [v^{\text{ac}}]_{\nu'}, \quad [\mathcal{D}_{\text{el},2}^{\text{ac}}(\mathbf{q})] = \sum_{\nu\nu'} [v^{\text{ac}}]_{\nu}^* [\mathcal{D}^{(\text{el},2)}(\mathbf{q})]_{\nu i}^{\nu' j} [v^{\text{ac}}]_{\nu'} \quad (\text{IX4})$$

where $[\mathcal{D}_{\text{el}}^{\text{ac}}(\mathbf{q})] = [\mathcal{D}_{\text{el},2}^{\text{ac}}(\mathbf{q})] + [\mathcal{D}_{\text{el},1}^{\text{ac}}(\mathbf{q})]$. In a more compact form,

$$[\mathcal{D}_{\text{el},1}^{\text{ac}}(\mathbf{q})]_i^j = \frac{1}{M_{\text{CN}}} \sum_n^{\text{occ.}} \sum_{n'}^{\text{unocc.}} \sum_{\mathbf{k}}^{\text{FBZ}} \frac{\text{Tr} \left[P_n(\mathbf{k}) \cdot [f_i(\mathbf{k} + \mathbf{q}) - f_i(\mathbf{k})] \cdot P_{n'}(\mathbf{k} + \mathbf{q}) \cdot [f_j(\mathbf{k}) - f_j(\mathbf{k} + \mathbf{q})] \right]}{E_n(\mathbf{k}) - E_{n'}(\mathbf{k} + \mathbf{q})} + \text{H.c.},$$

$$[\mathcal{D}_{\text{el},2}^{\text{ac}}(\mathbf{q})]_i^j = \frac{1}{M_{\text{CN}}} \sum_n^{\text{occ.}} \sum_{\mathbf{k}}^{\text{FBZ}} \text{Tr} \left[\left(M_{ij}(\mathbf{k}) - M_{ij}(\mathbf{k} + \mathbf{q}) \right) \cdot P_n(\mathbf{k}) \right] + \text{H.c.}, \quad (\text{IX5})$$

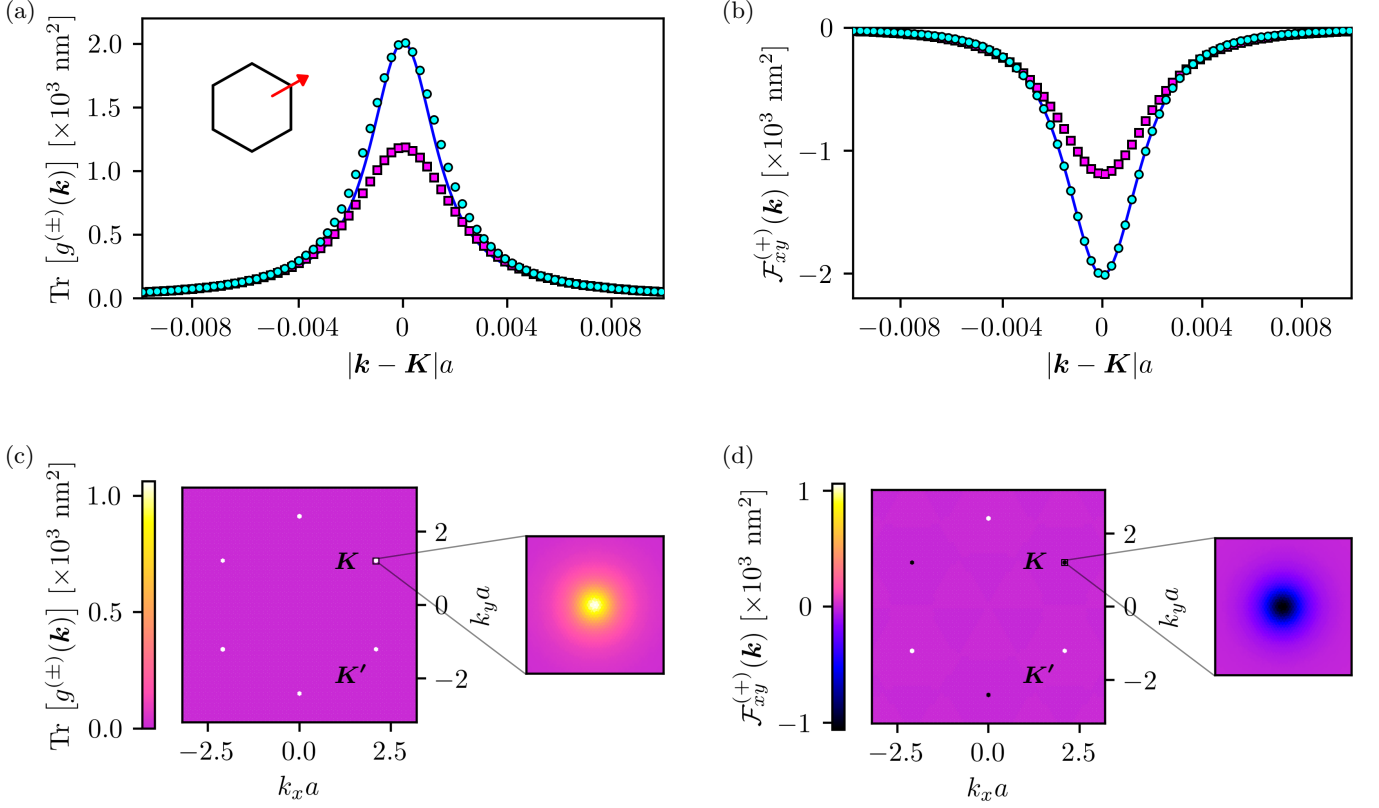


FIG. 2. (Color online) Regularized QGT for gapped graphene. For better illustration, results in this figure have been calculated with a large gap of $\Delta = 20$ meV. (a) Trace of the Fubini-Study metric $g_{ij}^{(\pm)}(\mathbf{k})$ — which is the same for both conduction and valence bands due to the quasi-exact particle-hole symmetry in the vicinity of the \mathbf{K} point—plotted along the path in the FBZ shown as a red arrow in the inset. Cyan circles: numerical results obtained within the NN tight-binding model. Magenta squares: analytical results obtained within the NNNN model. Solid blue line: analytical results for massive Dirac fermions. (b) The only non-zero component of the conduction-band Berry curvature, $\mathcal{F}_{xy}^{(+)}(\mathbf{k}) \equiv -2 \text{Im } \mathcal{Q}_{xy}^{(+)}(\mathbf{k}) = \mathcal{F}_{yx}^{(-)}(\mathbf{k})$, plotted along the same path as in panel (a). The valence-band curvature is identical apart from a sign. Legend is the same as in panel (a). (c)-(d) 2D color plots of $g_{ij}^{(\pm)}(\mathbf{k})$ and $\mathcal{F}_{xy}^{(+)}(\mathbf{k})$ calculated within the NNNN model as functions of \mathbf{k} . The insets provide a zoom-in view of the \mathbf{K} point, where the singularity discussed in the text has been cured.

where \cdot denotes the matrix product. For the case of a single Dirac node, we observe that

$$\begin{aligned} f_i(\mathbf{k}) &= i\gamma \partial_{k_i} h(\mathbf{k}) = i\gamma \hbar v_F \sigma_i, \\ M_{ij}(\mathbf{k}) &= (\gamma \delta_{ij} - \gamma^2 \partial_{k_i, k_j}^2) h(\mathbf{k}) = \gamma \delta_{ij} h(\mathbf{k}). \end{aligned} \quad (\text{IX6})$$

From $f_i(\mathbf{k}) = i\gamma \hbar v_F \sigma_i$, we find

$$f_i(\mathbf{k} + \mathbf{q}) - f_i(\mathbf{k}) = 0, \quad (\text{IX7})$$

thus concluding that $[\mathcal{D}_{\text{el},1}^{\text{ac}}(\mathbf{q})] = 0$. The total electronic contribution to the dynamical matrix, projected on the acoustic mode, is vanishing:

$$\begin{aligned} [\mathcal{D}_{\text{el}}^{\text{ac}}(\mathbf{q})]_j^i &= \frac{1}{M_{CN}} \sum_n^{\text{occ.}} \frac{1}{\Omega} \int_{|\mathbf{k}| < \Lambda} \delta_{ij} \gamma \text{Tr} \left[\left(h(\mathbf{k}) - h(\mathbf{k} + \mathbf{q}) \right) \cdot P_n(\mathbf{k}) \right] \\ &= \delta_{ij} \gamma \frac{v_F}{M_{CN}} \sum_n^{\text{occ.}} \frac{1}{\Omega} \int_{|\mathbf{k}| < \Lambda} \text{Tr} \left[(q_x \sigma^x + q_y \sigma^y) \cdot P_n(\mathbf{k}) \right] \\ &= -\delta_{ij} \gamma \frac{v_F}{M_{CN}} \sum_n^{\text{occ.}} \frac{1}{\Omega} \int_{|\mathbf{k}| < \Lambda} \left[q_x \sigma^x \frac{k_x}{\sqrt{k_x^2 + k_y^2}} + q_y \sigma^y \frac{k_y}{\sqrt{k_x^2 + k_y^2}} \right] = 0. \end{aligned} \quad (\text{IX8})$$

We next discuss the geometric contribution $[\mathcal{D}_g^{\text{ac}}(\mathbf{q})]$. We emphasize that $[\mathcal{D}_g^{\text{ac}}(\mathbf{q})]$ is a non-analytical function of \mathbf{q} , and thus a direct Taylor expansion in small \mathbf{q} fails to describe the long-wavelength behavior. In fact, by trying to perform the latter, we obtain

$$[\mathcal{D}_g^{\text{ac}}(\mathbf{q})]_i^j \approx \frac{-\gamma^2 v_F}{2M_C \Omega} \int_0^\Lambda dk \frac{1}{k^2} \begin{pmatrix} q_x^2 + 3q_y^2 & 2q_x q_y \\ 2q_x q_y & 3q_x^2 + q_y^2 \end{pmatrix} + O(\mathbf{q}^3) \quad (\text{IX9})$$

where Λ is a once again the ultraviolet cutoff, and Ω is the area of the Brillouin zone. In addition, we replace the momentum summation with an integral, as $\frac{1}{N} \sum_{\mathbf{k}} \rightarrow \frac{1}{\Omega} \int_{\mathbf{k}}$. We observe that the coefficient of the \mathbf{q}^2 term diverges due to the infrared (small k) divergence of the integral $\int_0^\Lambda 1/k^2 dk$. This divergence reflects the non-analytical properties of the $[\mathcal{D}_g^{\text{ac}}(\mathbf{q})]_i^j$. To directly prove this non-analyticity, we focus on the specific case of $\mathbf{q} = (q_x, 0)$ to simplify the problem. We first evaluate the $i = x, j = x$ component which gives

$$\begin{aligned} [\mathcal{D}_g^{\text{ac}}((q_x, 0))]_x^x &= \frac{v_F \gamma^2}{\Omega M_C} \int_{|\mathbf{k}| < \Lambda} \\ &(-1) \left[k_y^2 q_x \left(6k_x^5 + 23k_x^4 q_x + k_x^2 q_x \left(11\sqrt{k_x^2 + k_y^2} \sqrt{(k_x + q_x)^2 + k_y^2} + 28k_y^2 + 27q_x^2 \right) \right. \right. \\ &+ k_x \left(k_y^2 \left(6\sqrt{k_x^2 + k_y^2} \sqrt{(k_x + q_x)^2 + k_y^2} + 23q_x^2 \right) + 6q_x^2 \sqrt{k_x^2 + k_y^2} \sqrt{(k_x + q_x)^2 + k_y^2} + 6k_y^4 + 11q_x^4 \right) \\ &+ q_x \left(k_y^2 \left(3\sqrt{k_x^2 + k_y^2} \sqrt{(k_x + q_x)^2 + k_y^2} + 7q_x^2 \right) + q_x^2 \sqrt{k_x^2 + k_y^2} \sqrt{(k_x + q_x)^2 + k_y^2} + 5k_y^4 + 2q_x^4 \right) \\ &\left. \left. + k_x^3 \left(6\sqrt{k_x^2 + k_y^2} \sqrt{(k_x + q_x)^2 + k_y^2} + 12k_y^2 + 35q_x^2 \right) \right) \right] \\ &\left[(k_x^2 + k_y^2)^{3/2} ((k_x + q_x)^2 + k_y^2)^{5/2} \left(\sqrt{k_x^2 + k_y^2} + \sqrt{(k_x + q_x)^2 + k_y^2} \right) \right]. \end{aligned} \quad (\text{IX10})$$

We could then let

$$\begin{aligned} k_x &\rightarrow p_x q_x, \\ k_y &\rightarrow p_y q_x, \end{aligned} \quad (\text{IX11})$$

thus obtaining

$$[\mathcal{D}_g^{\text{ac}}((q_x, 0))]_x^x = \frac{v_F \gamma^2 |q_x|}{\Omega M_C} C_{\Lambda/|q_x|},$$

with

$$\begin{aligned} C_{\Lambda/|q_x|} &= \int_{|\mathbf{p}| < \Lambda/|q_x|} \\ &(-1) \left[p_y^2 \left(6p_x^5 + 23p_x^4 q_x + p_x^2 \left(11\sqrt{p_x^2 + p_y^2} \sqrt{(p_x + 1)^2 + p_y^2} + 28p_y^2 + 27 \right) \right. \right. \\ &+ p_x \left(p_y^2 \left(6\sqrt{p_x^2 + p_y^2} \sqrt{(p_x + 1)^2 + p_y^2} + 23 \right) + 6\sqrt{p_x^2 + p_y^2} \sqrt{(p_x + 1)^2 + p_y^2} + 6p_y^4 + 11 \right) \\ &+ \left(p_y^2 \left(3\sqrt{p_x^2 + p_y^2} \sqrt{(p_x + 1)^2 + p_y^2} + 7 \right) + \sqrt{p_x^2 + p_y^2} \sqrt{(p_x + 1)^2 + p_y^2} + 5p_y^4 + 2 \right) \\ &\left. \left. + p_x^3 \left(6\sqrt{p_x^2 + p_y^2} \sqrt{(p_x + 1)^2 + p_y^2} + 12p_y^2 + 35 \right) \right) \right] \\ &\left[(p_x^2 + p_y^2)^{3/2} ((p_x + 1)^2 + p_y^2)^{5/2} \left(\sqrt{p_x^2 + p_y^2} + \sqrt{(p_x + 1)^2 + p_y^2} \right) \right]. \end{aligned} \quad (\text{IX12})$$

Here, we comment that $[\mathcal{D}_g^{\text{ac}}((q_x, 0))]_x^x$ only depends on $|q_x|$ instead of q_x . In the $|q_x| \rightarrow 0$ limit, we find

$$[\mathcal{D}_g^{\text{ac}}((q_x, 0))]_x^x = \frac{v_F \gamma^2 |q_x|}{\Omega M_C} C_{\Lambda/|q_x|} \approx \frac{v_F \gamma^2 |q_x|}{\Omega M_C} C_{\Lambda/|q_x| \rightarrow \infty}, \quad (\text{IX13})$$

where we defined the real coefficient $C_\infty = C_{\Lambda/|q_x| \rightarrow \infty}$ by letting $\Lambda \rightarrow \infty$. This coefficient is evaluated numerically, yielding

$$C_{\Lambda/|q_x| \rightarrow \infty} = -5.08. \quad (\text{IX14})$$

Therefore, we conclude that

$$[\mathcal{D}_g^{\text{ac}}((q_x, 0))]_x^x \approx -5.08 \frac{v_F \gamma^2 |q_x|}{\Omega M_C}, \quad (\text{IX15})$$

which is indeed a non-analytical function of q_x since it depends on the absolute value of q_x . Similarly, for the other three components of the dynamical matrix, we find

$$\begin{aligned} [\mathcal{D}_g^{\text{ac}}((q_x, 0))]_x^y &\approx \frac{v_F \gamma^2 |q_x|}{\Omega M_C} \times 0 \approx 0 \\ [\mathcal{D}_g^{\text{ac}}((q_x, 0))]_y^x &\approx \frac{v_F \gamma^2 |q_x|}{\Omega M_C} \times 0 \approx 0 \\ [\mathcal{D}_g^{\text{ac}}((q_x, 0))]_y^y &\approx -2.09 \frac{v_F \gamma^2 |q_x|}{\Omega M_C} \end{aligned} \quad (\text{IX16})$$

Therefore, we have proved the non-analytical nature of the $\mathcal{D}_g^{\text{ac}}((q_x, 0))$.

To further understand the behaviors of the Dirac node, we also consider the Hamiltonian of the gapped Dirac node

$$h_{\text{gap}}(\mathbf{k}) = \begin{pmatrix} \Delta/2 & v_F(k_x - ik_y) \\ v_F(k_x + ik_y) & -\Delta/2 \end{pmatrix} \quad (\text{IX17})$$

with the following eigenvalue and eigenvectors

$$\begin{aligned} \varepsilon_{\pm, \mathbf{k}} &= \pm \sqrt{v_F^2 |\mathbf{k}|^2 + \frac{\Delta^2}{4}} \\ U_+(\mathbf{k}) &= \frac{1}{\sqrt{2\varepsilon_{+, \mathbf{k}}(\varepsilon_{+, \mathbf{k}} + \frac{\Delta}{2})}} \begin{pmatrix} \varepsilon_{\mathbf{k},+} + \frac{\Delta}{2} \\ v_F(k_x + ik_y) \end{pmatrix}, \quad U_-(\mathbf{k}) = \frac{1}{\sqrt{2\varepsilon_{\mathbf{k},+}(\varepsilon_{\mathbf{k},+} + \frac{\Delta}{2})}} \begin{pmatrix} v_F(ik_y - k_x) \\ \varepsilon_{\mathbf{k},+} + \frac{\Delta}{2} \end{pmatrix} \end{aligned} \quad (\text{IX18})$$

We now evaluate the electronic contributions to the dynamical matrix of the acoustic mode. We first consider $[\mathcal{D}_{\text{ele}}^{\text{ac}}(\mathbf{q})]_i^j$. We notice that, for the gapped Dirac node,

$$\begin{aligned} f_i(\mathbf{k}) &= i\gamma \partial_{k_i} h(\mathbf{k}) = i\gamma v_F \sigma_i \\ M_{ij}(\mathbf{k}) &= (\gamma \delta_{i,j} - \gamma^2 \partial_{k_i, k_j}^2) h(\mathbf{k}) = \delta_{i,j} \gamma h(\mathbf{k}) \end{aligned} \quad (\text{IX19})$$

Then we observe

$$f_i(\mathbf{k} + \mathbf{q}) - f_i(\mathbf{k}) = 0 \quad (\text{IX20})$$

Therefore, from (IX5), we conclude that the total electronic contribution of the gapped Dirac node gives

$$\begin{aligned} [\mathcal{D}_{\text{el}}^{\text{ac}}(\mathbf{q})]_i^j &= \delta_{i,j} \gamma \frac{v_F}{M_C N} \sum_n^{\text{occ.}} \frac{1}{\Omega} \int_{|\mathbf{k}| < \Lambda} \text{Tr} \left[(q_x \sigma^x + q_y \sigma^y) \cdot P_n(\mathbf{k}) \right] \\ &= -\delta_{i,j} \gamma \frac{v_F}{M_C N} \sum_n^{\text{occ.}} \frac{1}{\Omega} \int_{|\mathbf{k}| < \Lambda} \left[q_x \sigma^x \frac{k_x}{\sqrt{k_x^2 + k_y^2 + \frac{\Delta^2}{4}}} + q_y \sigma^y \frac{k_y}{\sqrt{k_x^2 + k_y^2 + \frac{\Delta^2}{4}}} \right] = 0 \end{aligned} \quad (\text{IX21})$$

which also vanishes. We next evaluate the geometric contribution. Since the finite Δ removes the singular behaviors of the Dirac node, we could perform a direct expansion in powers of \mathbf{q} which gives

$$\begin{aligned} [\mathcal{D}_g^{\text{ac}}(\mathbf{q})]_i^j &= \frac{\gamma^2 \pi v_F^4}{4M_C \Omega} \int_0^\Lambda k dk \frac{1}{[\Delta^2/4 + v_F^2 k^2]^{7/2}} \times \\ &\quad \begin{pmatrix} -(\Delta^4 (2q_x^2 + q_y^2)) + \Delta^2 k^2 v_F^2 (5q_x^2 + q_y^2) + k^4 v_F^4 (q_x^2 + 3q_y^2) & -q_x q_y (\Delta^4 - 4\Delta^2 k^2 v_F^2 + 2k^4 v_F^4) \\ -q_x q_y (\Delta^4 - 4\Delta^2 k^2 v_F^2 + 2k^4 v_F^4) & -(\Delta^4 (q_x^2 + 2q_y^2)) + \Delta^2 k^2 v_F^2 (q_x^2 + 5q_y^2) + k^4 v_F^4 (3q_x^2 + q_y^2) \end{pmatrix}_{ij} \end{aligned} \quad (\text{IX22})$$

We introduce the auxiliary variable $k = y\Delta/v_F$, and find

$$[\mathcal{D}_g^{\text{ac}}(\mathbf{q})]_i^j = \frac{\gamma^2 \pi v_F^2}{4M_C \Delta^5 \Omega} \int_0^{v_F \Lambda / \Delta} y dy \frac{1}{[1/4 + y^2]^{7/2}} \times \begin{pmatrix} -((2q_x^2 + q_y^2)) + y^2(5q_x^2 + q_y^2) + y^4(q_x^2 + 3q_y^2) & -q_x q_y(1 - 4y^2 + 2y^4) \\ -q_x q_y(1 - 4y^4 + 2y^4) & -((q_x^2 + 2q_y^2)) + y^4(q_x^2 + 5q_y^2) + y^4(3q_x^2 + q_y^2) \end{pmatrix}_{ij} \quad (\text{IX23})$$

By performing the integral on y , we find

$$[\mathcal{D}_g^{\text{ac}}(\mathbf{q})]_i^j = \frac{8\gamma^2 \pi v_F^2}{15\Delta M_C \Omega} \times \begin{pmatrix} \frac{(1-5\eta^2(9\eta^2+4))q_y^2 - 3(5\eta^2(\eta^2+2)-1)q_x^2}{(4\eta^2+1)^{5/2}} - 3q_x^2 - q_y^2 & -\frac{2(-15\eta^4+5\eta^2+(4\eta^2+1)^{5/2}-1)q_x q_y}{(4\eta^2+1)^{5/2}} \\ -\frac{2(-15\eta^4+5\eta^2+(4\eta^2+1)^{5/2}-1)q_x q_y}{(4\eta^2+1)^{5/2}} & \frac{(1-5\eta^2(9\eta^2+4))q_x^2 - 3(5\eta^2(\eta^2+2)-1)q_y^2}{(4\eta^2+1)^{5/2}} - q_x^2 - 3q_y^2 \end{pmatrix} + \text{H.c.}, \quad (\text{IX24})$$

where

$$\eta = \frac{v_F \Lambda}{\Delta}. \quad (\text{IX25})$$

To get a simple formula, we could let $\Lambda \rightarrow \infty$, which then gives

$$[\mathcal{D}_g^{\text{ac}}(\mathbf{q})]_i^j \approx \frac{-8\gamma^2 \pi v_F^2}{15\Delta M_C \Omega} \begin{pmatrix} 3q_x^2 + q_y^2 & 2q_x q_y \\ 2q_x q_y & 3q_y^2 + q_x^2 \end{pmatrix}, \quad (\text{IX26})$$

We can see that the dynamical matrix of the acoustic mode is proportional to $1/\Delta$, which diverges as $\Delta \rightarrow 0$, which also reflects the non-analytical behaviors of the geometric contribution of the gapless Dirac node ($\Delta \rightarrow 0$).

Appendix X: Quantum geometric velocity renormalization for the EFK Hamiltonian

In this section, we consider the velocity renormalization from the EFK Hamiltonian defined in appendix VI. The geometric terms in the dynamical matrix are

$$D_g^{(1)}(q) = \frac{1}{M} \frac{2}{N} \sum_k^{\text{FBZ}} \left\{ \frac{1}{E_-(k) - E_+(k+q)} (F(-, k, +, k+q)F(+, k+q, k) - F^E(-, k, +, k+q)F^E(+, k+q, k)) + \text{H.c.} \right\},$$

$$D_g^{(2)}(q) = \frac{1}{M} \frac{2}{N} \sum_{k\tilde{k}}^{\text{FBZ}} \sum_{\alpha} \left[\delta_{\tilde{k},0} - \delta_{\tilde{k},k} \right] \left\{ [M^{\text{E-g}}(\tilde{k})]_{\alpha}^{\alpha'} + [M^g(\tilde{k})]_{\alpha}^{\alpha'} \right\} [P_n(k)]_{\alpha'}^{\alpha} + \text{H.c.}, \quad (\text{X1})$$

where $F(n, k, n', k')$, $F^E(n, k, n', k')$ is given by

$$F^E(nk, n'k') = \sum_{\alpha\alpha'} [U_n^{\dagger}(\mathbf{k})]_{\alpha} \left\{ [f^E(k')]_{\alpha}^{\alpha'} - [f^E(k)]_{\alpha}^{\alpha'} \right\} [U_{n'}(\mathbf{k}')]_{\alpha'},$$

$$F(nk, n'k') = \sum_{\alpha\alpha'} [U_n^{\dagger}(\mathbf{k})]_{\alpha} \left\{ [f(k')]_{\alpha}^{\alpha'} - [f(k)]_{\alpha}^{\alpha'} \right\} [U_{n'}(\mathbf{k}')]_{\alpha'}, \quad (\text{X2})$$

The leading order term in q of the dynamical matrix is thus given by

$$D_g^{(1)}(q) = \frac{1}{M} \frac{2}{N} \sum_k^{\text{FBZ}} \left\{ \frac{1}{E_+(k) - E_-(k)} \left(\text{Tr} \left[P_- \left(\partial_k f(k) \right) P_+ \left(\partial_k f(k) \right) \right] - \text{Tr} \left[P_- \left(\partial_k f^E(k) \right) P_+ \left(\partial_k f^E(k) \right) \right] \right) \right\} q^2 + \text{H.c.} + O(q^4)$$

$$D_g^{(2)}(q) = -\frac{1}{M} \frac{2}{N} \sum_k^{\text{FBZ}} \left\{ \text{Tr} \left[\left(M^{\text{E-g}}(\tilde{k}) + M^g(\tilde{k}) \right) P_n(k) \right] \right\} q^2 + \text{H.c.} + O(q^4) \quad (\text{X3})$$

where M is the mass of each atom in the chain. The quantities $f^g(\mathbf{k})$, $f^E(\mathbf{k})$ are given by

$$f^g(k) = \frac{1}{2(t^2 - \tilde{t}^2)\cos(2ak) - 4\delta t\cos(ak) + \delta^2 + 2t^2 + 2\tilde{t}^2} \times$$

$$\begin{pmatrix} -4ia\gamma\tilde{t}^2\sin(ak)(\delta\cos(ak) - 2t) & -2a\gamma\tilde{t}((\delta^2 + 4t^2)\cos(ak) - \delta t(\cos(2ak) + 3)) \\ 2a\gamma\tilde{t}((\delta^2 + 4t^2)\cos(ak) - \delta t(\cos(2ak) + 3)) & 4ia\gamma\tilde{t}^2\sin(ak)(\delta\cos(ak) - 2t) \end{pmatrix},$$

$$f^E(k) = \frac{1}{2(t^2 - \tilde{t}^2)\cos(2ak) - 4\delta t\cos(ak) + \delta^2 + 2t^2 + 2\tilde{t}^2} \times$$

$$\begin{pmatrix} 2ia\gamma\sin(ak)(\delta - 2t\cos(ak))(\delta t - 2(t^2 - \tilde{t}^2)\cos(ak)) & -4a\gamma\tilde{t}\sin^2(ak)(\delta t - 2(t^2 - \tilde{t}^2)\cos(ak)) \\ 4a\gamma\sin^2(ak)(\delta t - 2(t^2 - \tilde{t}^2)\cos(ak)) & -2ia\gamma\sin(ak)(\delta - 2t\cos(ak))(\delta t - 2(t^2 - \tilde{t}^2)\cos(ak)) \end{pmatrix}. \quad (\text{X4})$$

while $M^{E-g}(k) + M^g(k)$ is given by

$$M^{E-g}(k) + M^g(k) = \frac{2a^2\gamma^2\tilde{t}^2}{(-4\delta t\cos(ak) + 2(t^2 - \tilde{t}^2)\cos(2ak) + \delta^2 + 2t^2 + 2\tilde{t}^2)^2} \begin{pmatrix} m_{11} & m_{12} \\ m_{12}^* & -m_{11} \end{pmatrix}$$

$$m_{11} = \delta(2\cos(2ak)(\delta^2 + 4t^2 + 2\tilde{t}^2) - 3\delta t\cos(3ak) + t^2\cos(4ak) - \tilde{t}^2\cos(4ak) + 15t^2 - 3\tilde{t}^2)$$

$$- t(9\delta^2 + 16t^2)\cos(ak)$$

$$m_{12} = \frac{1}{\tilde{t}} \left[i\sin(ak)(-6\delta t\cos(ak)(\delta^2 + t^2 + 3\tilde{t}^2) + 6\delta^2 t^2\cos(2ak) - 2\delta t^3\cos(3ak) + 2\delta t\tilde{t}^2\cos(3ak) \right.$$

$$\left. + \delta^4 + 6\delta^2 t^2 + 4\delta^2 \tilde{t}^2 + 16t^2 \tilde{t}^2) \right] \quad (\text{X5})$$

Incorporating the formulas above, we obtain the velocity renormalization given by

$$D_g(q) = -\frac{1}{M} \frac{2}{N} \sum_k \frac{a^4\gamma^2\tilde{t}^2}{(-4\delta t\cos(ak) + 2(t^2 - \tilde{t}^2)\cos(2ak) + \delta^2 + 2t^2 + 2\tilde{t}^2)^{7/2}}$$

$$\left(-14\delta^5 t\cos(3ak) - 11\delta^4 t^2\cos(4ak) + 20\delta^4 \tilde{t}^2\cos(4ak) + 92\delta^3 t^3\cos(3ak) \right.$$

$$+ 12\delta^3 t^3\cos(5ak) - 204\delta^3 t\tilde{t}^2\cos(3ak) - 12\delta^3 t\tilde{t}^2\cos(5ak) + 8\delta^2 t^4\cos(4ak)$$

$$- 88\delta^2 t^2\tilde{t}^2\cos(4ak) + 80\delta^2 \tilde{t}^4\cos(4ak) - 2\delta t\cos(ak)[61\delta^4 + 4\delta^2(53t^2 + 37\tilde{t}^2) - 8(123t^4 - 206t^2\tilde{t}^2 + 43\tilde{t}^4)]$$

$$+ \cos(2ak)(13\delta^6 + 72\delta^4(t^2 + \tilde{t}^2) + 16\delta^2(5t^4 + 22t^2\tilde{t}^2 + 5\tilde{t}^4) - 384(t^6 - t^2\tilde{t}^4)) - 504\delta t^5\cos(3ak)$$

$$- 56\delta t^5\cos(5ak) + 1136\delta t^3\tilde{t}^2\cos(3ak) + 112\delta t^3\tilde{t}^2\cos(5ak) - 632\delta t\tilde{t}^4\cos(3ak) - 56\delta t\tilde{t}^4\cos(5ak) + 304t^6\cos(4ak)$$

$$- 608t^4\tilde{t}^2\cos(4ak) + 304t^2\tilde{t}^4\cos(4ak) + 3\delta^6 + 339\delta^4 t^2 - 28\delta^4 \tilde{t}^2 - 728\delta^2 t^4 + 1272\delta^2 t^2\tilde{t}^2 - 160\delta^2 \tilde{t}^4 - 688t^6 + 1632t^4\tilde{t}^2$$

$$\left. - 688t^2\tilde{t}^4 \right) q^2 + O(q^4) \quad (\text{X6})$$

This gives the non-zero and non-divergent contribution to the velocity of the acoustic mode.

* guglielmo.pellitteri@sns.it

- [S1] G. Grosso and G. Pastori Parravicini, *Solid State Physics, 2nd edition* (Academic Press, Oxford, 2014).
[S2] B. A. Bernevig and T. L. Hughes, *Topological Insulators and Topological Superconductors* (Princeton University Press, Princeton and Oxford, 2013).
[S3] R. Resta, The insulating state of matter: A geometrical theory, *Eur. Phys. J. B* **79**, 121 (2011).
[S4] J. P. Provost and G. Vallee, Riemannian structure on manifolds of quantum states, *Comm. Math. Phys.* **76**, 289 (1980).
[S5] J. Yu, C. J. Ciccarino, R. Bianco, I. Errea, P. Narang, and B. A. Bernevig, Non-trivial quantum geometry and the strength of electron-phonon coupling, *Nature Phys.* **20**, 1262 (2024).

- [S6] G. F. Giuliani and G. Vignale, *Quantum Theory of the Electron Liquid* (Cambridge University Press, Cambridge, 2005).
- [S7] J. J. Sakurai and J. Napolitano, *Modern Quantum Mechanics, 2nd edition* (Cambridge University Press, Cambridge, 2017).
- [S8] G. M. Andolina, F. M. D. Pellegrino, V. Giovannetti, A. H. MacDonald, and M. Polini, Cavity quantum electrodynamics of strongly correlated electron systems: A no-go theorem for photon condensation, *Phys. Rev. B* **100**, 121109 (2019).
- [S9] S. Baroni, S. de Gironcoli, A. Dal Corso, and P. Giannozzi, Phonons and related crystal properties from density-functional perturbation theory, *Rev. Mod. Phys.* **73**, 515 (2001).
- [S10] P. Giannozzi, S. Baroni, N. Bonini, M. Calandra, R. Car, C. Cavazzoni, D. Ceresoli, G. L. Chiarotti, M. Cococcioni, I. Dabo, A. Dal Corso, S. de Gironcoli, S. Fabris, G. Fratesi, R. Gebauer, U. Gerstmann, C. Gougoussis, A. Kokalj, M. Lazzeri, L. Martin-Samos, N. Marzari, F. Mauri, R. Mazzarello, S. Paolini, A. Pasquarello, L. Paulatto, C. Sbraccia, S. Scandolo, G. Sclauzero, A. P. Seitsonen, A. Smogunov, P. Umari, and R. M. Wentzcovitch, QUANTUM ESPRESSO: a modular and open-source software project for quantum simulations of materials, *J. Phys. Condens. Matter* **21**, 395502 (2009).
- [S11] P. Giannozzi, O. Andreussi, T. Brumme, O. Bunau, M. Buongiorno Nardelli, M. Calandra, R. Car, C. Cavazzoni, D. Ceresoli, M. Cococcioni, N. Colonna, I. Carnimeo, A. Dal Corso, S. de Gironcoli, P. Delugas, R. A. DiStasio, A. Ferretti, A. Floris, G. Fratesi, G. Fugallo, R. Gebauer, U. Gerstmann, F. Giustino, T. Gorni, J. Jia, M. Kawamura, H.-Y. Ko, A. Kokalj, E. Küçükbenli, M. Lazzeri, M. Marsili, N. Marzari, F. Mauri, N. L. Nguyen, H.-V. Nguyen, A. Otero-de-la-Roza, L. Paulatto, S. Poncé, D. Rocca, R. Sabatini, B. Santra, M. Schlipf, A. P. Seitsonen, A. Smogunov, I. Timrov, T. Thonhauser, P. Umari, N. Vast, X. Wu, and S. Baroni, Advanced capabilities for materials modelling with Quantum ESPRESSO, *J. Phys. Condens. Matter* **29**, 465901 (2017).
- [S12] G. Prandini, A. Marrazzo, I. E. Castelli, N. Mounet, and N. Marzari, Precision and efficiency in solid-state pseudopotential calculations, *npj Comput. Mater.* **4**, 72 (2018).
- [S13] A. Dal Corso, Pseudopotentials periodic table: From H to Pu, *Comput. Mater. Sci.* **95**, 337 (2014).
- [S14] J. P. Perdew, K. Burke, and M. Ernzerhof, Generalized gradient approximation made simple, *Phys. Rev. Lett.* **77**, 3865 (1996).
- [S15] S. Grimme, Semiempirical GGA-type density functional constructed with a long-range dispersion correction, *J. Comput. Chem.* **27**, 1787 (2006).
- [S16] M. Methfessel and A. T. Paxton, High-precision sampling for Brillouin-zone integration in metals, *Phys. Rev. B* **40**, 3616 (1989).
- [S17] H. J. Monkhorst and J. D. Pack, Special points for Brillouin-zone integrations, *Phys. Rev. B* **13**, 5188 (1976).
- [S18] T. Sohler, M. Calandra, and F. Mauri, Density functional perturbation theory for gated two-dimensional heterostructures: Theoretical developments and application to flexural phonons in graphene, *Phys. Rev. B* **96**, 075448 (2017).
- [S19] S. Reich, J. Maultzsch, C. Thomsen, and P. Ordejón, Tight-binding description of graphene, *Phys. Rev. B* **66**, 035412 (2002).
- [S20] M. I. Katsnelson, *The Physics of Graphene, 2nd edition* (Cambridge University Press, Cambridge, 2020).